

Bioactive coatings to control marine biofouling

DISSERTATION

zur Erlangung des akademischen Grades

**Doctor rerum naturalium
(Dr. rer. nat.)**

vorgelegt

der Fakultät Mathematik und Naturwissenschaften
der Technischen Universität Dresden

von

MSc. Mariana Tasso

geboren am 14.09.1976 in Buenos Aires

Eingereicht am 10.07.2009

Die Dissertation wurde in der Zeit von 02/2006 bis
06/2009 im Leibniz Institut für Polymerforschung Dresden angefertigt.

Tag der Verteidigung: 12.11.2009

Gutachter:

Prof. Dr. Carsten Werner
Prof. Dr. Katrin Salchert

Bioactive coatings to control marine
biofouling

Mariana Tasso

“In all things of nature there is something of the marvelous”

Aristotle (384 BC – 322 BC), *Parts of Animals*

Contents

1	Preface	1
2	Aim of the work	5
3	Theoretical basis	9
3.1	Marine biofouling	9
3.1.1	Main marine biofoulers and their adhesion strategies	12
3.2	Marine biofouling control	17
3.2.1	Enzymes as antifouling agents	19
3.3	Enzymes	21
3.3.1	General properties	21
3.3.2	Proteases and the subtilisin-like group of proteases	23
3.3.3	Subtilisin A	26
3.3.4	Applications of enzymes	27
3.4	Enzyme immobilization	28
3.5	Maleic anhydride copolymer thin films	30
3.6	Surface analysis of the bioactive maleic anhydride layers	33
3.6.1	Ellipsometry	33
3.6.2	High performance liquid chromatography	35

3.6.3	Absorbance spectroscopy	37
3.6.4	Confocal laser scanning microscopy	39
3.6.5	Atomic force microscopy	40
3.6.6	Surface wettability	42
3.7	Biofouling quantification	43
4	Results and Discussion	47
4.1	Immobilized enzyme layer	47
4.1.1	Enzyme layer thickness	48
4.1.2	Enzyme surface concentration	50
4.1.3	Enzyme activity	53
4.1.4	Surface morphology and wettability	56
4.2	Enzyme layer stability in aqueous media	58
4.3	Antifouling and fouling-release potential of Subtilisin A in solution	62
4.4	Antifouling and fouling-release potential of immobilized Subtilisin A	67
4.4.1	Assays with spores of <i>Ulva linza</i>	67
4.4.2	Assays with cells of <i>Navicula perminuta</i>	75
4.4.3	Assays with cyprids of <i>Balanus amphitrite</i>	80
5	Conclusions	87
6	Summary	93
7	Materials and Methods	95
7.1	Materials	95

7.2	Experimental marine organisms	98
7.3	Experimental techniques	100
7.3.1	Ellipsometry	100
7.3.2	High performance liquid chromatography	101
7.3.3	Absorbance spectroscopy	103
7.3.4	Confocal laser scanning microscopy	104
7.3.5	Atomic force microscopy	107
7.3.6	Surface wettability	107
7.3.7	Cell density	108
7.3.8	Cell adhesion strength	109
7.4	Polymer film preparation	110
7.5	Covalent immobilization of Subtilisin A	111
7.6	Enzyme layer characterization	113
7.7	Enzyme layer stability in aqueous media	115
7.8	Biological assays with micro and macrofoulers	116
	Abbreviations	123
	List of Figures	127
	List of Tables	131
	References	133
	Acknowledgements	147

Chapter 1

Preface

Marine biofouling is defined as the undesirable accumulation of biological material (microorganisms, plants, and animals) on man-made surfaces immersed in seawater [1; 2]. Bacteria are ubiquitous colonizers of many types of surfaces and are the first at gaining immersed substrata, which in turn are already covered by a conditioning film formed by adsorbed organic molecules [3; 4]. Along with bacteria, a myriad of other organisms settle on surfaces, settlement representing a crucial step in their life cycle as it allows the transition from planktonic to adult stages. Bacterial colonization of a surface is followed by a progressive accumulation of microorganisms, like fungi and microalgae, that together form a complex structure called biofilm [5]. Biofilms act as attractors for more visible foulers, such as macroalgae and the hard-shelled invertebrates (hydroids, barnacles, tubeworms and bivalves) [1; 2; 4]. The complex processes of exploration in search of an appropriate substratum for settlement, local sensing of surface properties and recognition of specific surface ligands, selection of a settlement location, and final commitment to settlement, vary amid different organisms and species [3; 6; 7; 8]. However, adhesion-mediating substances are a common feature for most individuals in the marine environment. Bacteria and diatoms use extracellular polymeric substances (EPS) to bind to surfaces and to hold the biofilm structure, which are primarily polysaccharides with only a minor fraction of proteins [5; 7; 9], although for some bacterial and diatom species high glycoprotein contents have been revealed [10–14]. Algae largely rely on

(glyco)proteins [15] whereas barnacles and mussels depend almost exclusively upon proteinaceous adhesives to guaranty a holdfast to surfaces [6; 16; 17]. Despite the substantial efforts undertook in this direction, the detailed composition of the adhesives produced by micro and macrofoulers is still not fully unveiled. The chemical sequencing of the adhesive molecules, their interplay with specific recognizable surface-related factors, the evolving structure and properties of the holdfasts and pads from the initial settlement steps to the formation of a secure bond between the cell wall (or the functional body part used for that purpose) and the surface itself, and the laws behind the interactions between the various adhesive components, are all at the focus of dedicated investigations [6; 9; 13; 18–21].

Proteins have been recognized as constituents of the adhesives produced by several organisms [2]. Due to their capability to cleave ester bonds in proteins, proteases emerged as potential candidates to control biofouling in an environmentally-friendly manner without threatening marine life. Enzymes are biodegradable compounds whose expected mode-of-action and consequences of use oppose to those of the currently employed biocides and non-biodegradable, prone-to-accumulation antifouling substances [2; 22]. Proteases could destabilize the biofilm matrix, degrade the adhesive substances secreted by biofilm-forming microorganisms, modify the settlement behavior of those organisms responding to biofilm-related cues to settle, and interfere with the primary and secondary adhesion of macrofoulers by degrading the proteinaceous component of the secreted adhesives [2; 3; 22] (Figure 1.1). Investigations on the potential of a spectrum of proteases to reduce settlement levels onto target surfaces and/or to diminish the strength of adhesion of the organisms to the substratum (so that removal by application of mild forces could sweep fouling away) are well-documented in the literature [14; 23–26]. So far, however, reports have broadly focused in the use of commercial preparations of the proteases together with additives, stabilizers and other components, as well as in the incorporation of commercial or pure preparations into potential antifouling paints and coatings [27; 28]. When commercial preparations are employed, biological results are

shadowed by the spurious effects of residual non-enzymatic components and by the limited knowledge of the actual surface concentration and activity of the enzyme when these preparations are incorporated onto coatings. Hence, to extract any conclusion about the impact of the soluble or matrix-incorporated enzyme on the observed biological response becomes hardly possible.

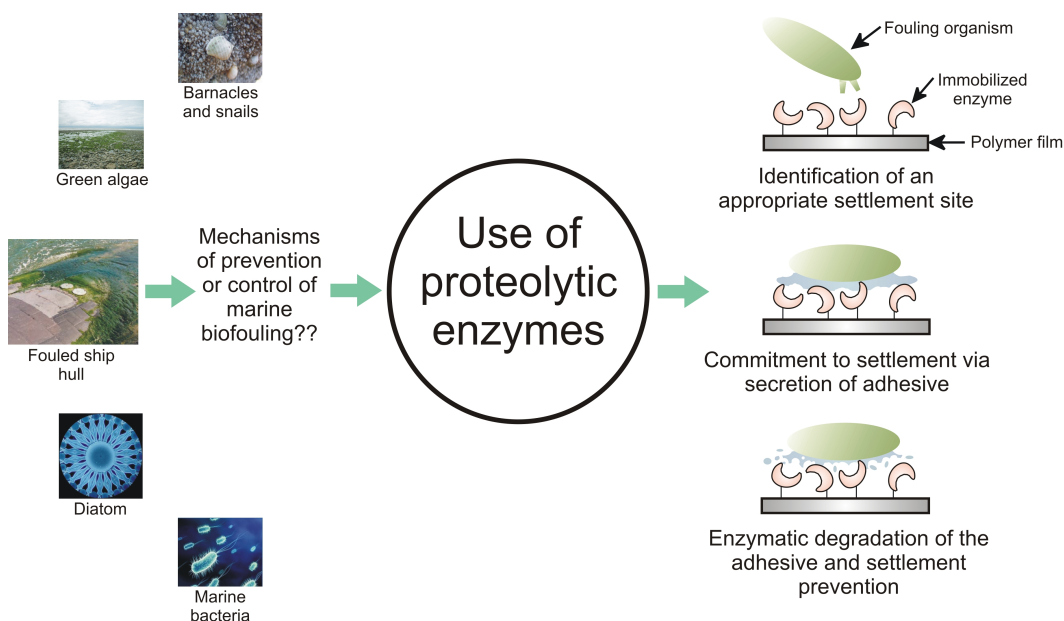


Fig. 1.1. Many marine organisms colonize immersed man-made surfaces causing substantial economic losses and lowering the life expectancy and performance of materials and devices in contact with sea water. A promising strategy to prevent and/or control marine biofouling is based on the use of proteolytic enzymes. The rationale behind this idea lies in the capability of proteases to degrade the proteinaceous component of the secreted adhesives used by most marine organisms to secure an anchorage to surfaces. By doing so, enzymes could deter settlement without compromising the health and viability of these organisms (since the target is expected to be the secreted adhesive and not the cell body) acting then as environmentally-friendly antifouling and/or fouling-release compounds.

As a strategy to evaluate the potential role of proteases as ‘destabilizers’ of adhesion processes in the marine environment, the immobilization of the protease Subtilisin A (or Subtilisin Carlsberg, pure formulation) to polymeric maleic anhydride-based nanocoatings [32; 33; 36] was proposed. In this work, the

enzyme was covalently-bound to the surface of poly(ethylene-*alt*-maleic anhydride) and poly(octadecene-*alt*-maleic anhydride) copolymer films *via* the spontaneous reaction of the anhydride moieties with the amine groups of the lysine residues of the protein. Two distinct copolymer surfaces were selected in an attempt to evaluate the dependence of the immobilized enzyme layer features on the physicochemical characteristics of the base polymer carrier. The enzyme-containing coatings were extensively characterized and tested as model coatings with three of the most relevant and ubiquitous biofouling organisms: spores of the green alga *Ulva linza*, cells of the diatom *Navicula perminuta*, and cyprid larvae of the barnacle *Balanus amphitrite*.

Results are presented which concern the characterization of the immobilized enzyme layer in terms of immobilized protein amount and activity, enzyme layer roughness and wettability, and enzyme layer stability upon incubation in aqueous media. The outcome of the biological assays with marine organisms is related to the antifouling (*i.e.* settlement inhibition) and fouling-release capability of a group of bioactive coatings of increasing activity and surface concentration. The experimental findings are thoroughly discussed *vis-à-vis* the physicochemical characteristics of the bioactive layers, with particular emphasis on the role of the base copolymer carrier as ‘determiner’ of the final properties of the bioactive layers.

Chapter 2

Aim of the work

The colonization of immersed surfaces by a myriad of marine organisms is a complex, multi-stage, species-specific process giving rise to economic and environmental costs [1; 29]. This unwanted accumulation of organisms in the marine environment, called biofouling, has been attacked from different fronts, going from the ‘problem-elimination-as-problem-solving’ strategy (essentially through the use of biocides) to more elaborated and environmentally-friendly options based on the principle of ‘non-stick’ or ‘easy foul-release’ surfaces, which do not jeopardize marine life viability [4; 30].

Several marine organisms rely on proteinaceous adhesives to secure a holdfast to surfaces [2]. Proteolytic enzymes have been demonstrated to be effective agents against settlement and settlement consolidation onto surfaces of marine bacteria, algae, and invertebrates, their proposed mode-of-action being the enzymatic degradation of the proteinaceous components of the adhesives ([22] and references therein). So far, however, the evidence remains inconclusive since most of the published investigations refer to commercial preparations where the enzyme is mixed with other components, like additives, which obviously act as additional experimental variables [23; 24]. Besides that, reports on the effects of soluble, free enzyme molecules onto the adhesives produced by various marine species largely exceed those involving surface-bound enzyme and are usually deprived of a discussion about the impact of additional factors, like the relative fractions of adsorbed-to-the-surface *vs.* soluble enzyme over time, or the levels of

retention of enzymatic activity during the length and in the conditions of the biological assays [12; 25; 26; 28].

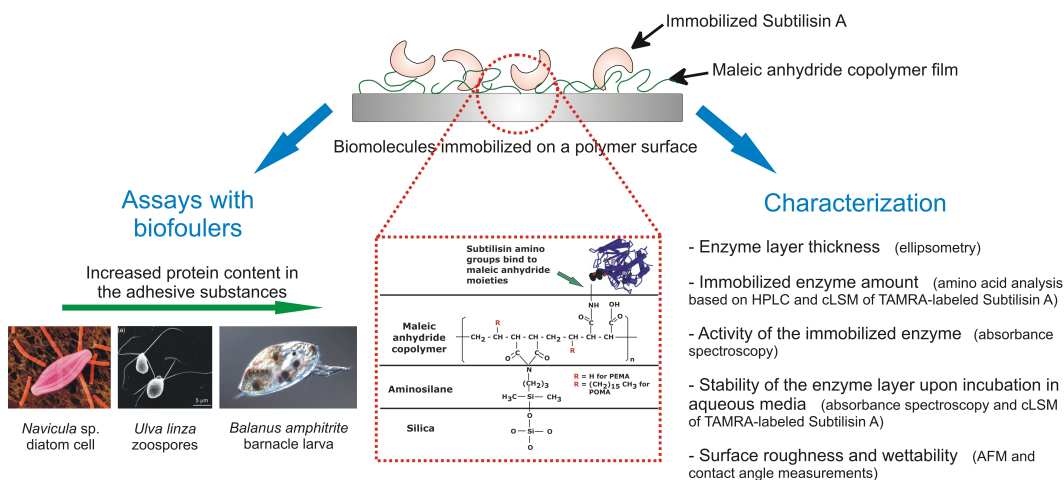


Fig. 2.1. Strategy towards the goal. The protease Subtilisin A is immobilized onto maleic anhydride copolymer thin films of distinct characteristics. The enzyme-containing coatings are characterized to unveil properties such as enzyme layer thickness and immobilized amount, catalytic activity, surface roughness and wettability, and stability upon incubation in aqueous solutions. The bioactive coatings are thereafter used in biological assays with three marine biofouling organisms: diatoms, algae, and barnacles. Controlled variations in the surface properties of the bioactive coatings are utilized as experimental variables to evaluate the biological response in model assays with the mentioned organisms.

This work aims at providing clear, conclusive evidence about the potential of serine proteases to target the adhesives produced by a group of model marine biofoulers. The strategy towards the goal consists in the preparation and characterization of maleic anhydride copolymer nanocoatings modified by a surface-bound enzyme, Subtilisin A, the active constituent of the commercial preparations reported as effective against biofouling [23; 24]. The enzyme-containing maleic anhydride copolymer films are to be characterized and thereafter tested in biological assays with three major biofoulers: spores of the green alga *Ulva linza*, cells of the pennate diatom *Navicula perminuta*, and cyprid larvae of the barnacle *Balanus amphitrite*. The purpose of the biological assays is to elucidate the efficacy of the immobilized catalyst to discourage settlement

and/or to facilitate removal of these organisms from the bioactive layers (Figure 2.1).

Maleic anhydride copolymer thin films were selected as immobilization platforms for the protease due to their tunable physico-chemical properties (obtained through variation of the comonomer unit) [31–34] and reactivity towards proteins and biomolecules [35–38]. The physico-chemical characteristics of the base polymer carrier are expected to dictate the final enzymatic properties of the immobilized biocatalyst as well as to be responsible for non-specific interactions related to biofouling and/or fouling-release. Therefore, extensive efforts are to be directed towards the characterization of the immobilized enzyme layer in terms of surface concentration, enzyme activity, surface wettability and roughness, and stability upon incubation in aqueous media. Moreover, since the process of adhesion depends upon several surface-related parameters, like wettability and roughness [39–42], the obtainment of bioactive layers in which only one parameter is varied at the time is a crucial requirement to be fulfilled in order to thoroughly comprehend the impact of the immobilized enzyme alone onto the organisms' response. For this reason, the preparation of bioactive layers of graded activity (or surface content) at constant surface wettability, roughness and topography is to be sought.

Chapter 3

Theoretical basis

3.1 Marine biofouling

Biofouling reflects the undesirable accumulation of organic material and a multitude of other forms of life, from unicellular to invertebrates, on man-made surfaces (Figure 3.1). Only in the marine environment, more than 4000 species of marine organisms are recognized as responsible for biofouling [43]. Biofouling is a worldwide problem affecting a multitude of industrial process, including pulp and paper manufacturing and food processing, bridge pillars, biomaterials, fish nets, cooling systems, and ship hulls. The cumulative cost of marine biofouling may run into billions of dollars per year worldwide, which explains the outstanding interest in the development of effective and economical control measures [28; 44].

Marine biofouling is a multistage and complex process involving an interplay between the substrate and the organisms that (actively or not) choose that substratum for settlement in what is a crucial step for their future development. The first stage of marine biofouling is characterized by the rapid accumulation of organic molecules (mostly proteins and polysaccharides) on the surface to form a conditioning film. Shortly after, a microbial biofilm develops in virtue of the attachment of single cell organisms, such as bacteria and diatoms. The presence of a microbial biofilm can provide cues that facilitate (or inhibit [28]) the settlement of more complex organisms, like algal spores and protozoa, which

attach to the surface by partially displacing the biofilm. These microfoulers, *i.e.* algae spores and protozoa in their early stages of settlement, can grow and become macrofoulers (*e.g.* after germination of algal spores into plants).

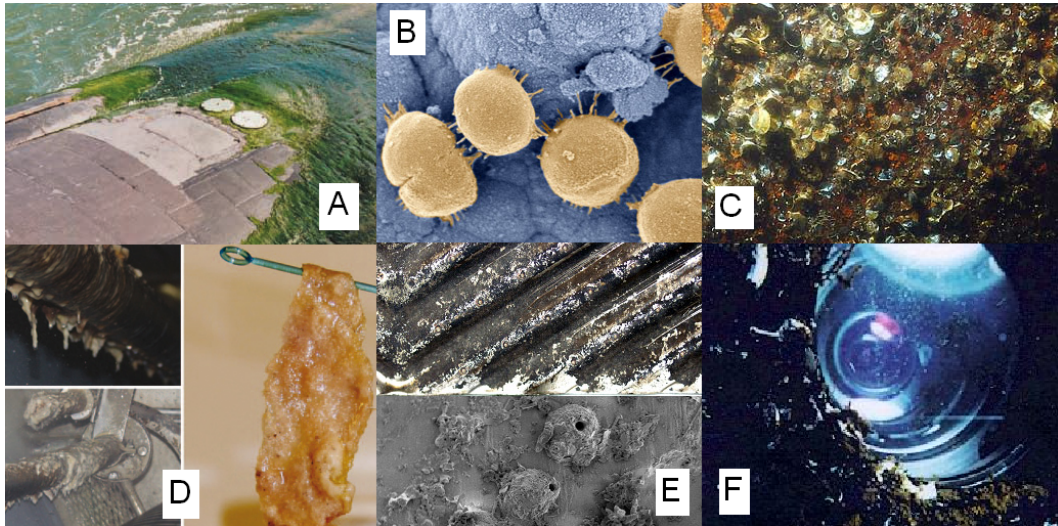


Fig. 3.1. Examples of biofouling, A: immersed structure fouled by green algae (Callow and Callow 2002 [4]); B: *Staph. epidermidis* causes fouling of medical implants; C: hard foulers on a ship's hull; D: microbial slimes in a paper machine; E: industrial lamellar coolers are troubled with deposits that cause large losses of heat-exchange capacity; F: immersed camera lens protected with an antifouling coating. Except for A, all images were free of access from internet.

As indicated in the temporal sequence of the biofouling process depicted in Figure 3.2, tertiary colonizers complete the biofouling sequence when settling into the already formed fouling community and subsequently growing into relative large and visible adults (macrofoulers) [45]. Barnacles and tubeworms are examples of hard calcareous macrofoulers, while the green seaweed *Ulva* (*Enteromorpha*) is the most common and troublesome algal macrofouler [46].

Biopolymers are utilized by all organisms to gain attachment to surfaces and for numerous other functions in varied environments, which explains their evolution into a diversity of chemical compositions [47]. The biofouling phenomena has been found to be regulated by several surface-related factors, such as surface energy, elastic modulus, frictional slippage, thickness ([39] and references therein), surface roughness and topography [40–42; 48; 49], and

surface chemistry [44; 50; 51]. Since the colonization of surfaces by more complex organisms is preceded by the formation of a biofilm, the following paragraphs will then describe this process, leaving the details about the gain of the surface by higher organisms to the next section.

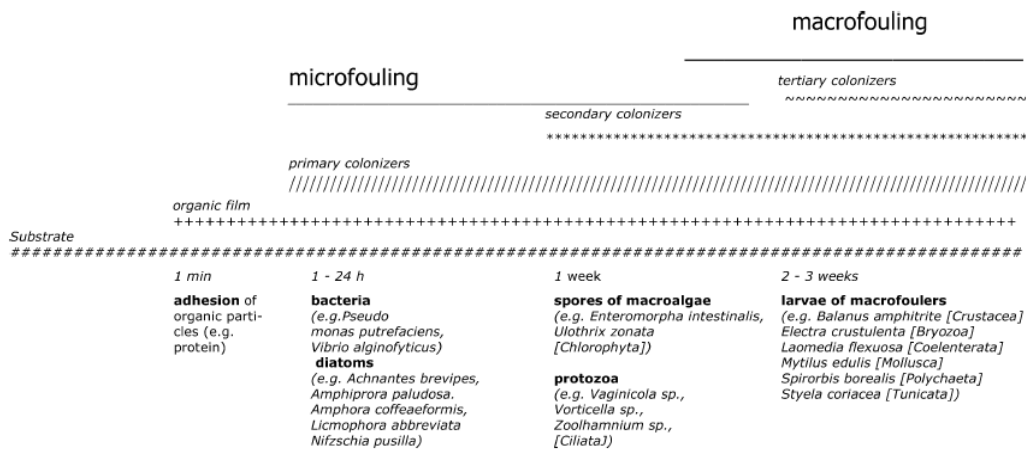


Fig. 3.2. Temporal sequence of the biofouling process (Yebra *et al.* 2004 [1]).

Biofilm is a bacterial (and diatom [9]) community which adheres to biotic and abiotic surfaces and it is embedded in a polymeric matrix composed mainly of polysaccharides, proteins [2], nucleic acids, lipids, cellular debris, and inorganic compounds such as salts [25; 5]. Proteins have been shown to account for up to 30 % of the total extracellular polymeric substances (EPS) in *Pseudomonas aeruginosa* biofilm and to be the major constituent of the EPS secreted by *Pseudoalteromonas* sp. D41 upon adhesion [14]. The biofilm matrix is largely a hydrated gel composed of water (97 %) and EPS which fulfills different functions associated with the formation and regulation of the biofilm community (e.g. providing bacterial protection and communication) [52]. Transition from the single-cell (planktonic) mode of growth to a complex structure such as the biofilm occurs in a sequential, developmental process. The process of adhesion to a surface, *i.e.* the first step of biofilm formation, is strongly affected by physico-chemical properties of both bacterial cells and surfaces, such as electric charge and hydrophobicity [3]. Bacteria colonize a surface thanks to appendages and

envelope structures such as flagella, pili, peptidoglycan or adhesin [14], have a reversible attachment [2] and display selectivity in their choice of a substrate. Upon establishment of a biofilm community, the adaptation of cells to the biofilm lifestyle, their joint response to external stimuli, and the regulation of exopolysaccharide biosynthesis to maintain the biofilm structure, are all controlled by a mechanism called *quorum* sensing, which implies the recognition of a *quorum* of neighboring cells [3]. Tackling either the accumulation of EPS on surfaces or the *quorum* sensing mechanism (or both) appears to be a promising strategy to effect biofilm viability and with it the cues leading to accumulation of other organisms [3; 5; 53].

3.1.1 Main marine biofoulers and their adhesion strategies

A myriad of organisms are responsible for marine biofouling [1; 46; 54]. Colonization of a surface is a ‘must’ in the life history of bacteria, micro and macrofoulers since it allows transition from a planktonic larval to a sessile adult stage. Apart from bacterial biofilms (already discussed in the previous section), the most common marine biofoulers (due to their widespread presence in ocean waters around the world) are the green alga *Ulva linza* [46] and several species of barnacles and tubeworms [29; 55; 56]. Some of these organisms were taken as ‘model’ organisms in research studies dedicated to assess the antifouling and fouling-release potential of surfaces, as well as to elucidate the adhesion mechanisms and the nature of the adhesive substances secreted (a successful example concerns investigations of mussel adhesive proteins and synthesis of biomimetic adhesives [21]). Within the frame of this work, three marine organisms were utilized: spores of the green alga *Ulva linza*, cells of the diatom *Navicula perminuta*, and larvae of the barnacle *Balanus amphitrite*, whose main characteristics are described below.

Ulva linza spores

Ulva linza is a common, green macroalga found throughout the world in the upper intertidal zone of seashores and as a fouling organism on a variety of man-made structures including ship's hulls [46]. Tolerance to a wide range of salinities and water qualities, together with the production of large number of propagules (zoospores) (Figure 3.3 A), contribute to the ecological success of this cosmopolitan genus [57]. Zoospores are quadriflagellate, pear-shaped cells of 5 – 7 μm length [57], which colonize substrata by secretion of a glycoprotein adhesive. Spore germination occurs within a few hours after settlement, cell division and growth giving rise to sporelings (young plants) [8]. Settlement of spores is an active process involving 'exploration' in search for a substratum, a pre-settlement, 'probing' behavior of a candidate surface with multiple spinning movements on the apical papilla, followed by a permanent phase of commitment, characterized by discharge of adhesive-containing cytoplasmic vesicles as the cell contracts against the surface depositing an adhesive pad, and final adsorption of flagella with further formation of a cell wall [4; 8]. After secretion, the formed adhesive pad (Figure 3.3 B) undergoes a hardening process, which increases its stiffness providing a secure holdfast to the surface [58]. Adhesion of *Ulva linza* zoospores is seen as an extension of the cell wall synthesis as adhesive secretion continues after settlement and the nature of the adhesive appears to be related to a constituent of the normal plant cell wall [8].

The zoospores glycoprotein adhesive is mostly protein with ~ 17 % N-linked glycan [15]. Settlement and adhesion of zoospores are influenced by several surface-related factors, such as topography [40; 48], wettability [50; 59–62], surface chemistry [43; 51; 63], surface energy [51], release of H_2O_2 from coatings [64], and surface elastic modulus and thickness [65].

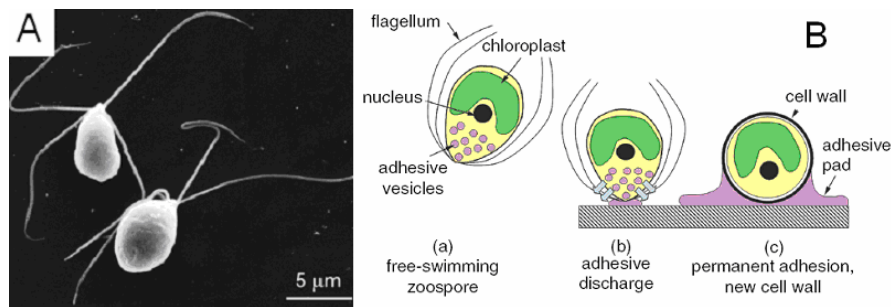


Fig. 3.3. A: SEM image of swimming, quadriflagellate zoospores of *Ulva linza* (Callow and Callow 2002 [4]); B: Course of events involved in the settlement and adhesion of zoospores of *Ulva linza* (Callow and Callow 2006 [8]).

Navicula perminuta diatom cells

Diatoms are a diverse and abundant group of unicellular protists that typically adhere to submerged surfaces, including sand and rock, grow on macroalgae, or even form large colonial mats that bind loose, sandy surfaces [9]. Benthic diatoms have been identified as major foulers of artificial surfaces placed in the marine environment, being able to resist different hydrodynamic regimes and detachment forces from the substrata. Diatom morphology is characterized by a highly ornamented, siliceous cell wall (frustule). *Navicula perminuta* is a benthic (in opposition to planktonic) diatom of bilateral symmetry (or pennate) (Figure 3.4). The diatom frustule is composed of two overlapping thecae (an epitheca and hypotheca) that join together in a similar manner as a Petri dish producing a joint region where girdle bands are observable.

Diatoms secrete EPS from numerous openings located in the silica wall and from an elongate slit, the raphe, running the length of each valve. Secretion of adhesive mucilages through the raphe results in cell-substratum adhesion and a form of cell motility called gliding. As the cell is thrust forward, extracellular adhesives are constantly being secreted from the raphe, thus providing a seamless supply of adhesive mucilage whose trail may be used as a signaling cue for the settlement of other organisms [9]. Diatoms are carried out to surfaces by currents or gravity, hence they contact surfaces passively (*i.e.* without selection) [7]. Primary adhesion in diatoms involves the cell contacting the surface and

‘inspecting’ it in search for a microhabitat (gliding), whereas secondary adhesion is associated with the formation of complex gregarious (sessile) structures (e.g. pads, stalks) when a suitable place has been located. Adhesion in diatoms is reversible: cells can detach from surfaces, as for example when nutrients are depleted.

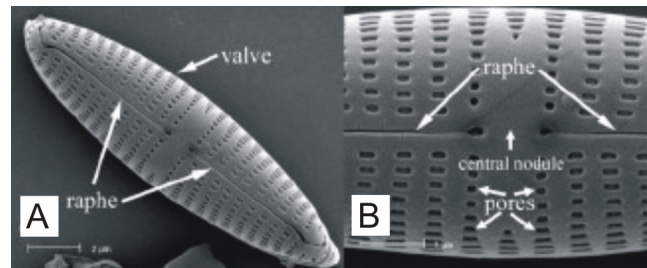


Fig. 3.4. SEM images of the pennate diatom *Navicula* sp. of bilateral cell symmetry. Each theca includes an elongated slit (A, B), termed the raphe, from which adhesive mucilage is secreted.

Images from Molino and Wetherbee 2008 [9]; scale bars = 2 μm (A); 1 μm (B).

Diatoms adhesive is predominantly polysaccharide with minor fractions of protein [7; 9], although for some species high glycoprotein contents have been revealed [10–12; 13]. As for other biofoulers, settlement and adhesion strength of diatoms are affected by surface-related properties like wettability [23; 50; 60], surface chemistry [43; 63], or surface lubricity [66].

Balanus amphitrite barnacle cyprids

Balanus amphitrite is a sub-tropical sessile crustacean covered by calcareous shell plates [6] considered to be a serious pest because it rapidly colonises immersed man-made objects and is widespread throughout the sub-tropics [55]. Barnacle larvae (cyprids) (Figure 3.5 A) explore a surface by ‘walking’ using a pair of attachment organs, or ‘antennules’, which secrete an adhesive from unicellular glands (Figure 3.5 B). In this exploratory phase, cyprids are capable of detaching, leaving behind blobs of temporary adhesive ‘footprints’. The temporary adhesive does not disperse in water, it is resistant to biodegradation, and also operates as a signalling molecule to induce the settlement of additional cyprids. After selection

of an appropriate site on which to settle, the cyprid stands on its head and releases proteinaceous cement onto the paired antennules. Initially fluid, this permanent cyprid cement flows around and embeds the attachment organs, curing within one to three hours to form a discrete matrix. The firmly attached organism subsequently metamorphoses into the calcified adult barnacle [4; 55]. As an adult, a third, discrete adhesive is produced, which is renewable and has 90 % protein content [6]. The adult cement forms a thin disc between the base plaque of an adult barnacle and the surface to which it is attached [6].

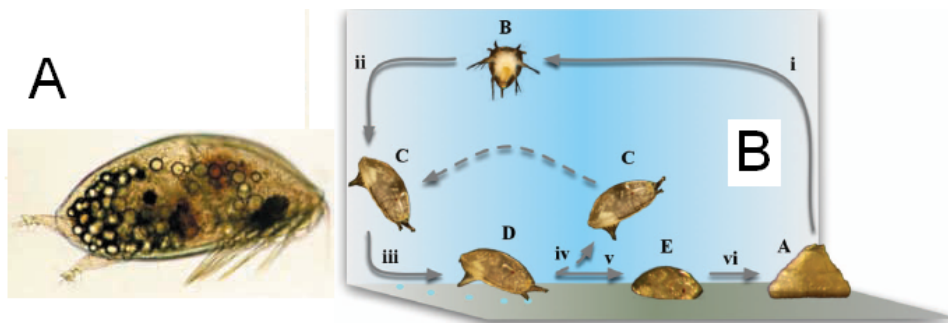


Fig. 3.5. A: the cyprid larva of *Balanus amphitrite* barnacle showing the two antennular appendages used to ‘walk’ and sense the surface prior to settlement (Callow and Callow 2002 [4]).

A cypris larva of *Balanus amphitrite* is ca. 500 μm long and 200 μm wide [55]; B: Settlement scheme of a cyprid followed by metamorphosis into an adult barnacle. A is a juvenile barnacle, which releases nauplii, B, into the water column. After feeding in the water column for days to weeks (i – ii), the nauplii metamorphoses into cyprids, C, which will explore surfaces (iii) depositing footprints (D). Cyprids may re-enter the water column (iv) or settle immediately (v). A permanently attached cyprid (E) will complete metamorphosis into a juvenile barnacle (A) within 12 h of permanent attachment (Aldred and Clare 2008 [55]).

Cyprid temporary adhesive, required for exploration and settlement by the larvae, is composed primarily of protein [16; 17] and demonstrated sensitivity to hydrolysis by proteolytic serine-proteases [23; 24]. Settlement of barnacle cyprids has been found to be controlled by the surface texture (and pattern [48]), local hydrodynamics, surface chemistry, surface colour and the presence of adult or cyprid conspecifics ([55] and references therein), as well as by the ratio between elastic modulus and thickness in silicone coatings [67] or by localized pulsed

electric fields [68]. The so-called adult settlement-inducing protein complex, a large glycoprotein [18; 20], and the proteinaceous footprints deposited during surface exploration are both considered to be inducers of gregarious settlement and have been shown to be related immunologically [19].

3.2 Marine biofouling control

Because of the vast array of organisms involved in marine biofouling and the complexity of the fouling process, development of an effective surface coating to combat biofouling remains a major technical challenge. Historically, the most effective approach to inhibit biofouling has been to utilize toxic compounds (biocides), such as organotin compounds, in a surface coating designed to allow for a gradual release into the aquatic environment. Although this approach has been very effective at controlling marine fouling, it has created significant environmental concern, ending in the ban of all new uses of organotin-containing antifouling (AF) coatings since 2003 [1; 29; 30; 69]. Similarly, the use of booster biocides (pesticides and herbicides), which are incorporated into copper-based AF systems, is also under scrutiny due to their toxic effects on the environment [30]. The environmental concerns associated with the use of AF coatings based on leachable biocides propelled efforts to develop non-toxic coatings which do not inhibit settlement, but, instead, allow for easy-removal of attached biofoulers. Marine coatings based on the “easy-release” approach have been referred to as fouling-release (FR) coatings. At present, the commercially-available FR coatings are polysiloxane-based materials, but fluoropolymer coatings are also in use [1]. Because of the low surface energy, low modulus and low surface roughness of polysiloxane coatings, they have been found to be the most effective for providing FR characteristics [1; 56; 67; 70; 71]. However, such FR coatings are only efficient if the vessel travels at relatively high speed and even then, fouling by slimes prevails, often necessitating underwater cleaning. A comparison of vessel speeds on fowl release properties showed that barnacles were removed at 7 knots

and that 18 knots was required to remove weeds, whereas a speed of 30 knots was ineffective in removing slime films ([30] and references therein).

Numerous alternative environmentally-benign technologies are being investigated, for example biomimetic surfaces that incorporate topographic features of shark skins [40; 48] or mollusc shells [49], pulsed electrical fields [68], surface-active coatings [43; 64], coatings that incorporate chemical defense molecules from marine organisms [72], and ‘non-stick’ surfaces [63; 73]. An alternative approach to generate low adhesion of fouling organisms is to incorporate enzymes into coatings. Interest in the potential of enzymes as AF agents has been active for the past 20 years and is well represented in the patent literature [22]. Enzymes are generally considered to be environmentally benign, as their proteinaceous nature would lead to rapid biological degradation in the marine environment. Strategies for the use of enzymes in AF technologies are varied, and may be classified as either ‘indirect’ where the enzyme liberates a secondary AF product using a substrate from the environment or from within the formulation, or ‘direct’ where the enzyme acts as either the primary AF agent or directly degrades the adhesive of the fouling organism [2; 22]. Nature is a source of instructive examples about the antifouling effect of enzymes: pilot whales were shown to constantly secrete hydrolytic enzymes that may help maintaining their outer surface clean by hydrolyzing adhesive glycoconjugates of early settling biofouling organisms [74]. Furthermore, reports on the use of antifouling compounds produced by bacteria (mostly enzymes) [30; 75] or on the direct incorporation of live bacterial cells into paints and hydrogels certainly widen opportunities to exploit natural antifouling strategies in industrial and naval applications [76; 77]. A legislative concern remains, however, about whether enzymes should be considered as biocides (*e.g.* cell wall degrading enzymes) or not (*e.g.* adhesive degrading enzymes) in view of their effect onto marine life viability [22].

3.2.1 Enzymes as antifouling agents

In a recent work, Kristensen *et al.* 2008 [2] review possible modes-of-action of enzymes proposing that enzymes could a) attack the adhesives produced by settling organisms, b) degrade biofilm matrix of proliferating settled organism, c) catalyze the release of AF compounds from surfaces, and d) obstruct intercellular communication during colonization or proliferation (*e.g.* by affecting *quorum*-sensing). The effectiveness of enzymatic preparations against biofilm formation associated with pathogenic bacteria [78] has already been shown, as well as against dental biofilms [79], industrial biofilms [80; 81], and marine bacteria ([25] and references therein). In a laboratory trial with several enzymes (proteases, lipases, glycosidases) used in solution, Leroy *et al.* 2008 [25] found that Savinase® (subtilisin) was the best at preventing adhesion and facilitating removal of *Pseudoalteromonas* sp. D41 bacterial cells onto/from polystyrene surfaces. The effectiveness of Savinase® was attributed to the high protein content of the secreted EPS and of the external cell layer of *Pseudoalteromonas* sp. Furthermore, the proteolytic enzymes pronase, trypsin, and chymotrypsin were shown to inhibit attachment of *Vibrio proteolytica* bacteria to the hydrophobic substratum polystyrene by > 97 %. The same enzyme treatments had no effect on attachment to hydrophilic substrata such as glass or tissue culture dishes, though [26]. When evaluating the effects of proteases onto diatom adhesives, Dugdale *et al.* 2005 [12] found that the adhesive pads produced by the diatom *T. undulatum* (a species secreting EPS with a fingerprint of modular proteins) were affected by treatment with proteases.

In trial assays with a wide spectrum of enzymes, Pettitt *et al.* 2004 [23] demonstrated the efficacy of commercial proteolytic enzymes in preventing settlement of barnacle *Balanus amphitrite* cyprids, as well as their effects on the attachment of *Navicula perminuta* diatoms and *Ulva linza* algal spores. Serine proteases (specially Alcalase®) had the broadest AF and FR potential towards all tested organisms over the experimental time frame. However, the adhesive of *Ulva linza* and the juvenile cement of *Balanus amphitrite* became progressively

less sensitive to hydrolysis by the proteases as they cured. In line with Pettitt's work, Aldred *et al.* 2008 [24] demonstrated that the mode-of-action of Alcalase® in preventing the settlement of cyprids was to degrade the proteinaceous temporary adhesive used by cyprids during exploration of the surface (glass) rather than deterring them from settling. The degradation of footprints was observed *via* AFM: footprints disappeared entirely within 30 min of exposure to the enzyme. Conversely, as observed by Pettitt *et al.* 2004 [23], cyprid permanent cement became resistant to attack by Alcalase within 15 h of expression.

In addition, Dobretsov *et al.* 2007 [28] investigated the effect of soluble proteases (commercial and produced by marine bacteria) on attachment of larvae of the bryozoan *Bugula neritina* on polystyrene plates, and found settlement inhibition to occur. When incorporating one protease produced by a bacterial isolate into a water-soluble paint, settlement inhibition of the barnacle *Balanus amphitrite* was also observed. In other studies with immobilized enzymes, Y. Kim *et al.* 2001 [27] incorporated proteases (pronase) onto polydimethylsiloxane films and into paints and demonstrated a decrease in protein binding with increasing the enzymatic activity of the coating. Similarly, Subtilisin A immobilized onto single wall carbon nanotubes and incorporated into polymethylmethacrylate films was shown to reduce the adsorption of human serum albumin and fibrinogen [82].

As exemplified above, it is clear that enzymes constitute an open avenue of investigation in AF research and that they may prove to be highly effective if technologies can be developed that can effectively exploit their action. It would be hoped that an active surface would prevent attachment of larvae/spores before the adult stage is reached through deterrence or interference with the temporary attachment mechanism of the organism [22]. Major concerns of enzyme-containing coatings are the incorporation of enzymes in the paint matrix, their compatibility with other paint components (like additives or surfactants), and adequate enzyme activity and stability in the very demanding conditions offered by the oceans' waters (*i.e.* pH, temperature, salinity).

3.3 Enzymes

3.3.1 General properties

Enzymes constitute a large group of proteins of distinguishable properties due to their capability to catalyze chemical reactions. Practically all of the numerous and complex biochemical reactions that take place in animals, plants, and microorganisms are regulated by enzymes [83]. As proteins, enzymes differ from carbohydrates and lipids in virtue of the presence of higher fractions of nitrogen in their structure, usually ranging from 15 % to 20 %.

Proteins (hence, enzymes) are polymers of the bifunctional monomers called amino acids. The resulting link between the carboxylic acid group of an amino acid and the amine group of another is an amide link (or peptide bond; NH – CO). Since water is released in this reaction, peptide bonds are inherently susceptible to cleavage by water (hydrolysis) in a reverse reaction.

As catalysts of chemical reactions, enzymes can speed up the reaction rate by $10^6 - 10^{12}$ times (see Carter and Wells 1988 for examples [84]), without (in addition) being altered or consumed at the end of the process. Enzymes work by lowering the ΔG of a reaction (*i.e.* the Gibbs energy barrier or activation energy), hence accelerating the formation/breakage of covalent bonds [85]. The reaction between enzymes and their ligands (called substrates) requires the intimate participation of some amino acid residues within the backbone of the enzyme molecule; the binding between the enzyme and its substrate occurring in a ‘groove’ or ‘pocket’ (the so-called active site of the enzyme) localized in the outer periphery of the enzyme molecule (Figure 3.6).

A measure of the efficacy of enzymes to bind to their substrate molecules is given by the enzyme activity. The activity of enzymes is defined as the rate of the enzymatic conversion reaction of the substrate and it is usually expressed as moles of substrate converted per unit time. The catalytic activity of enzymes can be determined by measuring either the formation of products or the disappearance of the substrate. Finding the adequate conditions to appropriately monitor the

enzyme activity requires the selection of a ‘complementary’ substrate and the optimization of the buffer, buffer pH (enzymes work in a narrow range of pH, outside of which denaturation, *i.e.* inactivation, occurs) and substrate concentration [86].

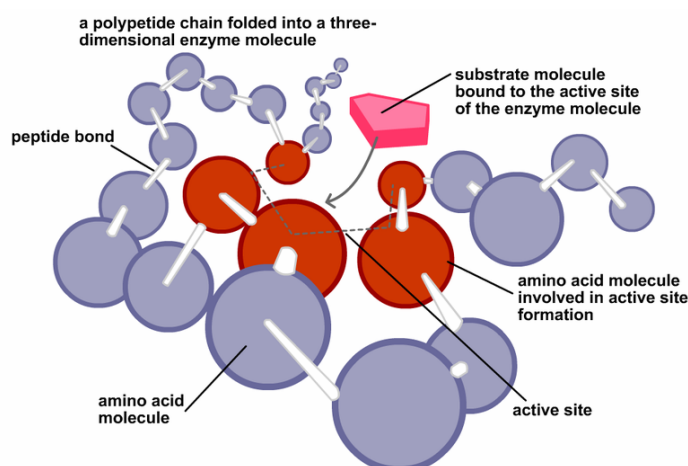


Fig. 3.6. Schematic depiction of the enzyme molecular structure with indication of the active site ‘pocket’ (in red color), whose shape illustrates the structural complementarity between the enzyme active site and the substrate molecule required to operate the reaction.

In addition to their activity, a characteristic feature of enzymes is their substrate-specificity: enzymes act on specific molecules and on particular types of chemical bond or functional groups to produce specific reactions. To bind with a specific substrate molecule, enzymes need to undergo slight conformational changes so as to provide a binding site that is complementary to the steric and electronic features of the substrate (Figure 3.7). The idea of the structural complementarity between the enzyme active site and the substrate molecule was first formulated by Fisher [87] through the so-called “lock and key model”. Shortly after Fisher’s formulation, the “induced-fit theory” came into scene to expand the lock and key model by considering that the enzyme segments involved in substrate binding are not rigid (as envisioned by Fisher) but adapt their local conformation to best fit the substrate molecule. A further improvement of the theories describing enzyme-substrate interactions proposed the complementarity between enzyme binding site and substrate ‘transition state structure’ rather than its ground

state [88]. On this understanding, much of the substrate specificity of enzymes appears to reside in transition state interactions with the active site.

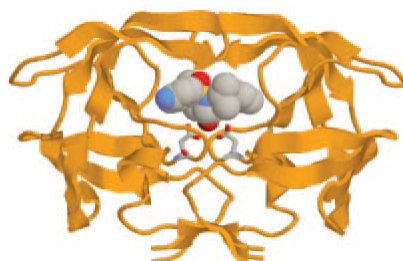


Fig. 3.7. Crystal structure of HIV protease (in yellow/orange color) with the substrate amprenavir bound to the complementary active site. The substrate is shown with carbon atoms in grey, oxygen in red, nitrogen in blue, and sulfur in yellow (Smyth 2003 [89]).

Well represented in the literature is the research dedicated to unveil the kinetic mechanisms behind the chemical conversion of substrates by enzymes and to explain the role of each active site residue onto it [90–94].

In as much as it concerns this study, the description of the relevant aspects of enzymes will be focused on the enzyme group of proteases and, in particular, on the group of subtilisin-like proteases to which the enzyme employed in this work (Subtilisin A) belongs.

3.3.2 Proteases and the subtilisin-like group of proteases

Proteases, also known as proteinases, peptidases or proteolytic enzymes, are the largest group of enzymes. Proteases belong to the class of enzymes known as hydrolases, which catalyze the reaction of hydrolysis of various bonds with the participation of a water molecule. Proteases are divided into six sub-groups: serine, threonine, cysteine, aspartate, and glutamic acid proteases, plus metalloproteases [95]. Unlike other groups of enzymes possessing high specificity, proteases are characterized by their capability to react with a wide spectrum of proteins. As they offer a broader cleavage specificity and are themselves also proteins, proteases are particularly susceptible to autolysis (*i.e.*

self-digestion), yielding multiple (intermediate) active forms and/or inactive degradation products [96; 97].

Proteases occur naturally in all organisms. These enzymes are involved in a multitude of physiological reactions from simple digestion of food proteins to highly-regulated cascades (*e.g.* the blood-clotting cascade, the complement system, apoptosis pathways, and breakdown and rebuilding of the extracellular matrix) [98 and other contributions herein].

Apart from their natural substrates, a vast range of synthetic substrates for proteases has been engineered [99; 84]. Most of the synthetic peptide substrates for proteinase activity assays are composed of a small peptide portion located on the amino-terminal side of the bond to be cleaved, and a leaving group that can be measured either directly or indirectly. Various techniques allow following the release of the leaving product, like photometry [100; 101], fluorimetry (including fluorescence resonance energy transfer) [102–105], electrochemical cells [106], radioactivity [107; 108], and other methods [109; 110].

Serine proteases are a sub-group among proteases present in virtually all organisms and functioning both inside and outside the cell. Serine proteases exist as two families: ‘the trypsin-like’ and the ‘subtilisin-like’, that have independently evolved a similar catalytic device characterized by the serine, histidine, aspartate triad, an oxyanion binding site, and possible other determinants that stabilize the transition state [84].

The subtilisin-like family of serine proteases (or simply subtilisins) is composed of proteases secreted by several strains of *Bacillus subtilis*, of which Subtilisin Carlsberg (or Subtilisin A) was the first to be isolated [111]. Since the discovery of the subtilisins, it has become evident that these enzymes manifest a broad specificity as proteases: during the purification of Subtilisin A, proteinase activity was observed on casein, hemoglobin, ovalbumin, and gelatin [112]. When tested with synthetic substrates, all the subtilisins showed a markedly higher activity on the esters of aromatic (included phenylalanine) amino acids than on those of aliphatic ones [99]. The rate limiting step of the catalytic reaction for subtilisins is acylation for amide bond hydrolysis and deacylation for ester

hydrolysis [99] (Figure 3.8). Subtilisins show a good stability in the pH range 7 – 10 [113; 114], possess two binding sites for calcium ions that stabilize their structure [100; 115], and contain no cysteine residue.

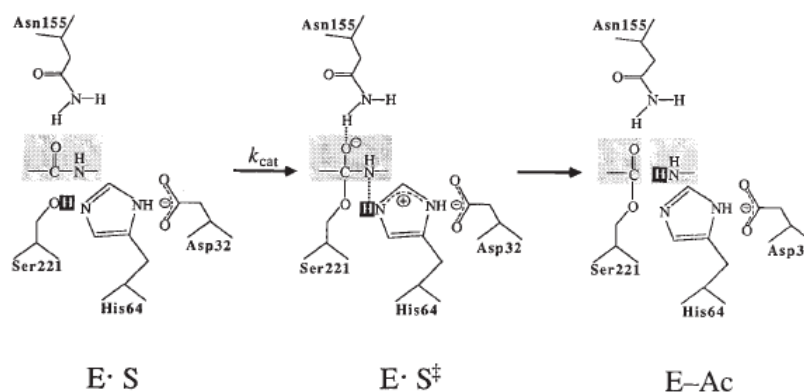


Fig. 3.8. Hydrolysis of peptide bonds by subtilisins. The scheme shows the rate limiting acylation step in subtilisins. ES = enzyme-substrate complex; ES^\ddagger = transition state complex ;

E-Ac = acyl-enzyme intermediate. From ES to ES^\ddagger , the proton on Ser221 (darkly shaded) is transferred to His64, thus permitting nucleophilic attack on the scissile peptide bond. The proton is then transferred to the amine leaving group to generate the E-Ac intermediate. Asp32 is believed to position the correct tautomer of His64 for catalysis in the ES complex and stabilize the protonated form of His64 in the ES^\ddagger complex. Some of the hydrogen bonds that form the ES^\ddagger complex are shown in dotted lines. In deacylation, these steps are reversed and water (as a nucleophile) replaces the amine leaving group (Carter and Wells 1988 [84]).

As for other enzymes, the specificity of subtilisins is largely determined by the local environment of amino acids directly contacting the substrate. Upon substrate binding, the binding site of subtilisins undergoes an induced-fit movement [116], whereas the rest of the backbone remains very rigid, with only a limited number of residues within the protein being involved in local mobility [117]. Several reports have demonstrated that modifications of amino acids within the catalytic triad of subtilisins by site-directed mutagenesis greatly reduce the turnover rate of the enzyme, and that the residues in the catalytic triad function in a strongly synergistic fashion [84; 118].

3.3.3 Subtilisin A

Subtilisin A (or Subtilisin Carlsberg; EC 3.4.21.62; peptidase S8 family), the proteolytic enzyme employed throughout this work, is a well-studied serine protease with high specificity to catalyze the hydrolysis reaction of proteins in aqueous media (see Rawlings and Barrett 1994 [119] for a review). The extra-cellular alkaline protease is produced by *Bacillus licheniformis*, has an average molecular weight of 27,280 Da, and 274 amino acids [99].

The complete amino acid sequence of the enzyme was first elucidated by Smith *et al*, 1966 [120]. During the purification of this enzyme, Güntelberg and Ottesen 1954 [112] reported that Subtilisin Carlsberg has an isoelectric point of 9.4 and a typical protein UV spectra. Subtilisin A was also found to be stabilized by Ca²⁺ ions and other salts [99], as for other subtilisins. The catalytic triad of this enzyme is composed of serine, histidine and aspartic acid residues at positions 221, 64, and 32, respectively [120; 121], with asparagine being important to form the oxyanion hole required during the catalytic process [95], as shown in Figure 3.8.

An unusual feature of the conformation of Subtilisin A is the high degree to which backbone chain segments tend to lie parallel to one another. Except for one of them, all the helical segments are approximately parallel, within $\pm 15^\circ$ to a common direction [122] (Figure 3.9 A). Subtilisin A has a preference for a large uncharged residue in P1 [114], average diameter of 4.5 nm [123] and contains nine surface-exposed lysine residues [124] (Figure 3.9 B). Lysine residues can participate in reactions with carboxylic acid, active ester, epoxy, and aldehyde functionalities of the binding surface [125] and are the most likely employed residues for covalent immobilization of the enzyme Subtilisin Carlsberg to the maleic anhydride copolymer layers used in this study.

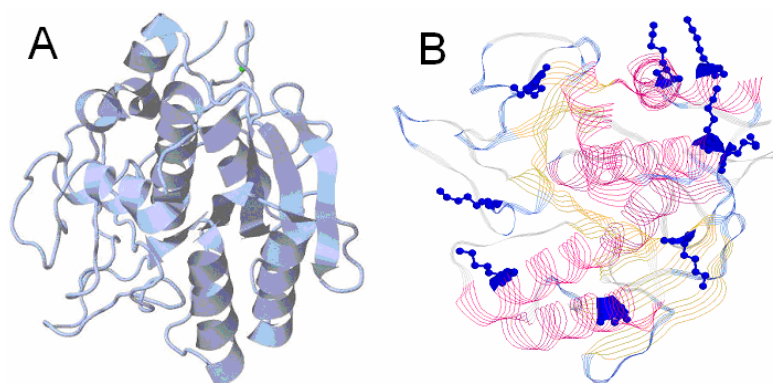


Fig. 3.9. Depiction of the molecular structure of Subtilisin A showing (A) the parallel alignment of molecular helices (graphic tool: Jmol v.11.6, Sun Microsystems Inc.), and (B) the surface location of lysine residues (graphic tool: RasMol Molecular Graphics v. 2.6, R. Sayle)

3.3.4 Applications of enzymes

The distinct catalytic properties of enzymes (*i.e.* high activity, selectivity, and specificity) have been exploited since the beginning of civilization in applications as varied as bread leavening, beer brewing or cheese ripening. More recently, enzymes became useful agents to sense blood sugar levels (glucose oxidase), in the determination of protein sequences (proteases) [126; 127], in protein biochips [125], and others. When utilized in biosensors, enzymes allow monitoring the levels of hormones, antigens, nerve gases, as well as the quality of air or water samples.

The ever expanding role of enzymes in industry and technology has been largely the result of an evolving understanding of protein function and structure. The wide use of enzymes for the fabrication of laundry detergents (proteases), in food processing (as for the clarification of juices or the development of flavor in cheeses) [99], bioreactors, and at the pharmaceutical industry highlights the valuable role and extent of application of enzymes at the industrial level.

Contrary to the non-biodegradability of a vast number of industrially-employed substances, enzymes provide an environmentally-friendly alternative in large-scale processes as they are biodegradable and not associated with the production of hazardous by-products or secondary waste. However, the

use of enzymes in industrial applications is still limited by several factors, namely their high cost, instability in aqueous and organic media, difficult recovery from the reactor effluents (due to their solubility in water), and availability in small amounts [128]. On this regard, strategies have been developed to increase the functionality and performance of enzymes in large-scale operations. Methodologies such as genetic and protein engineering [129], directed enzyme evolution [130], and protein immobilization to a support [131–134] are among the most actively investigated.

3.4 Enzyme immobilization

As referred in the previous section, the use of enzymes in large-scale operations is still limited. Enzyme immobilization constitutes an advantageous strategy to allow the economic reuse of enzymes in industrial applications, provide enhanced enzyme stability [135–137], selectivity and activity [138–140], and open the possibility to expand the intrinsic biocatalytic properties of enzymes to new fields, like biodefense [141], bioremediation [142–145] or antifouling [22; 28].

Immobilization strategies of molecules to a carrier support are various, ranging from the fundamental and well-established methods of adsorption, covalent binding, entrapment, or crosslinking [146] (Figure 3.10) to the recently-introduced combinatorial approaches, like modification of single enzyme molecules with a hybrid organic/inorganic polymer network for entrapment in nanoporous materials [147], crosslinking of covalently bound enzyme molecules to preserve native enzyme properties [148], or the incorporation of enzymes in plastic films by spin-coating and further cross-linking [149].

Despite being usually associated with simpler immobilization protocols, physical adsorption and entrapment methods frequently result in a progressive leakage of the biocatalyst from the support, causing a general decrease in performance. As a consequence, covalent immobilization strategies tend to prevail when reusability and extended lifetime are an issue.

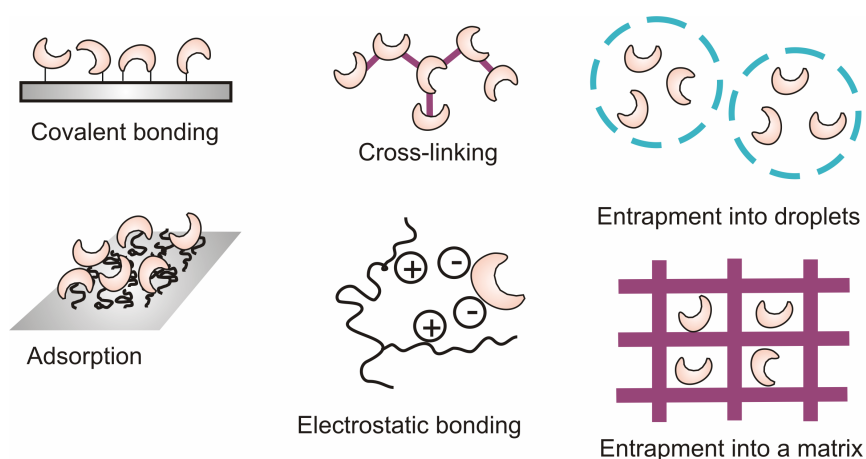


Fig. 3.10. Immobilization strategies (adapted from Trevan 1980 [146]).

Of particular importance in the field of immobilization techniques was the discovery that supports –besides functioning as carriers for enzyme immobilization– could modify intrinsic enzymatic properties (like activity, selectivity, or stability) depending on their physical and chemical characteristics [150–153]. Those findings widened the opportunities to improve the functionality of the immobilized biocatalyst through the selection of a suitable carrier.

In addition to the role of the binding chemistry, activity and stability retention of the immobilized enzyme can be synergistically enhanced by “directing” the immobilization of enzymes to the support. In site-directed immobilization schemes, all the enzyme active sites point ideally towards the solution –and therefore remain accessible for substrate binding– thanks to the introduction of a carrier-binding tag. The advantages of site-directed over random immobilization strategies (in which active sites result partially or totally blocked after binding) (Figure 3.11) are easily realized in terms of retained activity and enzyme stability when the optimized tag has been used [154; 155].

Taken together, the immobilization of enzymes to a support allows their reuse and has the potential to increase the catalytic performance of the enzyme as well as its stability, the conjunction of these properties being tunable by the selection of the appropriate binding chemistry.



Fig. 3.11. Schematic representation of random and site-directed enzyme immobilization. The active site of the protein is shown as an indentation. In random immobilization, the active site may be partially or totally blocked whilst in site-directed immobilization all active sites are fully accessible to the substrate (adapted from Wang *et al.* 2001 [155]).

3.5 Maleic anhydride copolymer thin films

Maleic anhydride (MA) copolymer films represent a versatile platform for the covalent and non-covalent immobilization of biomolecules [32; 35; 36; 156; 157]. Covalent binding of biomolecules occurs upon reaction of the anhydride moieties of the MA copolymer with diverse reactive groups [125], although the reaction with the amino group in the lysine residue of proteins is the most common example [32; 158–160]. Adsorption of molecules occurs at the hydrolyzed state of the copolymer film, protein adsorption and displacement of molecules at the surface being determined by the hydrophobicity of the copolymer (which increases with the chain length of the co-monomer) [161–164].

Different MA copolymers were obtained by variations in the comonomer unit. The physico-chemical characteristics of MA-*co*-ethylene, propylene, styrene, and octadecene polymers are available in the literature [31–34]. For the abovementioned copolymers, thin films of controllable wettability, thickness and surface roughness in the dry state [32–34], as well as of well characterized swelling behavior in solutions of various ionic strengths [31], were produced. The versatility of the gained polymeric supports for biomaterial applications was confirmed by investigations on cell adhesion and proliferation [158; 165]. Immobilization of enzymes (thrombomodulin) or of coagulation inhibitors to MA copolymer films resulted in anticoagulant surfaces [35; 37; 38].

Two MA copolymer films were used throughout this work: poly(ethylene-*alt*-maleic anhydride), PEMA, and poly(octadecene-*alt*-maleic anhydride), POMA whose most relevant properties are summarized in Table 3.1. The surface properties of MA copolymer films can be attributed to (and are determined by) the pendant aliphatic chain belonging to the comonomer unit. Hence, in the case of POMA, the long octadecene chain results in hydrophobic behavior, diminished swelling and hydrolysis of the copolymer in solution, whereas the short ethylene pendant chain in PEMA provides hydrophilic and high-swelling characteristics to these films.

Table 3.1. Survey of properties of the maleic anhydride copolymer films

	M_w ^{a)}	T dry ^{b)}	θ (H_2O) ^{c)}	γ ^{d)}	RMS ^{e)}	σ_{free} ^{f)}
POMA	30,000– 50,000	3.5 ± 1	100 ± 3	18.4 ± 1	0.32	9
PEMA	125,000	8 ± 1	70 ± 3	–	0.8	56

^{a)}: average molecular weight of the copolymers, $\text{g}\cdot\text{mol}^{-1}$; ^{b)}: thickness of the copolymer films determined by single wavelength ellipsometry in dry state (average of 4 different batches of 3 samples each), nm [166]; ^{c)}: static water contact angle of the copolymer layers, degrees (average of 2 different batches of 3 samples each) [167]; ^{d)}: surface free energy calculated from advancing contact angles, $\text{mJ}\cdot\text{m}^{-2}$ [34]; ^{e)}: RMS roughness obtained by AFM, nm [32]; ^{f)}: surface concentration of anhydride moieties on the copolymer layers determined by XPS after reaction with methionine amide hydrochloride, $\times 10^{13}\cdot\text{cm}^{-2}$ [33].

The preparation pathway of MA copolymer films onto solid supports (glass coverslips or silicon wafers) is schematically depicted in Figure 3.12. Due to the pre-treatment with hydrogen peroxide and aqueous ammonia, the inorganic surface is enriched with hydroxyl groups (see section 7.4 for details about the preparation of MA copolymer films). The reaction of the hydroxyl groups with 3-aminopropyldimethylethoxysilane in vapor phase produces a Si–O–Si bond and releases ethanol. The deposition of the MA copolymer film onto the

aminosilane-modified surface is carried out by spin-coating of organic solutions of the copolymers. The lone electron pair of the amine attacks one of the carboxyl carbons causing the anhydride bonds to be cleaved. Further conversion of the formed amide into an imide ring occurs upon heating (120°C). The resulting imide bond is more stable towards hydrolysis than the amides [156].

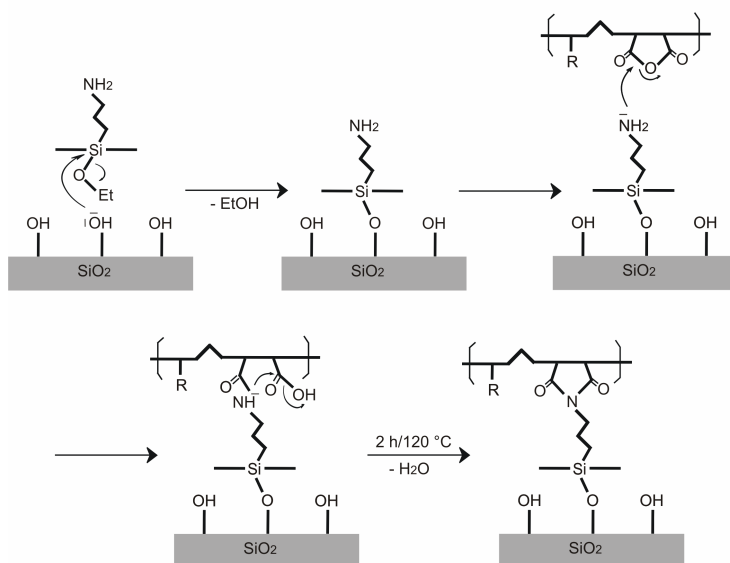


Fig. 3.12. Schematic depiction of the preparation of maleic anhydride (MA) copolymer thin films.

Derivatization of the MA copolymers

Amines ($R'-NH_2$ in Figure 3.13) comprised within many biomolecules can be attached *via* imide bonds to the MA copolymer films following the same mechanism used for MA preparation. Aminolysis of the anhydride moiety results in amide functions, which are converted into cyclic imides upon annealing (Figure 3.13). The protein used in this work, Subtilisin A, is thought to bind to the MA underlying layer by aminolysis through the lysine residues.

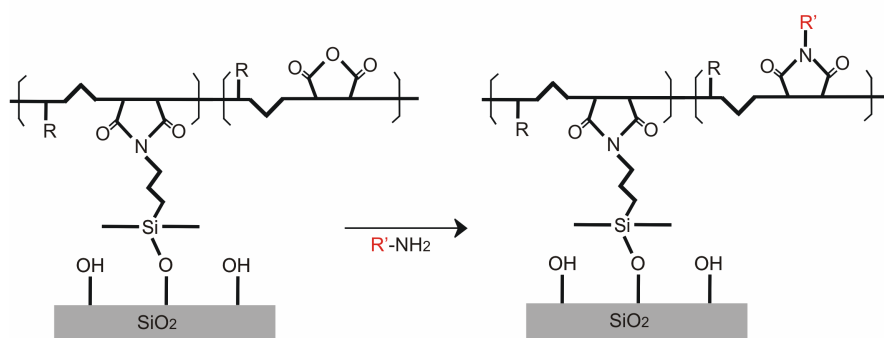


Fig. 3.13. Covalent immobilization of biomolecules to maleic anhydride copolymer films by aminolysis.

3.6 Surface analysis of the bioactive maleic anhydride layers

3.6.1 Ellipsometry

In the context of this work, single-wavelength ellipsometry measurements were performed on MA copolymer films onto which the enzyme Subtilisin A had been immobilized for the determination of layer thickness (see 7.3.1). The employed ellipsometry device utilizes a polarizer-compensator-sample-analyzer (PCSA) arrangement to measure polarization after reflection of the incident light beam. Further description will therefore focus on the relevant features of this arrangement rather than onto more general ellipsometry setups.

Ellipsometry measures the change in polarization state of light reflected (or transmitted) from the surface of a sample [168]. The polarization change is determined by the sample's properties, thus making ellipsometry a powerful technique for the investigation of fundamental physical parameters as layer thickness [169], optical constants [170], surface roughness, chemical composition and anisotropy [171; 172], or variations in the properties of layers (like swelling, adsorption [173–175] and binding [176] or desorption). In a typical PCSA setup, electromagnetic radiation, which is emitted by a light source, hits the surface at a given incident angle (ϕ_0), is reflected and finally collected in a detector after passing through an analyzer [177] (Figure 3.14).

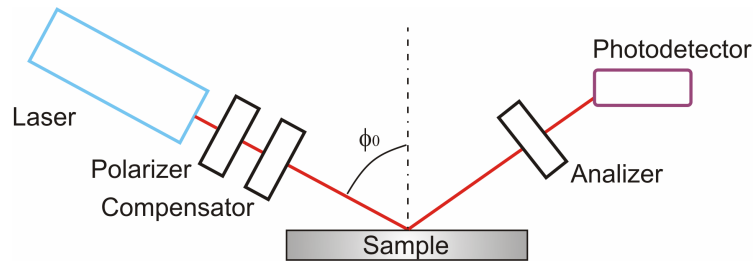


Fig. 3.14. Basic PCSA ellipsometry setup (adapted from Elwing 1998 [177]).

After the polarizer, the polarization is linear but turns elliptical after the compensator. The instrument changes the compensator angle until the reflected light from the sample is linearly polarized. The analyzer is thereafter orientated to extinguish the polarized light as detected by a photodetector (the reason why the technique is named null ellipsometry). The orientation of the polarizer P, of the compensator C and of the analyzer A allows to obtain the ellipsometric parameters of the sample (*i.e.* relative amplitude change, $\tan\psi$, and relative phase shift, Δ) as indicated in equations 3.1 and 3.2.

$$\tan(\psi)e^{i\Delta} = -\tan(A) \frac{\tan(C) - \tan(P - C)}{1 + i \tan(C) \tan(P - C)} \quad (3.1)$$

$$\text{where } \tan(\psi)e^{i\Delta} = \frac{r_p}{r_s} \quad (3.2)$$

and r_p ; r_s = amplitude of the parallel (p) and perpendicular (s) components of the beam after reflection and normalized to their initial values, respectively [168].

The polarization change depends on the layer thickness, the refractive index, n , and the surface morphology. Direct conversion of the measured ψ and Δ onto n (or onto thickness) is only possible in cases of isotropic, homogeneous and infinitely thick films. In all other cases a model of the layers must be established, which considers the optical constants and thickness parameters of all individual

optically-transparent layers. Iterative procedures (least-squares approximation) provide the best-fitting ψ and Δ values from which the optical constants and/or thickness of the sample are calculated [4; 31; 178].

In single-wavelength ellipsometry –which employs a monochromatic light source– the output is restricted to only one set of ψ and Δ values per measurement. Therefore, if the sample differs from the ideal substrate/layer/air scheme, it is hardly possible to determine n or thickness from this single pair of known parameters. Variations in the angle of incidence or in the wavelength range (spectroscopic ellipsometry) provide a means to determine n or thickness (or both) more accurately, as more data is acquired to feed the model [168; 178].

3.6.2 High performance liquid chromatography

High performance liquid chromatography (HPLC) was employed in this study to quantify the amount of immobilized enzyme onto the MA copolymer films used as carriers (see section 7.3.2). The separation of fluorescently-labeled single amino acids was carried out by gradient elution in reverse phase chromatography. Although a general description of this technique is provided below, most of the referred HPLC features allude in particular to the methodology and to the device utilized in this work.

HPLC is an analytical chromatographic separation technique in which the mobile phase is a liquid and the stationary phase is composed by an array of very small (3 – 10 μm) particles packed in a column. Separation of the analyte occurs through hydrophobic or affinity interactions between the stationary phase and the analyte flowing in the liquid phase at a high pressure. Analytes are eluted after a certain time (called retention time), which is a measure of the strength of their interaction with the stationary and mobile phases [179]. Separation of complex mixtures *via* HPLC has found applications in several fields, as for example in drug-screening [180; 181], pharmacology [182], forensic [183], identification of

extracts of marine organisms and plants [184], and in separation of polymerization products [185]. HPLC is usually combined with other techniques (*e.g.* neutron magnetic resonance [186], mass spectrometry [187; 188], solid phase extraction [182], and accelerator mass spectrometry [189]) to increase sensitivity, applicability range, and/or speed.

A standard HPLC setup consists of a column that holds chromatographic packing material, a pump, and a detector (Figure 3.15). HPLC is commonly divided in two types based on the polarity of the mobile and stationary phases: in normal phase chromatography the stationary phase is acidic and polar and the liquid phase is non-polar; in reversed phase chromatography the opposite occurs. The basis of a reverse phase chromatography (RPC) is a normal phase chromatography in which alkyl chains (usually with 18 or 8 carbon atoms) were bound to the stationary phase (generally, silica particles), turning it from polar to non-polar. RPC operates on the principle of hydrophobic interactions, which result from repulsive forces between the polar eluent, the relatively non-polar analyte, and the non-polar stationary phase. Separation occurs through the selective adsorption of the analyte to the stationary phase [179].

A further refinement of HPLC has been to vary the mobile phase composition during the analysis; this is known as gradient elution. The gradient separates the analyte as a function of its affinity for the current mobile phase composition relative to the stationary phase.

Due to their influence in the detection sensitivity and separation selectivity of HPLC, several operational parameters need to be considered, as the length and internal diameter of the column, the diameter and packing density of the particles in the stationary phase, and the pump pressure. Additionally, different detection methods can be implemented, being the absorption (UV, visible, and IR regions) and fluorescence (requiring a fluorescently-labelled analyte) detection methods the most common [179].

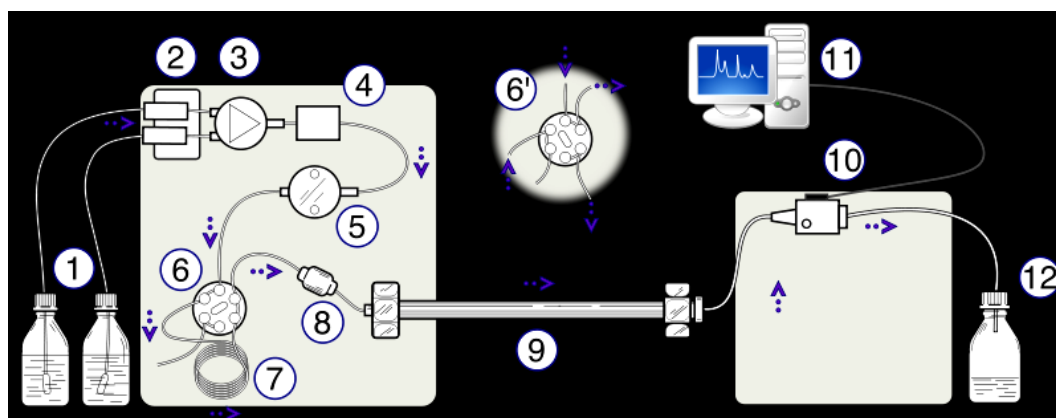


Fig. 3.15. Schematic representation of an HPLC unit. (1) Solvent reservoirs, (2) Solvent degasser, (3) Gradient valve, (4) Mixing vessel for delivery of the mobile phase, (5) High-pressure pump, (6) Switching valve in "inject position", (6') Switching valve in "load position", (7) Sample injection loop, (8) Pre-column, (9) Analytical column, (10) Detector (*i.e.* IR, UV), (11) Data acquisition, (12) Waste or fraction collector.

3.6.3 Absorbance spectroscopy

The activity of the immobilized enzyme was determined by means of absorbance spectroscopy. The conversion reaction of the substrate *N*-succinyl-Ala-Ala-Pro-Phe-pNA by the enzyme Subtilisin A yielded the chromophore phenylnitroaniline (pNa) as a product (see section 7.3.3 for details about activity determination). Due to its absorption peak at 410 nm, the presence of pNa in solution can be assessed by monitoring the absorbance of the sample at that wavelength [100; 109; 190].

Spectrophotometry works by measuring the relative amounts of radiant flux at each wavelength of the spectrum. Photons can interact with electrons in molecular orbitals and cause energy transitions between levels. Depending on the energy (or wavelength) of the photons, different processes can occur, including simple absorbance, reflection, scattering, fluorescence and luminescence (absorption of energy followed by emission at a lower energy), and photochemical reaction (absorbance with bond breakage) [191]. This explanation will focus on the simple absorbance process.

A spectrophotometer measures quantitatively the fraction of light that passes through a given solution. Light from a lamp is guided through a monochromator (or filter), then through the sample where it is partly absorbed, and finally reaches the detector (photodiode) (Figure 3.16). The obtained transmittance, T (relative percent of transmitted light) can be converted to an inverse logarithm function known as absorbance, A (or optical density, OD). Within small ranges, the Beer-Lambert law applies and allows to determine the concentration of a solute, C , from the absorbance values according to a linear relationship (Equation 3.3),

$$A = -\log_{10} T = \varepsilon C \quad (3.3)$$

where ε is the extinction coefficient of the sample [192].

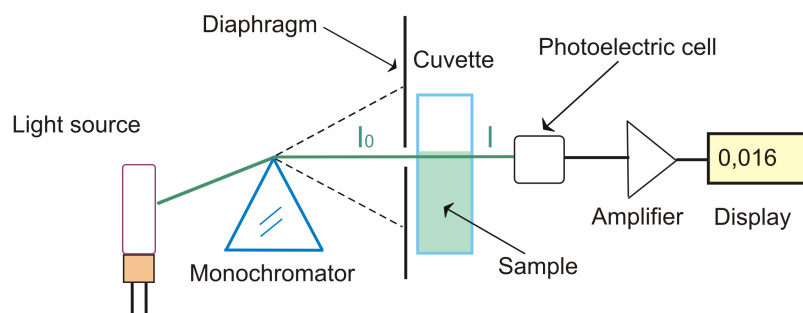


Fig. 3.16. Principle of absorbance spectroscopy.

Concerning the light source, either visible, infrared or ultraviolet can be used depending on the absorption profile of the analyte. An instrument capable of using visible light (usually with a tungsten or halogen lamp source) and UV light is known as a UV/Vis spectrophotometer. For the visible region of the spectrum, plastic cuvettes can be employed, whereas in the UV region quartz cuvettes are required.

3.6.4 Confocal laser scanning microscopy

Fluorescently-labeled Subtilisin A immobilized onto PEMA copolymer films was imaged *via* confocal laser scanning microscopy (cLSM). The fluorescence intensity of the uniformly-distributed labeled enzyme was determined onto samples of different characteristics and thereafter utilized to calculate the amount of protein bound to the surface (see section 7.3.4 for additional information).

cLSM is an optical microscopy technique based on conventional wide-field fluorescence microscopy. A key aspect in a confocal microscope is its ability to produce in-focus images of thick specimens by canceling interference intensity coming from outside this plane. Furthermore, cLSM provides the capacity for non-destructive optical sectioning of fluorescently-labeled samples as well as an enhanced image resolution based on the control of the confocal aperture (*i.e.* by elimination of higher orders of the diffraction pattern). Applications of cLSM include the imaging of biological specimens for the assessment of cell (or cell components) morphology [193; 194], characterization of heterogeneous surfaces [195], single-molecule imaging [196], protein adsorption [161; 197], and reactions at interfaces [198].

To image the specimen in the planar directions, a laser beam is deflected stepwise by a dichromatic (servo-controlled) mirror, directed towards the objective lens of the microscope, and focused on the sample (Figure 3.17). Ideally, the laser spot is focused into a small diffraction-limited volume to ensure higher image resolution. A mixture of emitted fluorescent light (of longer wavelength than the laser one) and reflected laser light from the illuminated spot is recollected by the objective lens and separated at the dichromatic mirror according to the wavelengths. Since the dichromatic mirror is transparent to longer wavelengths than the laser one, only the fluorescent light reaching the mirror effectively passes through it and is thereafter focused into a small pinhole (or confocal aperture), where out-of-focus light is suppressed. Finally, a photomultiplier detector collects the light energy coming from the focal plan and

produces an analog output signal, which is then digitalized and fed into a computer [199].

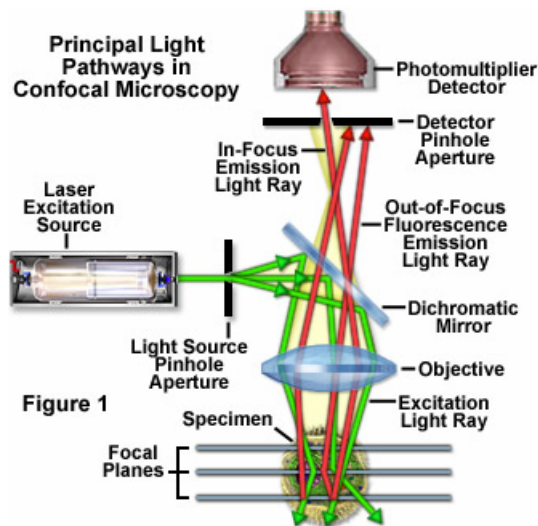


Fig. 3.17. Principle of the confocal microscope (www.microscopyu.com).

The selection of a desired laser wavelength occurs by means of excitation filters placed at the exit of the laser beam. Argon/Krypton and Helio/Neon lasers as well as high numerical aperture (NA) objectives (*e.g.* a 63x/1.4 NA) are commonly used [199].

3.6.5 Atomic force microscopy

Atomic force microscopy (AFM) was employed to investigate the surface roughness of the enzyme-containing coatings employed in the biological assays. Samples were evaluated in tapping-mode and in dry state (see section 7.3.5). The evaluation of surface-related properties, like surface roughness or phase distribution, is one of the main uses of AFM, although many others have been reported (*ex.* single-molecule imaging [200], cell adhesion studies [201], cell surface imaging [202; 203] or AFM-lithography for the patterning of nanostructures [204]).

The AFM scanning device is a probe tip (Si_3N_4 or Si) located at the end of a cantilever (Figure 3.18). When the tip interacts with the surface, small forces (usually less than 10^{-9} N) result and cause a deflection in the cantilever. This deflection, Δx , is proportional to the resulting forces, F , according to the Hooke's law (Equation 3.4), where k is the spring constant of the cantilever [205].

$$F = -k\Delta x \quad (3.4)$$

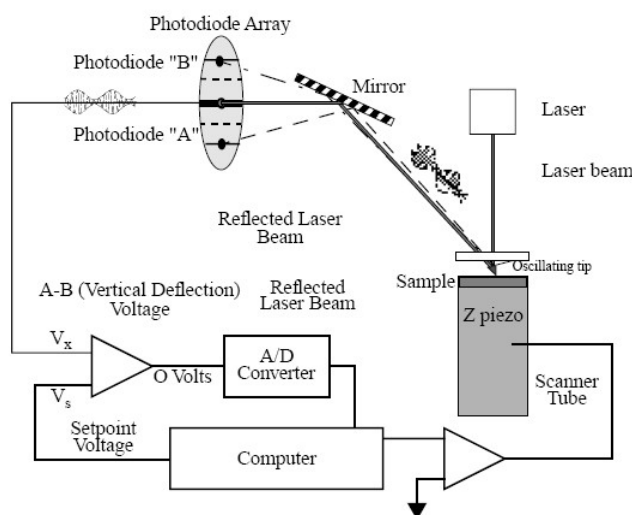


Fig. 3.18. Tapping mode AFM setup (BioScope™ instruction manual).

Different detection systems can monitor the cantilever displacement (*e.g.* tunneling current, interferometry and capacitance) but the optical detection is the most widely employed. In optical methods, a laser beam is reflected from the mirrored surface on the back side of the cantilever onto a position-sensitive photodetector. Feedback mechanisms from the photodetector enable the tip to maintain either a constant force (to obtain height information) or constant height (to obtain force information) above the sample [205].

The primary modes of operation of AFM are contact mode and tapping mode. In contact mode, the force between the tip and the surface is kept constant during scanning by maintaining a constant deflection of the cantilever. This

constant deflection results from the adjustment of the samples' height through a piezoelectric positioning element. The eventual damage of the surface, the tip, or the cantilever which may arise in contact mode makes the tapping mode preferable (especially in the case of surfaces of low elastic modulus and/or surface-bound compounds that may be displaced by or adsorbed onto the tip). In tapping mode, the cantilever is externally oscillated at or close to its fundamental resonance frequency or a harmonic. Changes in the oscillation amplitude or phase provide information about the sample's height distribution *via* software-assisted analysis of the piezo signal [205].

3.6.6 Surface wettability

In this study, sessile drop water contact angle measurements were carried out to determine the surface wettability of bioactive enzyme-containing coatings.

The contact angle, θ , is the angle at which a liquid/vapor interface meets a solid surface (Figure 3.19). The contact angle is specific for any given system, accounts for the properties of the solid surface (like roughness, homogeneity, stability), and is exploited as a measure of the surface wettability [206; 207].

In the thermodynamic equilibrium, the surface energies (σ and γ) of the solid (s), liquid (l), and vapor (v) phases must satisfy the Young's equation:

$$\sigma_s = \gamma_{sl} + \sigma_l \cos(\theta) \quad (3.5)$$

The Young equation assumes a perfectly flat, homogeneous and stable surface. As those conditions are hardly met in real situations, several alternative models were proposed to determine the surface energy of solids from contact angle data. The most known ones are those of Zisman, Fowkes, Owens-Wendt-Rabel-Kaelble and Oss-Chaudhury-Good [208–210], although the validity of the models is still a very debatable issue [211–213].

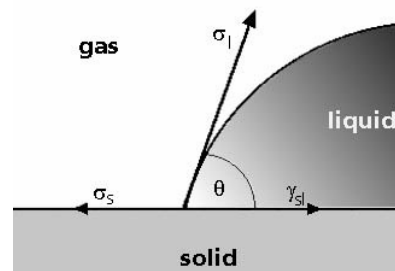


Fig. 3.19. Contact angle formation on a solid surface (www.kruss.info).

Contact angles can be measured by employing static or dynamic drops. In static contact angle measurements, a drop of liquid is produced on the surface, which is supposed to keep its volume constant during the measurement. Various interactions at the boundary surface can cause the contact angle to change considerably with time, thus introducing a source of error. In that case, dynamic contact angle measurements are preferred.

The shape of the deposited drop at the equilibrium position can be determined by diverse fitting methods. The tangent, circle, and Young-Laplace fitting methods are commonly employed. In this work, the CCD (charge-coupled device)-recorded image of a sessile drop was fitted by a general conic section equation (*i.e.* tangent method).

3.7 Biofouling quantification

Cell number

The quantification of settled cells of *Navicula perminuta* diatoms and of zoospores of the alga *Ulva linza* was performed by epifluorescence microscopy based in the autofluorescence of chlorophyll A in the chloroplast of zoospores and cells. The optical principle of epifluorescence microscopy is the same underlying principle of confocal laser scanning microscopy (see section 3.6.4 for details) but without the use of a confocal pinhole and of other sophisticated mechanisms, like

the servo-controlled deflection of the incident light during scanning of the sample. On the other hand, the enumeration of cyprid larvae of *Balanus amphitrite* either in the exploratory phase or after settlement was carried out by optical microscopy, whose mode of operation can be found in any elementary book.

Adhesion strength

The adhesion strength of the marine organisms evaluated in this study was assessed by considering the percentage of settled organisms being removed from the surface at a given impact pressure or shear stress. Forces normal (*Ulva* zoospores) and parallel (*Navicula* diatom cells) to the surface were applied by a modified water jet (WJ) apparatus [214] and a turbulent flow channel (FC) machine [215], respectively (see section 7.3.8 for details).

The semi-automated WJ apparatus provided a normal pressure as the water coming from a nozzle impinged on a relatively small spot on the surface (Figure 3.20). Computer-controlled movements of the sample holder allow to expose the mid-region of each sample to the water jet pressure. As described in Swain and Schultz 1996 [216], the applied water pressure to the surface can be obtained from the settings of the compressed air regulator by means of a calibration curve.

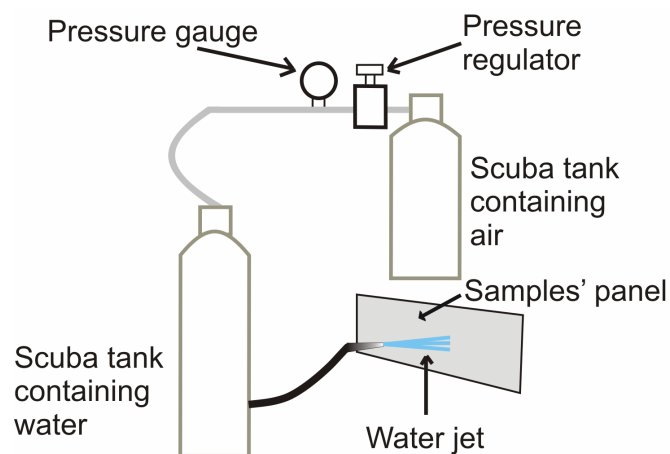


Fig. 3.20. Schematic view of the water jet apparatus (adapted from Swain and Schultz 1996 [216]).

The distribution of the water pressure on the surface decreases with the radius from the center of the impinged spot and becomes negligible at a radial distance of about 20 % of the distance from the nozzle to the surface [214]. In this impingement region, the maximum shear stress resulting from the applied pressure can be calculated as [214]:

$$\tau_{\max} = \frac{0.32\left(\frac{1}{2}\rho v_{jet}^2\right)}{\left(\frac{H}{d}\right)^2} \approx \frac{0.32(p_{jet})}{\left(\frac{H}{d}\right)^2} \quad (3.6)$$

where τ_{\max} = maximum wall shear stress, ρ = density of fluid (water), v_{jet} = mean velocity of jet at nozzle exit, H = distance from nozzle exit to surface, d = diameter of nozzle, and p_{jet} = the jet impact pressure. τ_{\max} constitutes a good approximation to the detachment forces experienced by the settled organisms whenever removal mechanisms based on shear (rather than on compressive/tensile) failure are dominant.

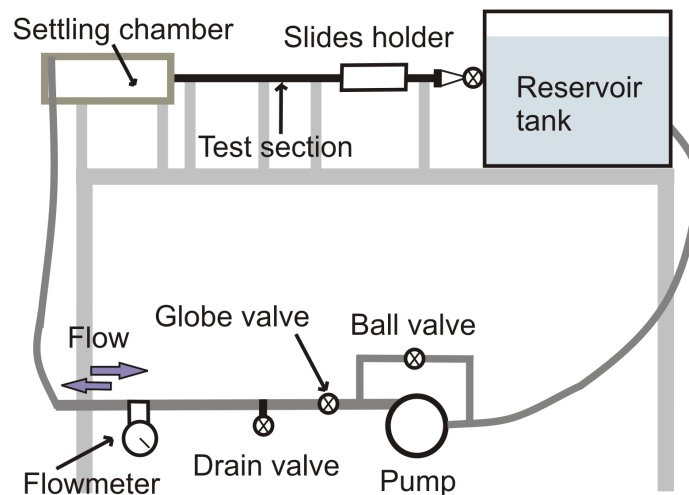


Fig. 3.21. Illustrative depiction of the turbulent flow channel device (adapted from Schultz *et al.* 2000 [215]).

The FC machine (Figure 3.21). was designed to measure the adhesion strength of microfouling organisms (algal spores and diatoms) in a rapid and repeatable manner at a laboratory scale. The apparatus is capable of producing a fully-developed turbulent flow and applies a constant wall shear stress to the surfaces under scrutiny [215]. The FC is composed by a pump used to deliver the flow in the water channel, two valves controlling the flow rate, a flowmeter, a settling chamber placed upstream of the test area, the test section containing the slide holder, and a discharge tank (Figure 3.21). The settling chamber is employed to improve flow uniformity and to lower the background turbulence in the test section [215]. The final wall shear stress applied in the sample section can be determined by using a calibration curve relating flow rate (the adjustable parameter through the pump valves) to wall shear stress.

Chapter 4

Results and Discussion

This chapter contains information which has already been published (see references [166] and [167]) together with complementary results and unpublished data (*i.e.* assays with cyprids of *Balanus amphitrite*; manuscript in preparation).

4.1 Immobilized enzyme layer

The protease Subtilisin A has nine [120; 124] typically surface-exposed Lysine residues, which are the most likely utilized reactive groups towards the anhydride moieties of the maleic anhydride copolymer films [125]. In this work, enzyme layers of controllable and distinguishable properties were produced by exposure of the MA copolymer films to variable concentration of the enzyme in solution (from 0.5 to 30 mg.ml⁻¹). Figure 4.1 schematically depicts the layered structure of the MA copolymer support and the posterior covalent binding of the enzyme to it. The physico-chemical characteristics of the immobilized enzyme layer onto the two selected MA copolymer films, PEMA and POMA, were thoroughly inspected; the layer thickness, surface concentration, and catalytic activity of the bioactive layers immobilized onto both copolymer films were determined and are presented in the following subsections.

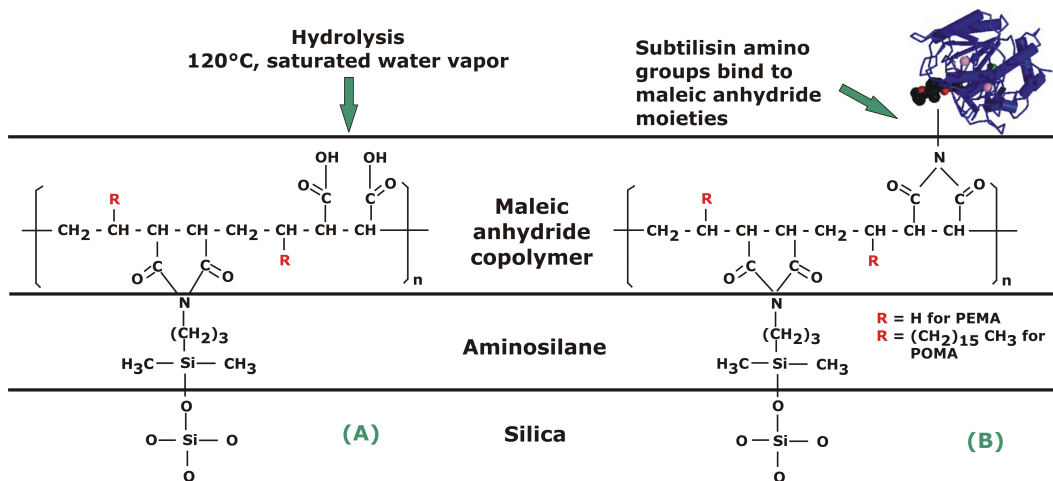


Fig. 4.1. Schematic depiction of (A) the maleic anhydride copolymer films used as substrate for the immobilization of the enzyme Subtilisin A, and (B) covalent binding of the enzyme to the maleic anhydride moieties (Tasso *et al.* 2009 [166]).

In principle, a vast majority of the immobilized enzyme molecules are thought to be covalently immobilized *via* the spontaneous aminolysis reaction occurring between the anhydride moieties of the MA copolymer films and the primary amino groups of the protein at alkaline pHs [36; 157; 158]. Nevertheless, the adsorption of enzyme molecules, which may be triggered by electrostatic interactions between the hydrolyzed copolymer layers and the solvated enzyme molecules, is a likely-to-occur process, which importance can not be underestimated. Aspects related to the eventual influences of adsorbed molecules on the investigated properties of the bioactive coatings will be further discussed in section 4.2 as part of the evaluation of the enzyme layer stability.

4.1.1 Enzyme layer thickness

The thickness of the enzyme layer immobilized onto PEMA and POMA copolymer thin films (as determined by single-wavelength ellipsometry) is represented in Figure 4.2 as a function of the enzyme concentration in solution ([Es]) utilized for immobilization.

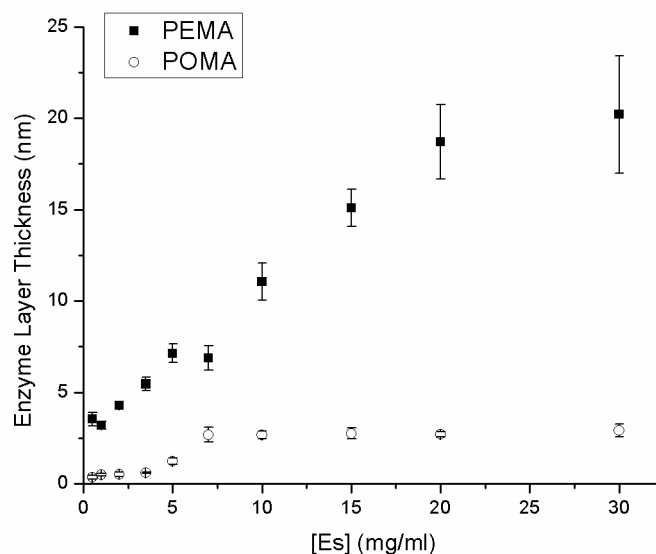


Fig. 4.2. Thickness of the enzyme layer immobilized onto PEMA and POMA copolymer films for variable concentrations of the enzyme in solution ($[Es]$) used for immobilization [166].

For the POMA-based bioactive coatings, the thickness *vs.* $[Es]$ curve showed an asymptotic behavior with a maximum enzyme layer thickness of 3 nm at $[Es] \approx 10 \text{ mg}\cdot\text{ml}^{-1}$. Due to the low-swelling of the POMA copolymer films during the immobilization process, a rather compact polymer layer is expected [31; 33] onto which the enzyme molecules would preferably spread and not interpenetrate. At saturation, the maximum thickness obtained onto POMA copolymer films (3 nm) could be associated to an enzyme monolayer when considering the enzyme has an average diameter of 4.5 nm [123].

Concerning the PEMA-based bioactive coatings, a constant thickness increase was obtained for increasing concentrations of the enzyme in solution with a probable saturation around $30 \text{ mg}\cdot\text{ml}^{-1}$. The 3D-like structure of the swollen PEMA films upon incubation in alkaline media, along with the availability of a higher density of anhydride functionalities ($56 \times 10^{13}\cdot\text{cm}^{-2}$) [33] than onto POMA films, might explain the presence of thicker enzyme layers onto PEMA copolymer films as entrapment and higher availability of anchoring points would promote retention of enzyme molecules on the surface.

4.1.2 Enzyme surface concentration

The amount of protein immobilized on the evaluated MA surfaces (or surface concentration), as quantified by AAA/HPLC and cLSM of TAMRA-labeled Subtilisin A, is presented in Figure 4.3 for the range of [Es] considered.

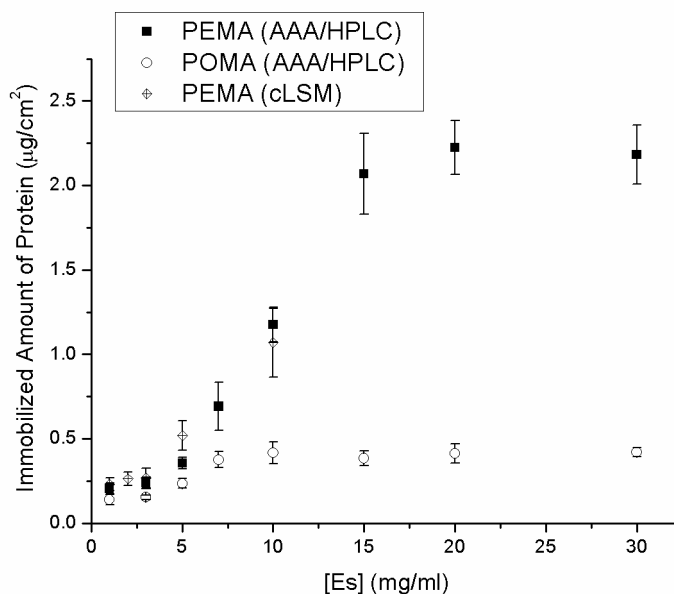


Fig. 4.3. Immobilized amount of protein onto PEMA and POMA copolymer films as a function of the enzyme concentration ([Es]) used for immobilization. Data determined by AAA/HPLC and cLSM of TAMRA-labeled Subtilisin A [166].

As for the thickness, the saturation level of the surface concentration was reached around $[Es] = 7 - 10 \text{ mg.ml}^{-1}$ for the POMA-based bioactive coatings, and at $[Es] \approx 20 \text{ mg.ml}^{-1}$ for the PEMA-based ones. Additional AAA/HPLC analysis of PEMA bioactive layers obtained with $[Es] = 50 \text{ mg.ml}^{-1}$ confirmed that the plateau in surface concentration was reached at $[Es] = 20 \text{ mg.ml}^{-1}$ (result not shown). At saturation, the immobilized enzyme amount onto PEMA films is five times higher than onto POMA films, in agreement with the thickness difference between both surfaces (*i.e.* 5 – 6 times higher thickness onto PEMA than onto POMA at saturation).

Assuming the immobilized enzyme has a globular non-deformed conformation (diameter of 4.5 nm) [123], the saturation level onto POMA coatings ($0.4 \mu\text{g}\cdot\text{cm}^{-2}$) can be associated to a complete surface coverage by the enzyme (*i.e.* a monolayer). At low enzyme surface concentrations, the immobilized enzyme is likely to undergo conformational changes, *i.e.* to unfold and spread so as to increase the contact area between the coating and the hydrophobic moieties of the enzyme. Since the anhydride density of the POMA coatings –which will determine the number of available binding sites for the enzyme– is one order of magnitude ($9 \times 10^{13}\cdot\text{cm}^{-2}$) [33] higher than the number of molecules immobilized on the surface (6×10^{12} enzyme molecules $\cdot\text{cm}^{-2}$), multi-point attachment of the enzyme to the surface and/or residual free anhydride moieties constitute a likely case.

In the low range of surface concentrations (*i.e.* below $0.5 \mu\text{g}\cdot\text{cm}^{-2}$), the protein amount values provided by AAA/HPLC were often questionable due to the exclusion of more than three amino acids from the fitting calculation, a problem essentially related to the closeness of the measured values to the detection threshold of the technique (100 ng). Fluorescence microscopy of TAMRA-labeled Subtilisin A was then proposed as a complementary methodology for the assessment of low surface concentrations. As presented in Fig. 4.3, the quantification of the immobilized enzyme amount onto PEMA films *via* cLSM was in good agreement with the results of AAA/HPLC, confirming that low immobilized protein amounts can be determined by combining both techniques [162], *i.e.* by converting qualitative cLSM data for the low surface concentration range into quantitative data by means of reliable AAA/HPLC-determined surface concentrations.

The 3D-like structure of the swollen PEMA copolymer films permitted penetration of enzyme molecules into the layer, which translated into higher loading capacities than onto the compact POMA copolymer films. Besides that, the high amounts of immobilized protein found onto PEMA copolymer films might also result from the contribution of the high electrostatic interaction

between the strongly acidic hydrolyzed PEMA and the positively charged Subtilisin A (pI 9.4 [112]) during the immobilization process.

For both MA copolymer layers evaluated, the surface concentration and enzyme layer thickness of immobilized Subtilisin A showed a good agreement, as represented in Figure 4.4. Based of these findings, the carrier-specific features of the immobilized enzyme layer found onto PEMA and POMA copolymer films are summarized in Figure 4.5.

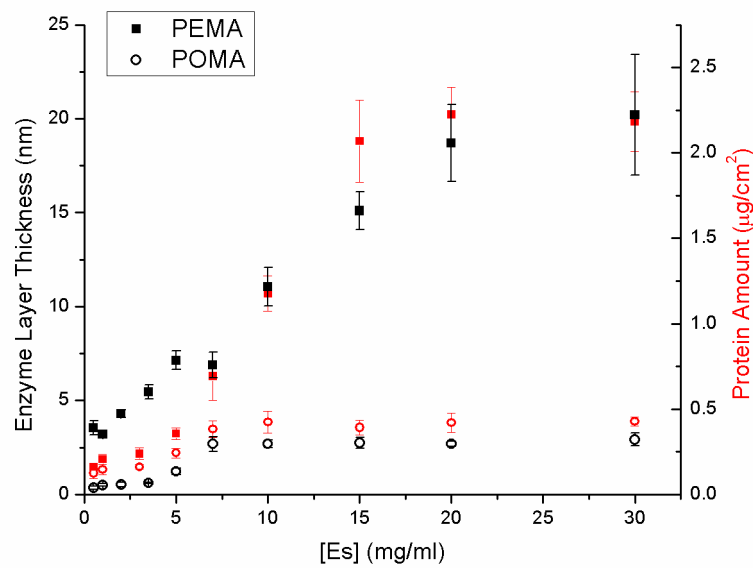


Fig. 4.4. Correspondence between enzyme layer thickness and surface concentration for Subtilisin A immobilized onto PEMA and POMA copolymer films [166].

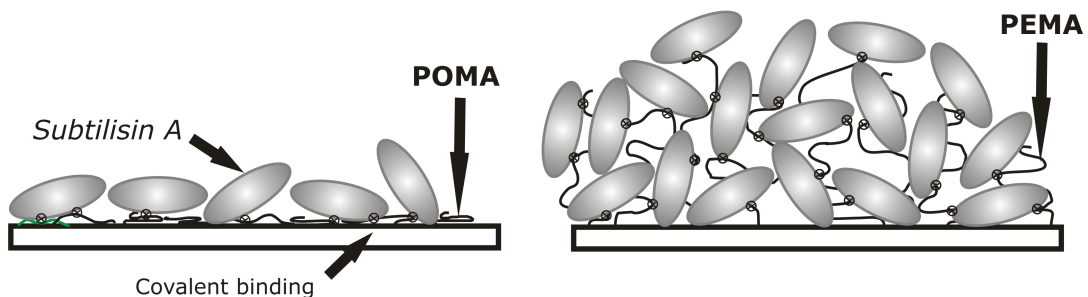


Fig. 4.5. Schematic representation of the proposed 2D and 3D structures of the bioactive POMA and PEMA copolymer layers (Tasso *et al.* 2009 [166]).

4.1.3 Enzyme activity

Initial activity

The catalytic activity of the enzyme-containing films is presented in Figure 4.6, as determined by absorbance spectroscopy (405 nm) following the cleavage of N-Suc-AAPF-pNA. The initial activity values of the bioactive layer immobilized onto POMA copolymer films reached a plateau at $[Es] \approx 10 \text{ mg.ml}^{-1}$, agreeing with the layer thickness and enzyme amount data. Since no increase in the immobilized enzyme amount occurs for $[Es] > 10 \text{ mg.ml}^{-1}$, the saturation of the initial activity in this range was predictable.

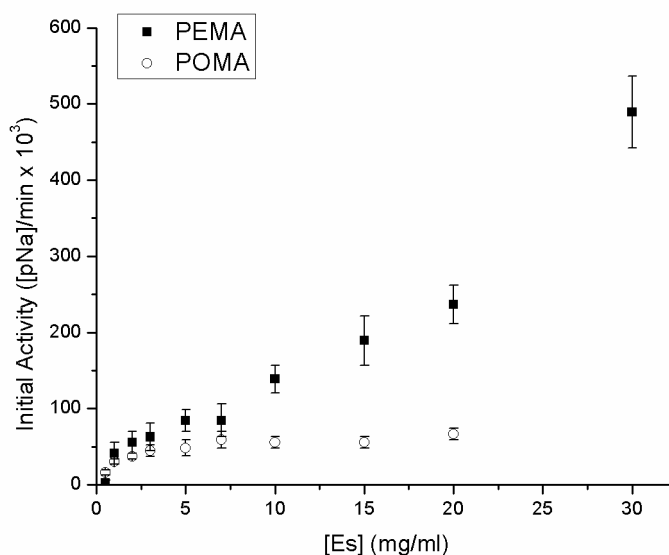


Fig. 4.6. Initial activity of the bioactive layers immobilized onto POMA and PEMA copolymer films using enzyme solutions of variable concentration ($[Es]$) for immobilization [166].

Contrarily, the enzyme-containing PEMA films exhibited a steady increase in initial activity, with a noticeable jump for coatings prepared using enzyme solution concentrations of 20 and 30 mg.ml^{-1} (Figure 4.6). This increase does not correlate with the invariant immobilized amounts (Figure 4.3) obtained for these two cases. Improved substrate accessibility –due to more suitable spatial

distribution and/or conformation of the enzyme molecules– might explain the increase in initial activity in this range. Another possible explanation is desorption of enzyme molecules from the PEMA film to the substrate solution during the activity assay. Desorption experiments (not included in this thesis) showed, however, that the amount of desorbed enzyme molecules after 3 h exposure to Milli-Q water remained within the detection limit of UV-spectroscopy at 280 nm ($< 200 \text{ ng.ml}^{-1}$).

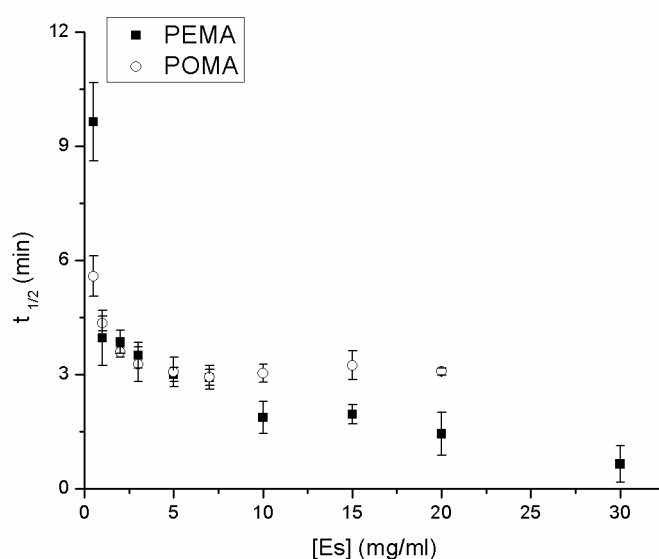


Fig. 4.7. $t_{1/2}$ (time required to consume half of the available substrate during the conversion reaction) for Subtilisin A immobilized onto POMA and PEMA films, as determined by calculations based on the fitted conversion curve.

In addition to the initial activity, the time required to consume half of the available substrate ($t_{1/2}$) was determined for the bioactive layers immobilized onto both copolymer films (Figure 4.7). The analysis of $t_{1/2}$ confirmed the initial activity results concerning the properties of the immobilized enzyme on the compared base coatings: saturation was reached at $[\text{Es}] \approx 5 \text{ mg.ml}^{-1}$ for POMA, with a $t_{1/2}$ of approx. 3 min, whereas a continuous decrease in $t_{1/2}$ was found for PEMA. Importantly, by considering the whole progress reaction curve and not

only its initial slope (as for the initial activity determination), the $t_{1/2}$ results largely supplement the initial activity data.

Specific activity

Figure 4.8 displays the specific activity (*i.e.* activity per immobilized enzyme molecule per unit area) vs. surface concentration for both enzyme-containing maleic anhydride copolymer films. In the lower surface concentration range, the catalytic turnover per molecule steeply increased with increasing surface concentration and reached a maximum at enzyme surface concentrations of about $0.2 \mu\text{g}\cdot\text{cm}^{-2}$ on both copolymer films. Interestingly, the maximum of the specific activity was reached at slightly higher enzyme surface concentrations on PEMA (considering the x-axis error bars), a result that might be attributed to the 3D characteristics and high negatively-charged surface of this polymer layer. Interpenetration and a high electrostatic interaction between the PEMA surface and segments of the enzyme molecules might reduce the degrees of freedom for those conformational changes required to convert the substrate and/or might lead to less advantageous molecular orientations than onto POMA films at similar surface concentrations. In the lower range of surface concentrations, the compact POMA layer appeared more convenient than the 3D-like PEMA films, as higher specific activities were obtained when using POMA for enzyme immobilization.

At higher surface concentrations, the obtained specific activities decreased, possibly due to limited substrate diffusion and/or restrictions in structural transitions of the enzyme within the more tightly packed bioactive layers (specially for PEMA-based bioactive layers). However, a dramatic increase in the specific activity (from $\sim 105 [\text{pNa}]\cdot\text{cm}^2\cdot\mu\text{g}^{-1}\cdot\text{min}^{-1}$ at $[\text{Es}] = 20 \text{ mg}\cdot\text{ml}^{-1}$ to $\sim 225 [\text{pNa}]\cdot\text{cm}^2\cdot\mu\text{g}^{-1}\cdot\text{min}^{-1}$ at $[\text{Es}] = 30 \text{ mg}\cdot\text{ml}^{-1}$) was observed for enzyme-containing PEMA copolymer films at the maximal surface concentration (point not included in Figure 4.8). This increase stems from the substantially higher initial activity of the PEMA bioactive layer obtained with $[\text{Es}] = 30 \text{ mg}\cdot\text{ml}^{-1}$ (Figure 4.6) compared to $[\text{Es}] = 20 \text{ mg}\cdot\text{ml}^{-1}$ at constant surface concentration.

Apparently, a more favorable distribution and/or conformation of the enzyme within the PEMA layer was feasible if enzyme immobilization was performed at accelerated transport conditions (*i.e.* using solutions of higher concentration).

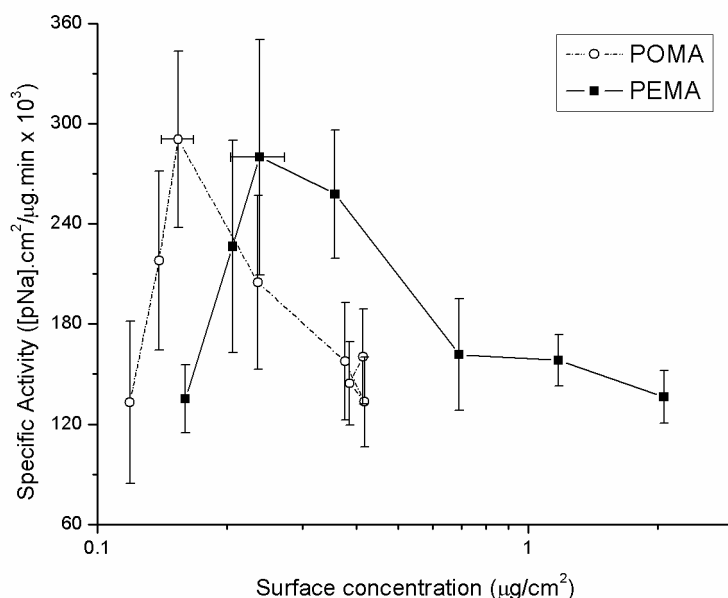


Fig. 4.8. Specific activity of Subtilisin A immobilized onto POMA and PEMA copolymer films as a function of the enzyme surface concentration (x-axis in \log_{10} scale) [166].

4.1.4 Surface morphology and wettability

The surface morphology and wettability of the bioactive coatings and controls used in the biological assays were characterized by AFM and static water contact angle measurements, respectively (Table 4.1). The assessment of the surface roughness and wettability of these coatings followed the need to narrow the space of variables affecting settlement and adhesion processes [40; 48; 50], thus emphasizing the decisive role of the graded activity in the final antifouling and fouling-release properties of the active coatings.

As a result of protein immobilization, POMA1 displayed a strong increase in hydrophilicity compared to the conditioned POMA base coating (*i.e.* 30° vs. 83°), whilst the static contact angle of PEMA1 was only slightly (10°)

higher than that of the conditioned PEMA. Interestingly, the water contact angles of all active coatings were found to oscillate around 30° and to be independent of the enzyme surface concentration and activity. The same applied to the denatured coatings, but with water contact angles around 50°. Moreover, due to protein denaturation (and exposure of the previously hidden hydrophobic segments of the molecule), denatured coatings resulted more hydrophobic than the active ones (*i.e.* 50° vs. 30°).

Table 4.1. Surface roughness and wettability of the surfaces tested in the biological assays

<i>Coating type</i>	<i>Coating label</i>	<i>[Es]</i> (<i>mg.mL⁻¹</i>) ^{a)}	<i>RMS</i> (<i>nm</i>) ^{b)}	θ_{static} (°) ^{c)}
Active coatings	POMA1	7	1.4 ± 0.2	29 ± 2
	PEMA1	3	0.6 ± 0.1	33 ± 1
	PEMA2	10	2.5 ± 0.5	34 ± 5
	PEMA3	20	2.6 ± 0.3	34 ± 3
	PEMA4	30	2.5 ± 0.2	30 ± 4
Denatured coatings	POMA1 – D	7	2.1 ± 0.3	53 ± 2
	PEMA1 – D	3	1.4 ± 0.2	47 ± 4
	PEMA2 – D	10	1 ± 0.2	56 ± 3
	PEMA3 – D	20	2.7 ± 0.3	53 ± 6
	PEMA4 – D	30	2.8 ± 0.3	49 ± 5
Conditioned base coatings	POMA	0	1.9 ± 0.2	83 ± 3
	PEMA	0	1 ± 0.4	20 ± 5

^{a)}: enzyme concentration in solution used during the immobilization process; ^{b)}: root mean square roughness (AFM); ^{c)}: static water contact angle.

The RMS roughness of all evaluated coatings (*i.e.* active, denatured, and conditioned base coatings) was in the range of 1 – 3 nm, as determined by AFM. Active and denatured coatings were characterized by similar surface roughness, independently of the enzyme surface concentration (and activity).

Based on the invariability of the surface roughness (RMS) and wettability (static contact angle) of the active coatings over the range of activities (and surface concentrations) considered, the evaluation of the biological response can be mostly restricted (and focused) to variations in only one parameter: the surface activity of the bioactive layers.

4.2 Enzyme layer stability in aqueous media

Extensive efforts were dedicated to the evaluation of the stability of the bioactive layers, essentially due to the need of ensuring the retention of enzymatic activity over the length of the biological assays. At first, the number of rinsing steps after enzyme immobilization was optimized to provide invariant surface concentrations on coatings obtained from different [Es] (AAA/HPLC measurements after 5, 8, and 10 rinsing steps with Milli-Q water; results not shown). Thereafter, the short-term desorption of enzyme molecules to the substrate solution (which could result in overestimated initial activities) was considered and found to be negligible, as mentioned in section 4.1.3 (UV-spectrometry of the aging solutions after 3 h incubation in Milli-Q water). For the long-term stability assessment, however, the bioactive coatings were exposed to Milli-Q water and to a substitute of artificial seawater (ASW*) for 6 and 24 h. The effect of the incubation treatment onto the set of bioactive coatings used in the biological assays was monitored following variations in the activity (absorbance spectroscopy) and in the surface concentration (cLSM of TAMRA-labeled Subtilisin A) of the immobilized enzyme layer. Furthermore, as the biological assays with barnacle cyprids spanned up to 48 h, the effect of a 48 h aging treatment in ASW* onto the activity of the bioactive layers was also evaluated.

As observed in Figure 4.9 (A) and (B), both incubation solutions, Milli-Q water on the first row and ASW* on the second row, resulted in similar deteriorating effects onto the monitored parameters (*i.e.* activity and surface concentration) after incubation for 6 and/or 24 h. The higher ionic strength of ASW*, when compared to Milli-Q water, could not be associated to any distinct effect, the dissimilarities between both solutions being generally unrelated. The initial activity of the evaluated samples decreased to *ca.* 40 % of the value without aging after 24 h incubation in either solution (Figure 4.9 (A)). This reduction in activity is partially due to the depletion in protein amount observed for these coatings (Figure 4.9 (B)). However, since the fraction of retained protein content on the coatings was found to be generally higher than the fraction of retained activity, denaturation processes (resulting in reduced activity at constant surface concentration) may significantly contribute to the activity loss. Protein denaturation might arise from the unfavorable pH conditions encountered during incubation (pH \sim 6.5 – 7) as Subtilisin A has an optimum pH range above 8 [112]. On the other hand, the observed decrease in surface concentration after incubation may arise from autolysis processes (mainly of molecules within the high enzyme surface concentration PEMA layers) and/or from desorption of initially-adsorbed-to-the-substrate or fragmented-after-autolysis protein molecules. On this respect, the analysis of incubation solutions after 6 h aging by absorbance spectroscopy at 280 nm revealed that the concentration of desorbed enzyme molecules is lower than 400 ng.ml^{-1} for all active coatings tested (results not shown).

As an interesting case for comparison purposes, the coatings of surface concentrations $0.24 \text{ }\mu\text{g.cm}^{-2}$ and $0.38 \text{ }\mu\text{g.cm}^{-2}$, which have similar initial activities without aging but were produced onto different copolymer substrate, were considered (see Table 4.2 for activities). For these coatings, the two distinct copolymer carriers were found to have no differential effect onto the residual activity and surface concentration after aging, indicating that the incubation in aqueous media has an overwhelming detrimental effect on the stability of the bioactive layers when compared to any effect of the copolymer carrier.

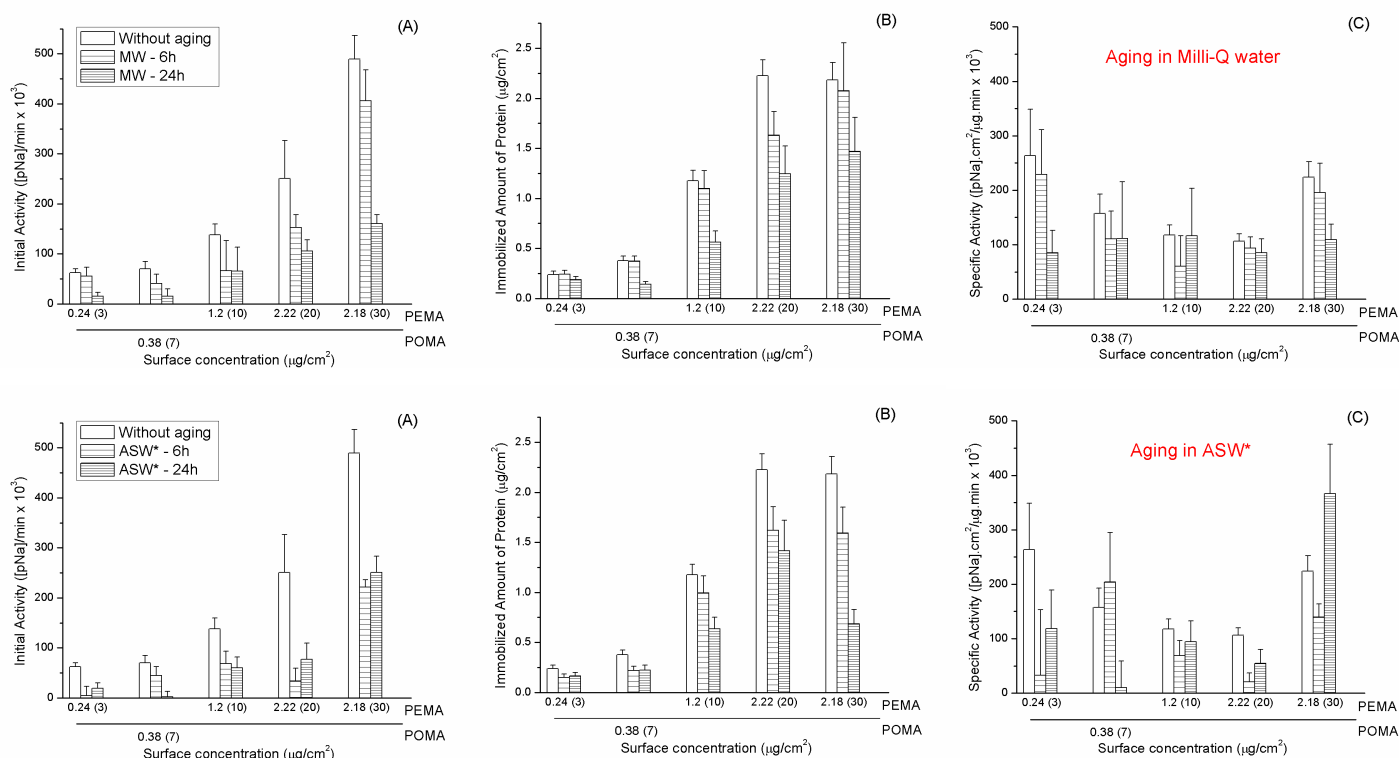


Fig. 4.9. (A) Initial activity, (B) immobilized amount of enzyme, and (C) specific activity of the bioactive coatings used in the biological assays before and after incubation in Milli-Q water (MW, first row [166]) and in ASW* (second row [167]) for 6 or 24 h. The x-axis represents the enzyme surface concentration after immobilization ($\mu\text{g}\cdot\text{cm}^{-2}$) and within brackets the enzyme concentrations in solution ($\text{mg}\cdot\text{ml}^{-1}$) used for enzyme immobilization. Legends PEMA and POMA refer to the copolymer film used for enzyme immobilization.

Upon incubation in both media, coatings with higher enzyme surface concentrations were found to be subjected to higher losses of initially-bound enzyme molecules as compared to coatings of lower surface concentrations. Autolysis processes might be of higher relevance for enzyme multilayers than for monolayers as molecules interact more strongly with their neighbors in densely-packed arrangements.

Regarding the specific activity after aging of the bioactive coatings in Milli-Q water, Figure 4.9 (C) (first row) shows that both the coating with the lowest and the highest surface concentrations exhibited a reduction in specific activity after incubation. The coatings with intermediate surface concentrations

were rather unaffected by aging in terms of the specific activity of the retained enzyme layer: the catalytic capability per enzyme molecule was conserved even when a fraction of the immobilized enzymes was lost. The same was not valid for the incubation in ASW*, where only the coating with surface concentration of $1.2 \mu\text{g}\cdot\text{cm}^{-2}$ kept its specific activity unmodified after 24 h incubation. The coating obtained with the highest concentration of enzyme in solution used during the immobilization process (*i.e.* $2.18(30) \mu\text{g}\cdot\text{cm}^{-2}$ in Figure 4.9 (C) second row) was the exception to the otherwise encountered decrease in specific activity. In this case, the substantial increase in specific activity can be mostly attributed to the lower retention of surface concentration compared to the retention of activity after incubation.

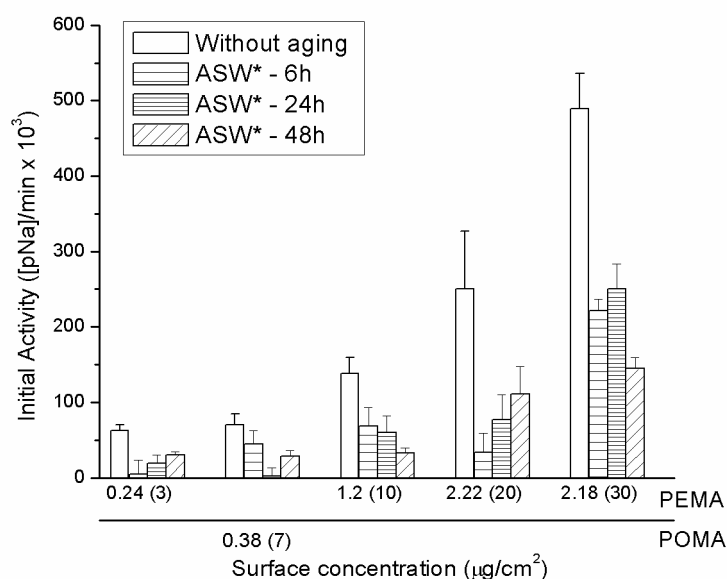


Fig. 4.10. Initial activity of the bioactive coatings used in the biological assays before and after incubation in ASW* for 6, 24 h, and 48 h. The x-axis represents the enzyme surface concentration after immobilization ($\mu\text{g}\cdot\text{cm}^{-2}$) and within brackets the enzyme concentrations in solution ($\text{mg}\cdot\text{ml}^{-1}$) used for enzyme immobilization. Legends PEMA and POMA refer to the copolymer film used for enzyme immobilization.

Incubation of the selected bioactive coatings in ASW* for 48 h (Figure 4.10) showed levels of activity retention comparable or slightly lower than those

obtained after 24 h aging. Even though the activity was lowered after incubation, the selected coatings preserved their original graded activities at the different incubation times. This is a fundamental result for the biological assays because it allows fulfilling the requirement of counting with coatings of increasing surface activity all over the length of the assay. The actual residual activities after the incubation times considered during the biological assays (*i.e.* 2.25 h for zoospores of *Ulva* and 5 h for cells of *Navicula*) were monitored *in-situ* by using additional slides. Residual activity values in ASW measured during the biological assays agreed with the trend observed in ASW*, *i.e.* no significant alteration in the gradation of the activity of the coatings was found (results not shown).

4.3 Antifouling and fouling-release potential of Subtilisin A in solution

Assays with zoospores of *Ulva linza*

Alcalase[®], a commercial preparation containing the serine protease Subtilisin A, has been shown to reduce the adhesion strength of spores of *Ulva* in a concentration-dependent manner [23]. To verify that this was also the case for pure Subtilisin A, spores were allowed to settle (attach) onto conditioned POMA and PEMA copolymer films for 45 min in the dark prior to washing and incubation in 0 (control), 8 or 50 $\mu\text{g}\cdot\text{ml}^{-1}$ Subtilisin A for 1.5 h. Settlement of *Ulva* zoospores onto the conditioned MA copolymer films was evenly distributed and not influenced by the various concentrations of Es employed: settlement onto PEMA + [Es] \approx 800 spores. mm^{-2} ; settlement onto POMA + [Es] \approx 70 spores. mm^{-2} , for [Es] = 0, 8, and 50 $\mu\text{g}\cdot\text{ml}^{-1}$. In opposition to the unaffected settlement, the adhesion strength of *Ulva* spores to the MA conditioned films was found to vary in a concentration-dependent manner, with different regimes for the two distinct copolymers (Figure 4.11). In the absence of the enzyme, the removal of spores of *Ulva* was lower from the hydrophilic conditioned PEMA surfaces

(static contact angle $20^\circ \pm 5^\circ$) than from the conditioned POMA films (static contact angle $83^\circ \pm 3^\circ$), in agreement with previous observations which showed that spores were more strongly attached to hydrophilic *cf.* hydrophobic surfaces [60]. Penetration of the secreted adhesive molecules onto the 3D-like structure of PEMA films together with the expected enhanced spreading of the adhesive onto the more hydrophilic PEMA interface [62] might explain the observed higher adhesion strength onto this coating. Under the presence of the enzyme in solution, however, removal of attached spores was more facilitated onto the hydrophilic PEMA conditioned films than onto its counterpart POMA (as indicated by the higher slope for PEMA in Figure 4.11). The ‘appealing’ character of conditioned PEMA films for *Ulva* settlement, and for stronger interactions between the adhesive molecules and the surface in the absence of enzyme, was found to turn into lower adhesion strengths than onto POMA conditioned films for $[Es] > 50 \mu\text{g}\cdot\text{ml}^{-1}$. These observations point at differential effects of the soluble enzyme onto the adhesive molecules bound to either MA conditioned surfaces.

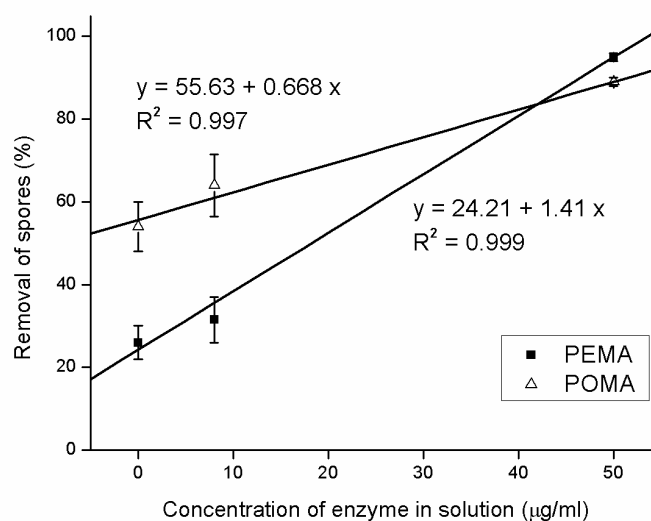


Fig. 4.11. Removal of spores of *Ulva* from conditioned POMA and PEMA films after incubation with 0 (control), 8 or $50 \mu\text{g}\cdot\text{ml}^{-1}$ Subtilisin A in ASW for 1.5 h and exposure to 60 kPa impact pressure. $N = 3$ (90 fields of view), error bars = ± 2 x standard error derived from arcsine-transformed data [167].

Assays with cells of *Navicula perminuta*

Navicula cells were allowed to settle onto conditioned MA copolymer films for 2h and thereafter exposed to 0, 8, 25, and 50 $\mu\text{g}\cdot\text{ml}^{-1}$ Subtilisin A in ASW for 3 h prior to removal by a wall shear stress of 35 Pa. Because *Navicula* cells are not selective during settlement and reach a surface only due to gravity, the settlement levels were not determined by any characteristic feature of the surfaces (settlement $\approx 450 \text{ cells}\cdot\text{mm}^{-2}$ onto both MA conditioned films at all [Es] used). As for *Ulva* spores, cells were evenly distributed on the tested surfaces and settlement was found to be unaffected by the different concentrations of Es employed. This indicates that *Ulva* spores and *Navicula* cells are not susceptible to removal by the handling steps after incubation with the different concentrations of Es when settled onto conditioned MA copolymer films.

In a similar way as for *Ulva* spores, and as already demonstrated for soluble Alcalase [23], the adhesion strength of *Navicula* cells (Figure 4.12) decreased with increasing concentrations of Subtilisin A in solution. Removal was higher onto PEMA conditioned films than onto POMA at all [Es] tested: the soluble enzyme seemed to have a more pronounced effect onto the adhesive curing and/or the interplay between the adhesive molecules and the surface when cells settled initially onto PEMA conditioned films.

Assays with cyprids of *Balanus amphitrite*

Results corresponding to the effect of 0, 0.5, 1, or 1.5 $\mu\text{g}\cdot\text{ml}^{-1}$ Subtilisin A in ASW onto the settlement of barnacle cyprids after 24 and 48 h are presented in Figure 4.13. Settlement was inhibited onto the conditioned POMA coatings at any of the [Es] and incubation times tested. The inhibitory character observed for the conditioned POMA film in the absence of enzyme seemed to have pre-determined the results found at other [Es]. As these coatings were not pre-leached in re-circulating seawater prior to the assays (the common practice in this case), release of inhibitory compounds from the POMA coatings could have occurred. However, since the chemicals used for the preparation of the POMA surfaces are

also used for the PEMA surfaces without signs of inhibition for the latter, the most likely explanation of the settlement inhibition observed for POMA conditioned films may be associated to additional surface-related inhibitory features, like their more hydrophobic character or different surface charge.

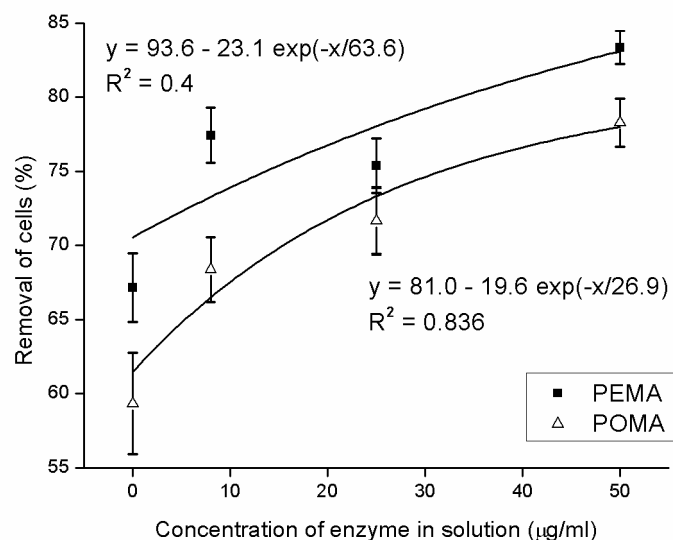


Fig. 4.12. Removal of cells of *Navicula* from conditioned POMA and PEMA films after incubation with 0 (control), 8, 25 or 50 $\mu\text{g}\cdot\text{ml}^{-1}$ Subtilisin A in ASW for 3 h and exposure to 35 Pa wall shear stress. $N = 3$ (90 fields of view), error bars = ± 2 x standard error derived from arcsine-transformed data.

In a comparative assay with immobilized Subtilisin A onto POMA films (including coatings POMA, POMA1, POMA1 – D, and the control AWG; see Table 7.3 for details about POMA1 and its denatured control POMA1 – D), all tested POMA-based coatings displayed inhibitory features, independently on whether the enzyme was immobilized (POMA1) or not (POMA) to the surface and on whether the bound-enzyme was active (POMA1) or not (POMA1 – D). The mean percentage settlement after 48 h was lower than 3% on all POMA coatings whereas it reached 50% (± 12 %) on the glass control AWG. As for the abovementioned assays with the enzyme in solution onto POMA coatings, the settlement-inhibitory properties of this carrier layer may have been still

'recognizable' by cyprids when an enzyme monolayer was immobilized onto it in either form, active or denatured. These observations illustrate about the 'conditioning' effect of the polymer carrier used for immobilization not only on the final properties of the bound catalyst but also on the final biological response. Based on these findings, the further evaluation of the bioactive coatings with barnacle cyprids was restricted to the use of PEMA as platform for enzyme immobilization.

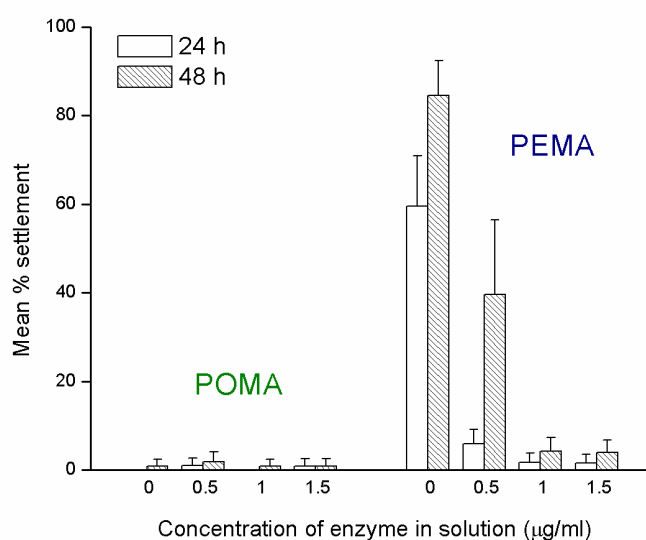


Fig. 4.13. Mean percentage settlement of *Balanus amphitrite* cyprids to conditioned POMA and PEMA films in the presence of 0 (control), 0.5, 1, and 1.5 $\mu\text{g}\cdot\text{ml}^{-1}$ Subtilisin A in ASW for 24 and 48 h. N = 6, error bars = \pm 95 % confidence intervals.

As indicated in Figure 4.13, in the absence of enzyme in solution the conditioned PEMA coatings were the most preferred substrate for settlement, being the mean percentage of settlement onto PEMA substantially higher than onto the controls, AWG and polystyrene dishes (AWG: 35 ± 5 % at 24 h, 65 ± 14 % at 48 h; Polystyrene dishes: 9 ± 5 % at 24 h, 18 ± 8 % at 48 h).

For the PEMA conditioned films, barnacle settlement was found to be dependent on the [Es] present in the liquid media together with cyprids. The strong inductive character of the conditioned PEMA film vanished at

[Es] $\approx 1 \mu\text{g}\cdot\text{ml}^{-1}$, revealing that relatively low [Es] are effective at deterring settlement of barnacle cyprids after 48 h incubation. This observation is in agreement with previous reports from Pettitt *et al.* 2004 [23] showing that Alcalase® had a minimum inhibitory concentration of $1.1 \mu\text{g}\cdot\text{ml}^{-1}$ for barnacle cyprid settlement onto polystyrene well plates. The enzyme in solution might degrade the temporary adhesive used by cyprids during exploration, hence making it difficult for them to finally commit to settlement, and/or eventually it might also target the cyprid permanent cement at the early settlement stages, as demonstrated by Aldred *et al.* 2008 [24] for Alcalase. Since the adhesives secreted by barnacle cyprids are mostly proteinaceous [16; 17], a marked impact of the broadly-specific enzyme Subtilisin A onto settlement was expected.

4.4 Antifouling and fouling-release potential of immobilized Subtilisin A

The activity and surface concentration of the enzyme-containing MA copolymer coatings used in the biological assays with micro and macrofoulers are presented in Table 4.2. Data are as reported in sections 4.1.2 (surface concentration) and 4.1.3 (initial activity).

4.4.1 Assays with spores of *Ulva linza*

PEMA bioactive coatings of increasing enzyme surface activity

The adhesion strength of spores to active PEMA coatings with increasing total activity of Subtilisin A was determined (see Table 4.2 for activities). Denatured coatings with the same immobilized protein content, and the PEMA conditioned copolymer film were included as controls.

Table 4.2. Initial activity and surface concentration of the active coatings used in the biological assays [167]

<i>Coating label</i>	$[Es]$ ($mg.ml^{-1}$) ^{a)}	σ ($\mu g.cm^{-2}$) ^{b)}	A ($[pNa].min^{-1} \times 10^3$) ^{c)}
POMA1	7	0.38 ± 0.05	59.2 ± 11
PEMA1	3	0.24 ± 0.03	62.8 ± 18
PEMA2	10	1.2 ± 0.1	138.7 ± 18
PEMA3	20	2.22 ± 0.2	236.3 ± 25
PEMA4	30	2.18 ± 0.2	489.4 ± 47

^{a)}: enzyme concentration in solution used during the immobilization process; ^{b)}: surface concentration of the immobilized enzyme layer (amino acid analysis based on HPLC); ^{c)}: initial activity of the immobilized enzyme layer (absorbance spectroscopy following the cleavage of *N*-succinyl-Ala-Ala-Pro-Phe-pNa at 405 nm).

As observed in Figure 4.14, initial settlement of spores on the PEMA active coatings was lower than on the denatured and conditioned coatings (see the caption of Figure 4.14 for data about the conditioned PEMA coating). Initial spore density on the PEMA active coatings also decreased as immobilized enzyme activity increased, a fact that is likely to be a consequence of the assay method. After the 45 min settlement period, all coatings were washed in ASW to remove unsettled (swimming) spores, before the incubation step proceeded. Consequently, the secreted adhesive of spores that settled rapidly could have been in contact with immobilized enzyme for up to 45 min, whilst others may have only been settled a few minutes, hence their adhesive would have been in contact with the immobilized enzyme for only a short period of time. A longer exposure to the immobilized enzyme and/or to higher concentrations of the enzyme on the surface is likely to have caused the adhesion strength of a proportion of settled spores to have weakened, resulting in an increasing amount being removed by the washing step.

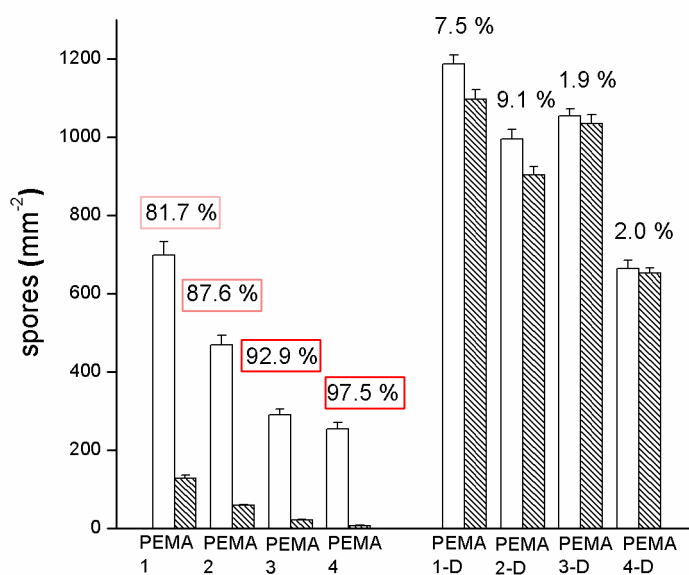


Fig. 4.14. Adhesion strength of adhered spores of *Ulva* to denatured (-D) and active coatings with increasing activity of Subtilisin A (see Table 4.2 for activities). White bars show spore density after settlement and washing, dark bars after exposure to an impact pressure of 34 kPa. The percentage figures show percent removal for each treatment. Settlement on PEMA conditioned films was 843 spores.mm⁻², with 2.3 % removal. N = 3 (90 fields of view), error bars = ± 2 x standard error [167].

The adhesion strength of spores was shown to be significantly ($p = 0.001$) influenced by the presence of active Subtilisin A immobilized on PEMA copolymer films in a concentration-dependent manner, with spore removal exhibiting a non-linear relationship with the activity of the immobilized protease over the range tested (Figure 4.15). Removal of spores from the denatured controls showed some significant differences ($p = 0.01$) between PEMA1-D / 2-D and PEMA3-D / 4-D, but there was no trend with increasing enzyme concentration, and removal was less than 10 % in all cases. With illustrative aims, photographs in Figure 4.16 show spores settled on active PEMA3 and denatured PEMA3-D coatings before and after exposure to the water jet pressure.

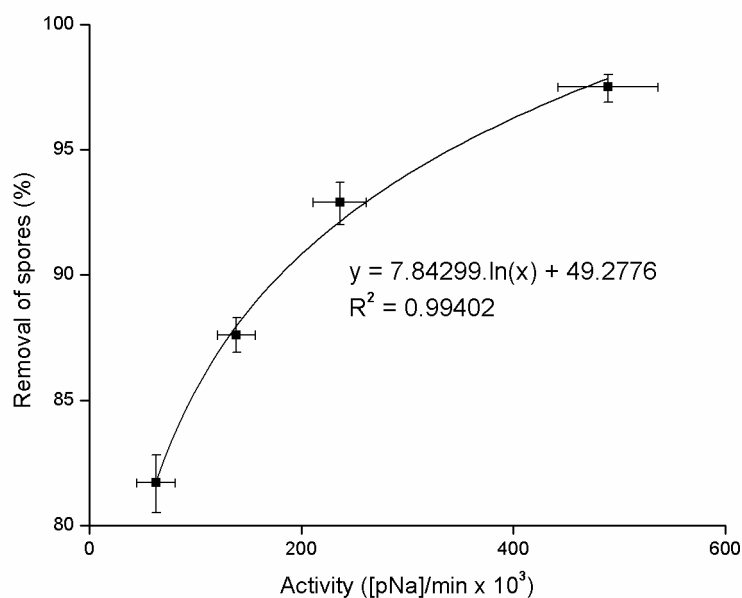


Fig. 4.15. Removal of adhered spores of *Ulva* from active PEMA coatings of increasing activity. Removal is calculated as a percentage of the settled population and is expressed as a function of the initial surface activity of the PEMA active coatings. For the y-axis: N = 3 (90 fields of view), error bars = ± 2 x standard error derived from arcsine transformed data. For the x-axis: N = 5, error bars = \pm standard deviation [167].

The decrease in adhesion strength found for coatings of increasing enzyme activity constitutes a proof of concept that immobilized proteases are able to affect the adhesion processes of *Ulva* spores to a given support, as occurred with soluble Alcalase [23]. Zoospores have been shown to be strongly attracted by the presence of the enzyme on the PEMA surface in either form, active or denatured. Even though the settlement levels were high in all coatings tested, almost 100 % removal could be attained with the coating of the highest activity (*i.e.* PEMA4), and removal was found to be dependent on the enzyme surface activity and concentration. The removal dependence with enzyme surface concentration and activity is likely to be the result of a stronger enzymatic action on the proteinaceous adhesive molecules as activity raises. Continuous cleavage (degradation) of the adhesive molecules could weaken the binding strength to the surface by effecting molecular cross-linking and/or the anchoring of the adhesive molecules to the support.

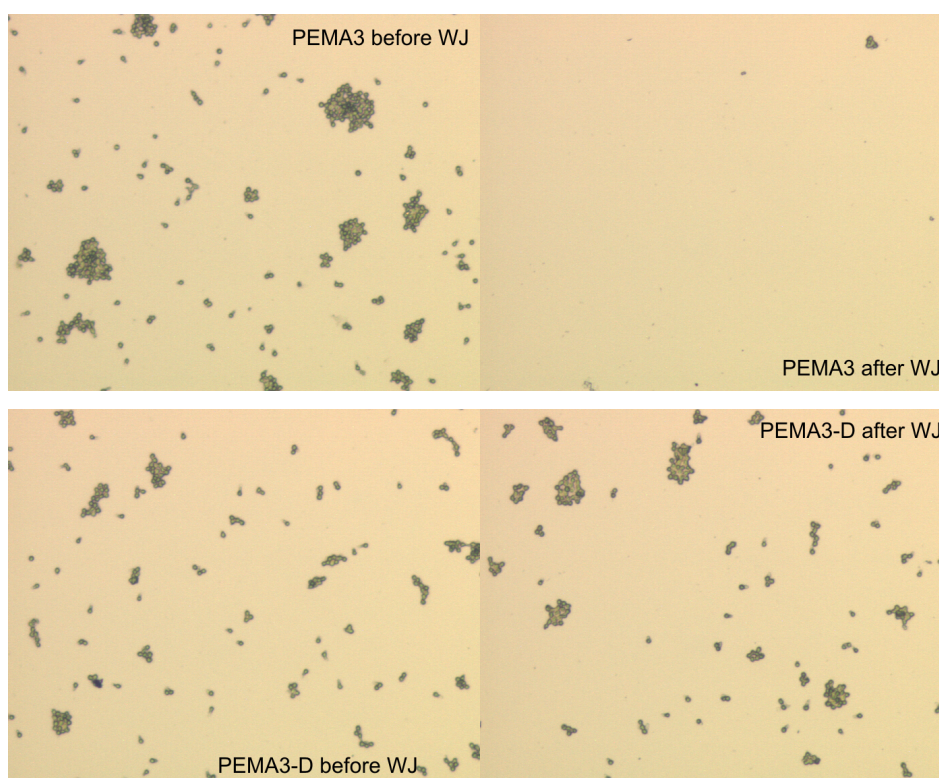


Fig. 4.16. Epifluorescence microscopy images of settled *Ulva* spores onto PEMA3 (first row) and PEMA3-D (second row) coatings, before and after the application of a removal pressure by using the water jet (WJ) apparatus (40x magnification).

Coating of similar enzymatic surface activity onto different copolymer supports

To investigate the influence of the physicochemical properties of the copolymer film used for enzyme immobilization on the antifouling efficacy of the immobilized biocatalyst, enzyme-containing coatings of similar activity (PEMA1 and POMA1; Table 4.2) were formulated onto different copolymer platforms. As enzyme activity was broadly equivalent (as well as surface roughness and wettability), removal of spores from these coatings could be related to any underlying effect of the base copolymer film on the adhesion strength (Figure 4.17).

There was a marked difference in the level of spore settlement on conditioned PEMA and POMA copolymer films, settlement on the former being approximately eight times greater. However, the level of settlement on POMA

films was increased when either active enzyme (POMA1) or denatured enzyme (POMA1-D) was attached to the films, such that within each pair of treatments (*i.e.* PEMA1/POMA1, PEMA1-D/POMA1-D) the level of initial spore settlement was approximately the same. Presumably spores were attracted to settle on the otherwise non-conductive POMA by the physical presence of either active or denatured enzyme protein on the surface. This effect has also been observed in previous studies of heat-denatured enzymes tested in solution (unpublished data from Prof. J. A. Callow's research group).

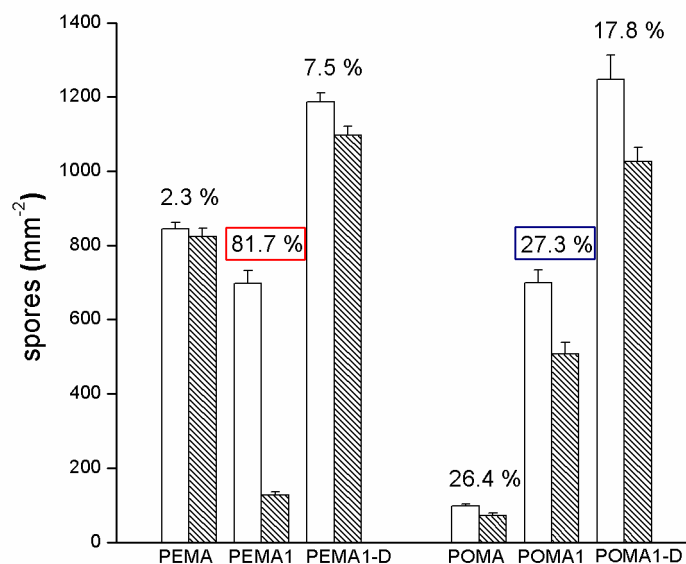


Fig. 4.17. Adhesion strength of spores of *Ulva* adhered to PEMA and POMA conditioned copolymer films, denatured coatings (PEMA1-D; POMA1-D) and active coatings (PEMA1; POMA1) with a Subtilisin A activity of approximately $60 [\text{pNa}].\text{min}^{-1} \times 10^3$. Bars show the mean number of spores before (white bars) and after (dark bars) exposure to an impact pressure of 34 kPa; the percentage figures show percent removal for each treatment.

N = 3 (90 fields of view), error bars = $\pm 2 \times$ standard error [167].

As observed in previous assays with Subtilisin A in solution (section 4.3), the strength of spore adhesion varied between the conditioned PEMA and POMA copolymer films, being significantly weaker (2.3 % vs. 26.4 % removal) on the latter ($p = 0.01$). In the case of the POMA coatings, the presence of Subtilisin A

had no influence on spore adhesion strength, whether the enzyme was active or denatured; the percentage removal of spores from POMA1 and POMA1-D did not differ significantly from POMA ($p = 0.01$). However, for the PEMA coatings, there were marked and statistically significant differences in adhesion strength. Active coating PEMA1 showed high levels of spore removal (82 %) compared to either the base polymer (2.3 %) or the denatured enzyme control (7.5 %): in both cases the levels of removal were significantly different ($p = 0.01$). Spore adhesion strength to the denatured PEMA1-D coating did not differ markedly to that on the conditioned coating.

The similar settlement levels observed for coatings PEMA1 and POMA1 could be attributed to the similar surface properties of both coatings, *i.e.* similar activity, surface roughness and wettability [50; 51]. However, the higher removal found for PEMA1 unveiled the impact of the physicochemical nature of the support on the ability of spores to adhere to surfaces, as the carrier determines the conformation and distribution of the immobilized enzyme molecules, hence their catalytic capabilities. A more favorable environment for the enzymatic cleavage of the proteinaceous adhesives, in terms of improved substrate accessibility and localized conditions (such as pH or surface charge) at the initial stages of spore settlement, might explain the increased removal observed for PEMA1.

Comparison between immobilized enzyme and equivalent amount of enzyme in solution

Coating PEMA3 has an immobilized amount of enzyme which is equivalent to an enzyme concentration in solution of $8 \mu\text{g}\cdot\text{ml}^{-1}$. This correspondence takes into account all molecules immobilized on PEMA3, either active or inactive, and provides an equivalent amount of enzyme in solution. It has to be noticed that, unlike the encountered fraction of the total immobilized molecules remaining active, all molecules in solution are expected to be active and kinetically more favored to catalyze the conversion of proteins than an equivalent amount of randomly immobilized enzyme molecules.

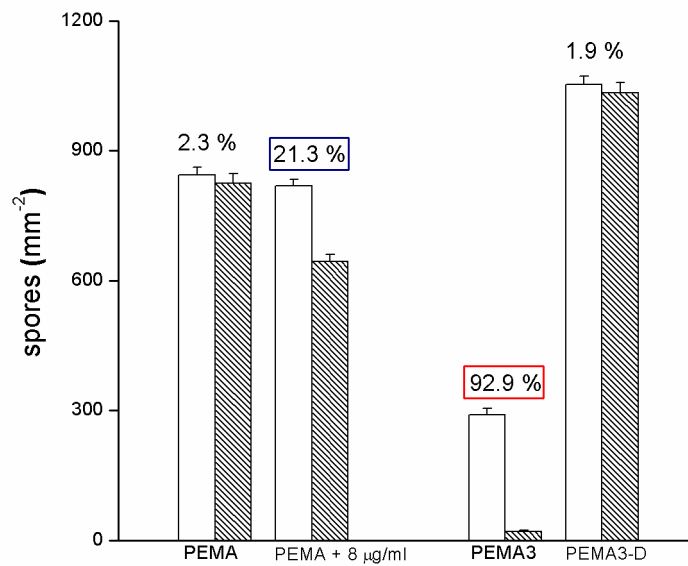


Fig. 4.18. Adhesion strength of adhered spores to the conditioned PEMA copolymer film, PEMA + 8 $\mu\text{g}\cdot\text{ml}^{-1}$, PEMA3 active coating, and PEMA3-D denatured coating. White bars show spore density after settlement and washing, dark bars after exposure to 34 kPa impact pressure.

The percentage figures show percent removal for each case. $N = 3$ (90 fields of view), error bars = $\pm 2 \times$ standard error [167].

As presented in Figure 4.18, PEMA3 and PEMA + 8 $\mu\text{g}\cdot\text{ml}^{-1}$ had very distinct settlement levels, PEMA3 having *ca.* three times lower settlement than PEMA + 8 $\mu\text{g}\cdot\text{ml}^{-1}$, whereas the latter had similar settlement levels as those found for the conditioned PEMA film. As a consequence of the experimental methodology, settled spores are constantly exposed to the immobilized enzyme whilst they are only exposed to the enzyme in solution after the initial settlement stage, when the first contact to the bare PEMA film occurred. Spores attached to the conditioned PEMA films, and thereafter exposed to the enzyme in solution during the incubation period, seemed not to have been affected by the washing step after incubation, as settlement onto them was comparable to that onto the control PEMA films. Contrarily, and as discussed for the assays with bioactive coatings of increasing activity, the quantified number of settled spores onto PEMA3 is likely to have been influenced by the washing step after incubation. The continuous contact of spores to the immobilized enzyme in PEMA3 might

have weakened the initial adhesion strength [4] of a fraction of settled spores so that the gentle washing step might have provided sufficient shear stress to remove part of the originally settled population.

Regarding the effectiveness of immobilized *vs.* soluble enzyme to decrease adhesion strength, the removal of spores from PEMA 3 was found to be more than four times higher than from the PEMA conditioned film incubated with $8 \mu\text{g}\cdot\text{ml}^{-1}$ Subtilisin A. Even though the activity of soluble Subtilisin A is more than one order of magnitude higher than that of PEMA3, the effect of the enzyme in solution onto the adhesion strength of *Ulva* spores is surpassed by the continuous effect of the enzyme localized at the interface between surface and adhesive.

4.4.2 Assays with cells of *Navicula perminuta*

PEMA bioactive coatings of increasing enzyme surface activity

Due to the generally lower adhesion strength of *Navicula* cells compared to that exhibited by spores of *Ulva*, the adhesion strength of diatom cells was determined by application of a shear stress parallel to the coating. As a consequence of the different hydrodynamic regimes (*i.e.* impact pressure for *Ulva* and shear stress for *Navicula*), results from the two species are not directly comparable.

Initially, equivalent levels of settlement are expected on all samples since *Navicula* cells are passively brought to surfaces by gravity and/or water currents. Because settlement levels are here quantified after a washing step, any variation in cell density among the tested surfaces is considered to stem from the simultaneous differences in cell adhesion strength to the coatings. As observed in Figure 4.19, the initial density of cells on the active and denatured coatings did not differ markedly, or vary systematically with enzyme activity, *i.e.* cells of *Navicula* appear not to be as susceptible to removal by the washing step as spores of *Ulva*.

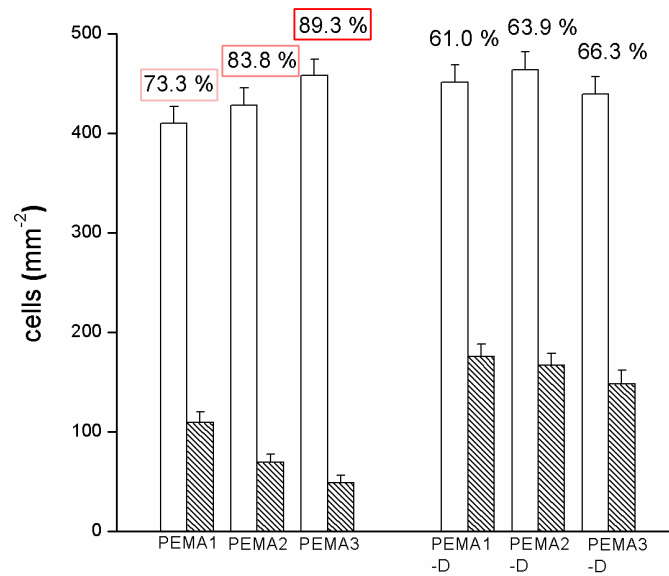


Fig. 4.19. Adhesion strength of cells of *Navicula* to denatured (-D) and active coatings with increasing activity of Subtilisin A (see Table 4.2 for activities). White bars show spore density after settlement and washing, dark bars after exposure to 35 Pa wall shear stress. The percentage figures show percent removal for each treatment. Settlement on PEMA conditioned films was 418 cells.mm⁻², with 67.2 % removal. N = 3 (90 fields of view), error bars = ± 2 x standard error [167].

Removal of cells by a wall shear stress of 35 Pa was in excess of 60 % for all coatings, however statistical analysis indicates that removal was significantly higher from active coatings than from denatured controls ($p = 0.001$), and showed a definite trend of increasing removal with increasing immobilized Subtilisin A activity (Figure 4.20). Although statistically significant differences in removal were found for the denatured coatings, removal only varied by 5.3 % with increasing enzyme concentration.

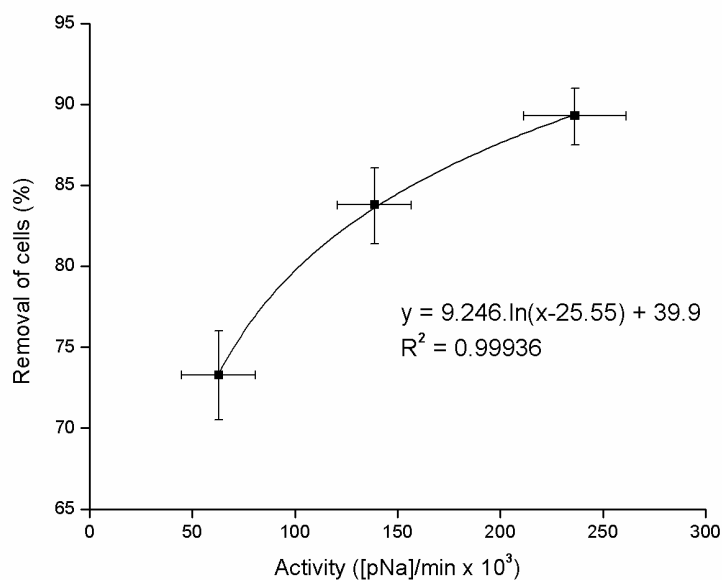


Fig. 4.20. Removal of adhered cells of *Navicula* from active PEMA coatings of increasing activity. Removal is calculated as a percentage of the settled population and is expressed as a function of the initial surface activity of the PEMA active coatings. For the y-axis: N = 3 (90 fields of view), error bars = ± 2 x standard error derived from arcsine transformed data.

For the x-axis: N = 5, error bars = \pm standard deviation.

Coating of similar enzymatic surface activity onto different copolymer supports

Settlement of diatom cells onto the PEMA-group of coatings was lower than onto the POMA-group ($p = 0.01$), coating PEMA1 having a significantly lower ($p = 0.001$) settlement level than coating POMA1 of similar activity (Figure 4.21). Since the water contact angles of these two coatings, as well as their RMS values and surface activities, are broadly equivalent, the lower number of diatom cells onto PEMA1 could be related (as for *Ulva*) to the washing step removing part of the settled population due to the weakening of the anchorage to the surface caused by enzymatic action.

Removal of diatom cells was higher onto the hydrophilic conditioned PEMA coating than onto the more hydrophobic POMA films, a result that is in correspondence with previous reports with hydrophilic mPEG-DOPA₃ surfaces [63]. Adhesion strength of *Navicula* cells to PEMA1 was significantly ($p = 0.001$)

lower than for POMA1 after a 3 h incubation period. In a similar way as for *Ulva* spores, the interaction between the secreted adhesive molecules and the enzyme immobilized onto PEMA appears to be weaker than in the case of the enzyme immobilized onto POMA, at equivalent surface activity. Specific features of the enzyme immobilized onto the 3D-like PEMA layers (*e.g.* conformation, orientation of active sites) might enhance the fouling-release capabilities of PEMA1 *cf.* POMA1 towards both algal species.

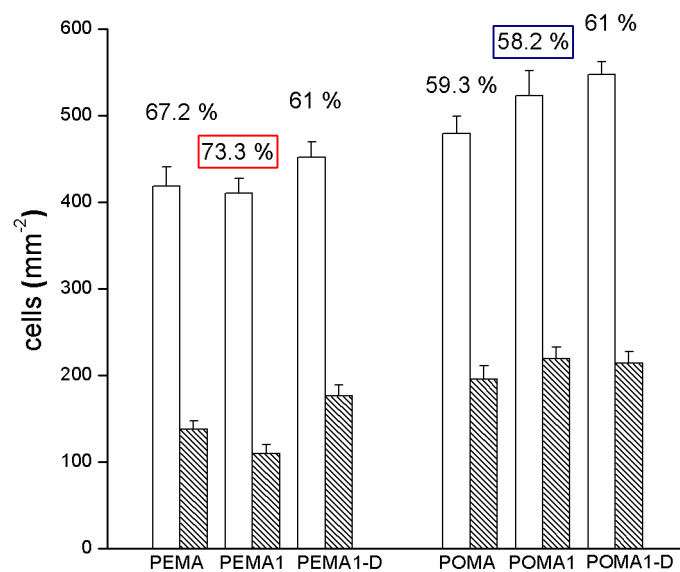


Fig. 4.21. Adhesion strength of cells of *Navicula* adhered to PEMA and POMA conditioned copolymer films, denatured coatings (PEMA1-D; POMA1-D) and active coatings (PEMA1; POMA1) with a Subtilisin A activity of approximately $60 \text{ [pNa].min}^{-1} \times 10^3$. Bars show the mean number of spores before (white bars) and after (dark bars) exposure to a wall shear stress of 35 Pa; the percentage figures show percent removal for each treatment.

N = 3 (90 fields of view), error bars = $\pm 2 \times$ standard error.

Comparison between immobilized enzyme and equivalent amount of enzyme in solution

No marked differences were found in the settlement levels of *Navicula* cells to PEMA3, the conditioned PEMA, PEMA + $8 \mu\text{g.ml}^{-1}$ Subtilisin A, and the

denatured control (Figure 4.22) after the washing step, probably obeying to the almost unchanged surface roughness and wettability of these coatings (there is a slight increase in contact angle from PEMA3 (~ 30 °) to PEMA3-D (~ 50 °) (Table 4.1), but perhaps not substantial to influence the after-washing settlement levels [50; 63]). Contrarily, removal from PEMA3 was significantly higher than from PEMA + 8 $\mu\text{g}\cdot\text{ml}^{-1}$ Subtilisin A ($p = 0.01$), suggesting that, as for *Ulva*, localization of enzyme activity to the adhesive:surface interface is more effective at reducing the adhesion strength of cells of *Navicula* than the equivalent amount of enzyme in solution.

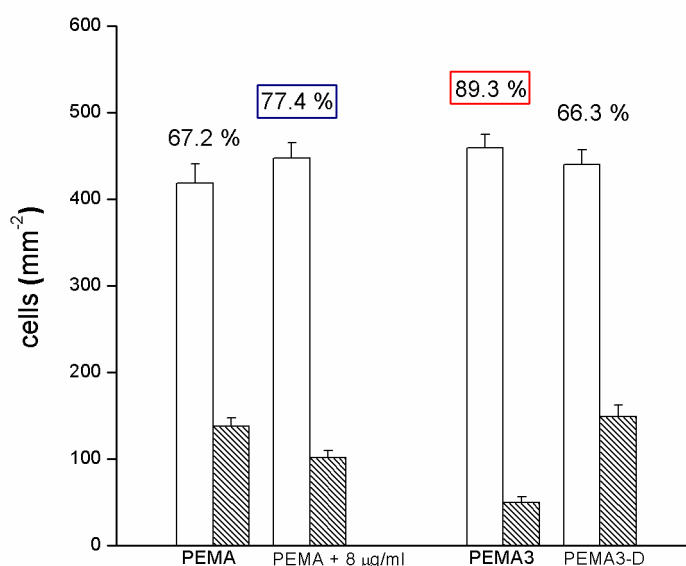


Fig. 4.22. Adhesion strength of diatom cells to the conditioned PEMA copolymer film, PEMA + 8 $\mu\text{g}\cdot\text{ml}^{-1}$, PEMA3 active coating, and PEMA3-D denatured coating. White bars show spore density after settlement and washing, dark bars after exposure to 35 Pa impact pressure.

The percentage figures show percent removal for each case. $N = 3$ (90 fields of view), error bars = ± 2 x standard error.

The effect of the immobilized enzyme in PEMA3 vs. an equivalent amount of enzyme in solution was less pronounced for *Navicula* cells than it was for *Ulva* spores: the percentage removal difference between PEMA3 and PEMA + 8 $\mu\text{g}\cdot\text{ml}^{-1}$ Subtilisin A being ~ 73 % for spores of *Ulva* and ~ 14 % for

Navicula cells. This difference between the two organisms might be attributed to different proportions of protein vs. glycans in their adhesives. The adhesive glycoprotein of *Ulva* is predominantly protein with approx. 17 % *N*-linked glycan [15] whereas diatom adhesives are complex mixtures of polysaccharide-based extracellular polymeric substances and minor protein fractions [7]. Another possibility is that the adhesives produced by diatoms on a surface are continually replenished as the diatom ‘glides’ over the surface [9], whereas adhesive release by settled spores of *Ulva* is largely a ‘one-off’ secretion [8].

4.4.3 Assays with cyprids of *Balanus amphitrite*

PEMA bioactive coatings of increasing enzyme surface activity

Barnacle cyprids of *Balanus amphitrite* were exposed to bioactive MA copolymer coatings of increasing activity and to denatured controls for 24 and 48 h to determine the mean percent settlement of these organisms to the tested surfaces. As explained in section 7.8, the usual methodology of the ‘drop’ settlement assay for barnacle cyprids failed as such when the hydrophilic bioactive PEMA coatings were tested and required a modification, which involved the deposition of a thin layer of wax around the central area occupied by the enzyme. When the wax ‘holding fence’ was introduced, cyprids were confined to the enzyme area, therefore only offered with the choice of settling either in-there or in the border interface between the wax fence and the enzyme area. Although the utilization of a wax fence solved the problem of the preferential cyprid settlement on the enzyme-free areas when no wax fence was used, it introduced an undesirable discontinuity (the border interface) to the surfaces under evaluation. This discontinuity was revealed to act as a magnet for cyprid settlement, and became the most preferred localization for settlement.

The obtained settlement levels onto the bioactive PEMA coatings remained low compared to the much higher settlement values of the denatured controls (Figure 4.23) after both incubation times. The difference in settlement

between active and denatured coatings was substantial after 24 or 48 h incubation (the average mean settlement after 48 h on the active coatings was of *ca.* 7 % vs. 52 % onto the denatured controls). No difference in settlement was found amid the bioactive coatings of increasing surface activity neither among the denatured controls ($p = 0.01$), in opposition to the concentration-dependent mechanism found for the enzyme in solution onto PEMA conditioned films (see Figure 4.13). The activity of the immobilized enzyme onto the coating of lowest activity (PEMA1) seemed to have been enough to reduce settlement to the very low levels observed, the increase in surface activity displaying then no further influence.

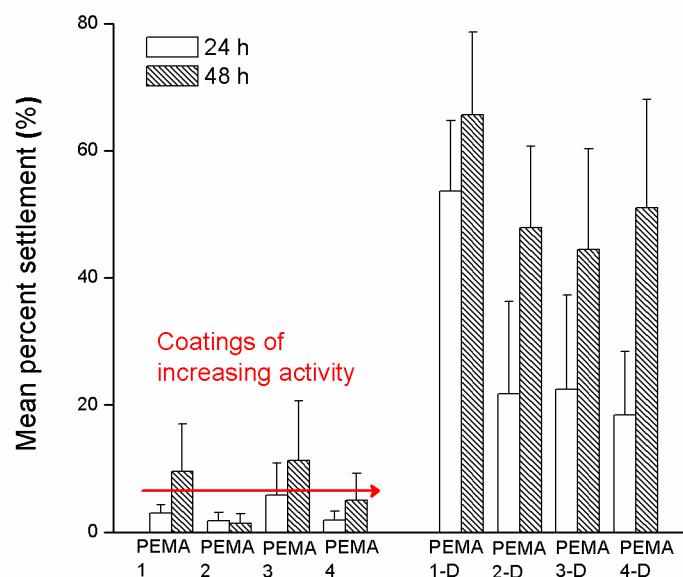


Fig. 4.23. Mean percent settlement of barnacle cyprids onto PEMA active coatings of increasing activity and the corresponding denatured controls (-D). Settlement is expressed as a percentage of the total number of cyprids dispensed on each slide. White bars show settlement after 24 h, dark bars after 48 h. The red arrow is located at a level corresponding to the average percent settlement of the active coatings. Settlement onto the AWG control slides was 33.3 ± 9.1 % after 24 h and 52.8 ± 5.3 % after 48 h. $N = 12$ (active coatings) or 6 (denatured coatings), error bars = ± 95 % confidence error.

As a result of the applied methodology, most of the settlement onto the bioactive coatings was found to occur at the interface between the enzyme area and the thin wax layer (Figure 4.24; PEMA1 on the first row), whereas a more even pattern was observed onto the denatured controls (Figure 4.24; PEMA1-D). Some of the individuals on the bioactive coatings settled in the nearness of the wax fence, others did it partly underneath (or above) the wax layer (see Figure 4.24; PEMA1 on the second row), but almost none settled in the enzyme area.

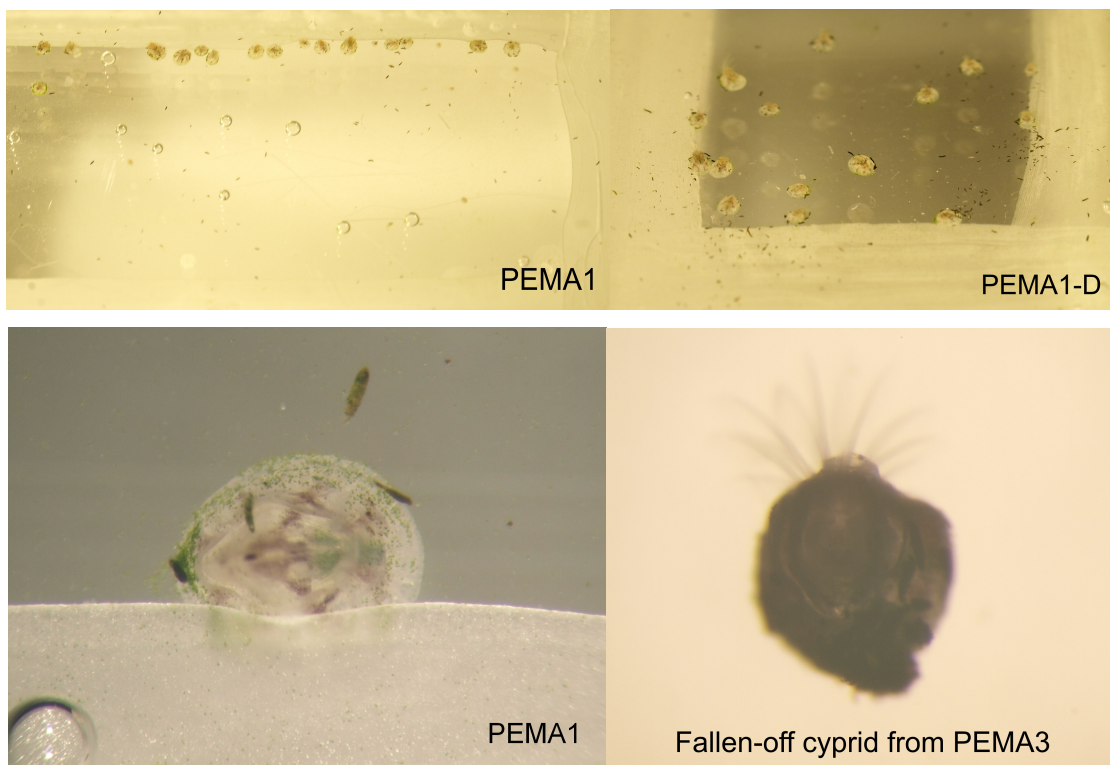


Fig. 4.24. First row: settlement distribution of barnacle cyprids onto active coating PEMA1 and denatured control PEMA1-D, as indicated in the photographs. Settlement onto these coatings is representative of the observations gained for all tested coatings; Second row: Barnacle cyprid settled in PEMA1 at the interface border between the enzyme area and the thin wax layer, possibly exploiting the enzyme-free regions (*i.e.* those underneath the wax layer or close to it) to dispense the adhesive and settle permanently; A fallen-off cyprid from PEMA3, moving its cirri as normal.

Results presented in Figure 4.23 account for the total number of settled cyprids, hence they include all settlement cases (*i.e.* near the border, in the central enzyme area, and partly underneath (or above) the wax layer). Since cyprids were offered

the same location choice among the different areas in the denatured controls, results from both active and denatured surfaces can be compared. Apart from the sheltered protection gained by settling in the areas close to the wax fence, additional reasons for choosing this location may lie in possible deleterious effects over the immobilized enzyme molecules introduced by the wax-dipping procedure, which could have caused conformation changes or, eventually, denaturation of a fraction of the immobilized molecules in the near-to-the-border areas.

Despite the experimental limitation introduced by the use of a wax fence, the total settlement onto the bioactive coatings resulted significantly lower than onto the denatured controls and the AWG slides ($p = 0.01$) at both incubation times, clearly highlighting the inhibitory effect displayed by the immobilized enzyme. Not only was the active immobilized enzyme obstructing settlement, but also caused a fraction of settled cyprids to be detached from the surface (Figure 4.25). A part of the population may have committed to settlement in the enzyme area, but the adhesion strength to the surface may have been weakened by the immobilized enzyme, so that slight movements of the slides during counting could have caused those cyprids to detach. A similar effect was observed with *Ulva* spores when increasing the activity of the immobilized catalyst (see section 4.4.1). The relative number of fallen-off cyprids (to the total number of settled) on the active coating was significantly ($p = 0.01$) higher than onto the denatured controls, without differences as activity increases. The average number of fallen-off cyprids was 43 % and 1 % for the active and denatured coatings, respectively. Fallen-off cyprids had a rounded shape (which is indicative of the first metamorphosis stages) and were found to behave as normal without any sign of compromise in their health or viability (Figure 4.24; fallen-off cyprid from PEMA3). This fact points at the non-biocidal character of the immobilized enzyme, a highly-appreciated feature in environmentally-friendly strategies for fouling control.

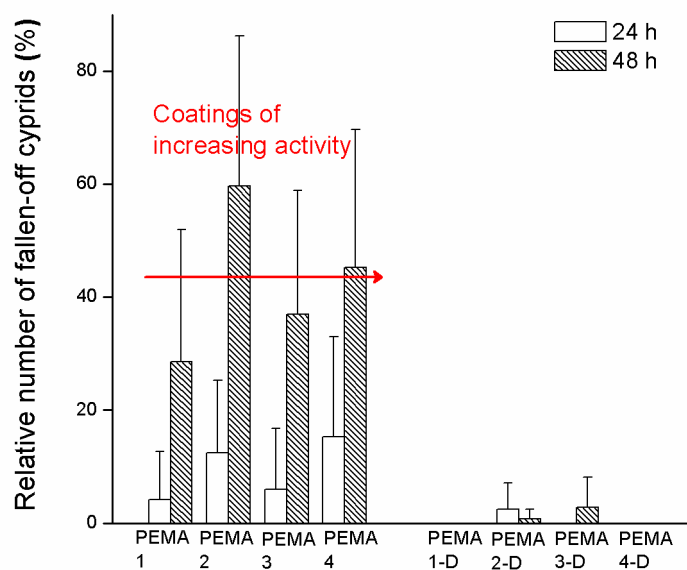


Fig. 4.25. Relative number of cyprids metamorphosed and fallen-off for PEMA active coatings of increasing activity and the corresponding denatured controls (-D). The relative number of fallen-off cyprids is calculated as the relative fraction of fallen-off to the total number of settled on each surface. White bars show settlement after 24 h, dark bars after 48 h. The red arrow is located at a level corresponding to the average relative number of fallen-off cyprids for the active coatings.

N = 12 (active coatings) or 6 (denatured coatings), error bars = \pm 95 % confidence error.

Comparison between immobilized enzyme and equivalent amount of enzyme in solution

Unlike previous observations with *Ulva* spores and *Navicula* diatoms (sections 4.4.1 and 4.4.2), the comparison between immobilized enzyme and equivalent amount of enzyme in solution did not yield any differences in the settlement of barnacle cyprids at any of the considered incubation times (Figure 4.26) ($p = 0.01$). For barnacle cyprids, the amount of enzyme immobilized on PEMA1 compares to $1 \mu\text{g}\cdot\text{ml}^{-1}$, a concentration of the enzyme in solution which was previously shown (see section 4.3) to result in very low settlement levels onto PEMA, possibly at the minimum reachable threshold as settlement with $1 \mu\text{g}\cdot\text{ml}^{-1}$ compared to that obtained with $1.5 \mu\text{g}\cdot\text{ml}^{-1}$ (see Figure 4.13).

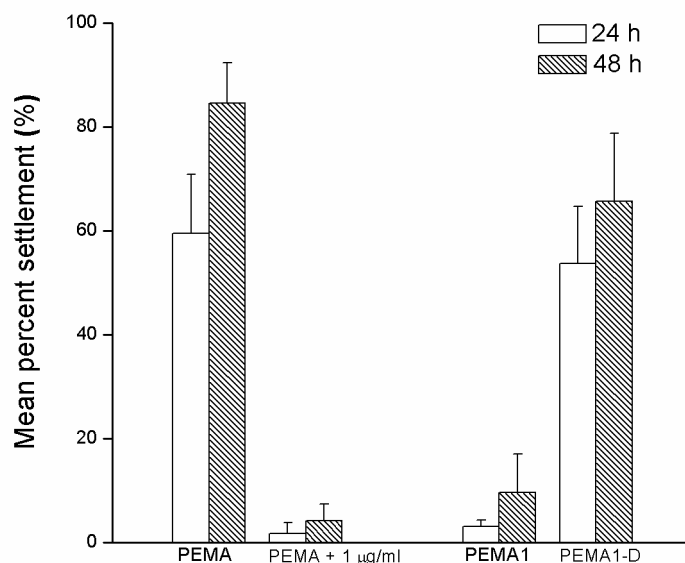


Fig. 4.26. Mean percent settlement of barnacle cyprids onto the conditioned PEMA copolymer film, PEMA + 1 $\mu\text{g}\cdot\text{ml}^{-1}$, PEMA1 active coating, and PEMA1-D denatured coating. Settlement is expressed as a percentage of the total number of cyprids dispensed on each slide. White bars show settlement after 24 h, dark bars after 48 h. N = 12 (active coatings) or 6 (denatured coatings and PEMA coating), error bars = \pm 95 % confidence error.

Despite the lower activity of the immobilized enzyme (when compared to equivalent amount of enzyme in solution) it appeared that localization of the enzyme at the interface between adhesive and surface together with the continuous cleavage capability provided by the immobilized catalyst, might have counterbalanced the lower activity levels regarding settlement of barnacle cyprids. Possibly, the time-scale of the settlement process in barnacle cyprids is large enough to allow the less kinetically-favored immobilized enzyme to act effectively onto the secreted adhesives and/or to hinder the mechanisms of recognition of substrate ligands required for successful settlement to occur.

Taking into account that the settlement levels obtained with the bioactive coating of the lowest activity (PEMA1) were very low and comparable to the saturation values obtained when testing various concentrations of the enzyme in solution (*i.e.* \sim 10 %), one could speculate about a cut-off activity for action (in a ‘one-or-nothing’ scheme), which should lie down the activity of PEMA1, or about

a gradual variation in the settlement levels as the activity of the immobilized catalyst increases. Further analysis and testing of these hypotheses could provide useful insights into the intricate mechanisms of barnacle cyprid adhesion to enzyme-containing coatings (results obtained; manuscript under preparation).

So far, an enzyme surface density of $0.24 \pm 0.03 \mu\text{g}\cdot\text{cm}^{-2}$ (activity of $62.8 \pm 18 [\text{pNa}]\cdot\text{min}^{-1} \times 10^3$) resulting from the exposure of PEMA copolymer films to $3 \text{ mg}\cdot\text{ml}^{-1}$ Subtilisin A (*i.e.* coating PEMA1) provided reasonable low settlement levels of barnacle cyprids after 48 h in laboratory-based tests. Since the strong effects observed onto settlement and strength of adhesion of barnacle cyprids were gained by using low amount of immobilized enzyme, these findings are considered to be certainly of interest to those involved in the design of antifouling surfaces incorporating active agents for practical applications.

Chapter 5

Conclusions

The serine protease Subtilisin A (the active constituent of the commercial preparation Alcalase®) was successfully immobilized onto two maleic anhydride copolymer films (PEMA and POMA) of distinct physico-chemical characteristics *via* the spontaneous reaction of the amine reactive groups of the enzyme with the anhydride moieties of the copolymer layers. Enzyme immobilization was random onto the copolymer carriers, a fact that presumably resulted in a fraction of the available enzyme active sites being impeded or prevented to react with the substrate molecules. The usual reduction in activity upon immobilization was thereafter observed with this strategy, reaching up to 60 % of the values without aging. The covalently-bound enzyme conserved nevertheless a remarkable capability to convert the chromogenic ester substrate *N*-succinyl-Ala-Ala-Pro-Phe-pNA, with $t_{1/2}$ values down one minute being achievable.

A thorough characterization of the enzyme layer immobilized onto the two distinct maleic anhydride copolymer films revealed the formation of distinguishable molecular arrangements onto each copolymer carrier: enzyme layers of higher thickness, surface concentration and activity were attainable when selecting PEMA as immobilization platform. Conversely, limited enzyme loading capacity as well as activity resulted from the use of POMA as carrier for immobilization (Figure 5.1). The obtained carrier-specific distribution and conformation of the bound enzyme molecules is in agreement with previous

research studies [150–153] about the ‘inductive’ and determining effect of the base platform on the resulting arrangement and final catalytic properties of the immobilized enzymes. The high-swelling and 3D-like structure of the PEMA copolymer films, together with their strong negatively-charged surface and higher density of anhydride moieties than the counterpart POMA, are suggested to have allowed enzyme interpenetration and strong electrostatic interactions, hence providing higher enzyme loadings (multilayers) and activities than onto POMA films. The enzyme monolayers found when using POMA as carrier for immobilization are considered to stem from the non-swelling behavior and more hydrophobic character of these copolymer layers, which would offer a rather compact 2D-like surface onto which the enzyme molecules would essentially ‘spread’. Molecular unfolding occurs to maximize the contact areas between the hydrophobic surface and the hydrophobic segments of the enzyme and prevents further immobilization of molecules once the surface becomes saturated with unfolded enzyme molecules. An indication of the higher area for enzyme anchorage resulting from the 3D *cf.* 2D structure of the two copolymer films tested came from the saturation concentrations encountered on both surfaces, *i.e.* 5 mg.ml⁻¹ for POMA *vs.* 20 mg.ml⁻¹ for PEMA.

Despite the enhanced activity observed when enzyme immobilization was performed onto PEMA copolymer films, the catalytic conversion per immobilized molecule had the same functional dependence with the surface concentration on both immobilization platforms, with a slight shift towards higher surface concentrations for PEMA films. The specific activity displayed a sharp increase in the low surface concentration range, reached a maximum at *ca.* 0.2 µg.cm⁻², and fell down hyperbolically in the high surface concentration range. The maximum in conversion capability per immobilized molecule occurs for a theoretical surface coverage by the enzyme of 80 % on both base copolymer layers. For higher surface coverages, the molecular catalytic efficacy decreases, with (PEMA) or without (POMA) an accompanying burst in activity. An enhanced conformation and flexibility of the enzyme molecules bound to POMA copolymer films in the low range of surface concentration could account for the slight shift in the specific

activity maximum and for the higher specific activities achieved onto POMA *cf.* PEMA. An optimized orientation of the active sites together with minimal restrictions for the molecular conformational changes required to convert the substrate would result in higher activity, hence in higher specific activities at any given surface concentration.

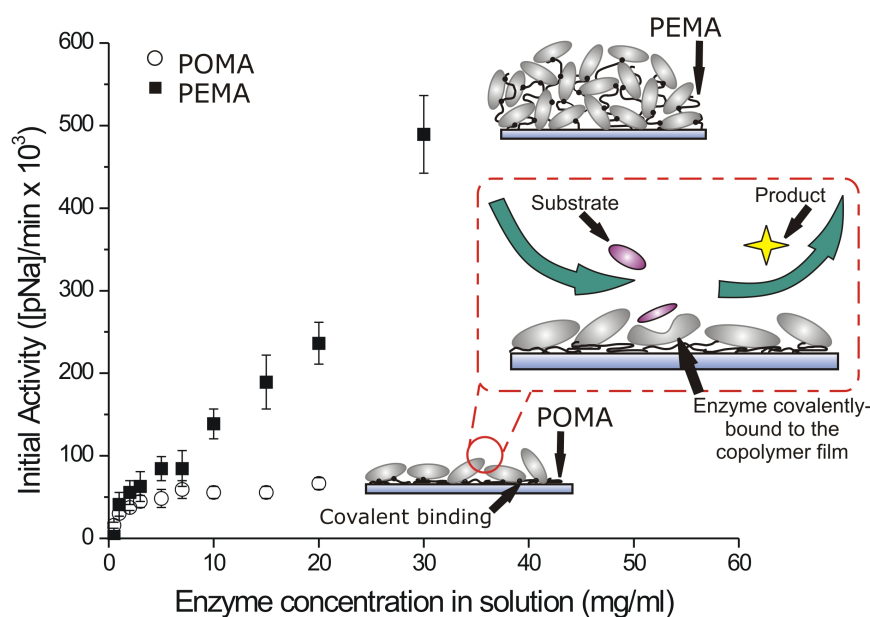


Fig. 5.1. Structure-property relationships for Subtilisin A immobilized onto PEMA and POMA copolymer thin films. Bioactive layers of higher thickness and surface concentration were obtained upon immobilization of the enzyme onto the hydrophilic, 3D-like PEMA film as compared to the enzyme monolayers resulting from immobilization onto the hydrophobic, 2D-like POMA surface. The enzymatic activity of the immobilized biocatalyst was higher when using PEMA *cf.* POMA as carrier for immobilization, in agreement with the higher enzyme loadings achieved onto the former. The activity was determined following the conversion reaction of the substrate N-Suc-AAPF-pNA into products (*i.e.* peptides and the chromophore pNa) by absorbance spectroscopy.

Exposure of the bioactive layers to aqueous media induced a pronounced fall in surface activity as well as in surface concentration, with no retrievable differences between the two incubation solutions of different ionic strength employed. The fall in activity upon incubation was partly dictated by the loss of immobilized

enzyme molecules from the surface, though higher depletions in activity than in protein amount reflect the additional effects of denaturation processes. During incubation, autolysis is probably playing a more important role than desorption of initially-adsorbed molecules as higher losses in protein amount on the surface were obtained for coatings of initially higher surface concentrations. The hydrolysis of enzyme molecules by their neighbors is expected to have a dependence with the surface density, whereas desorption is likely to be controlled and kept at a minimum level by the several washing steps implemented after enzyme immobilization. The residual activities after 48 h incubation in a substitute of artificial seawater lowered up to 40 % of the initial values, highlighting the need for improvement in the stability of the bioactive layers in aqueous media.

For the surface wettability and morphology of the enzyme layers used in the biological assays, essentially ‘nanorough’ surfaces (RMS = 1 – 3 nm) were obtained with invariant water contact angles over the range of increasing surface concentrations and activities considered. These findings allowed for the unequivocal evaluation of the biological response to the bioactive coatings only in terms of the surface activity as the main other surface-related parameters affecting adhesion phenomena (*i.e.* wettability and surface roughness) were found to be constant.

As previously demonstrated for the commercial preparation Alcalase® [23; 24], Subtilisin A (the active component of Alcalase) displayed antifouling and fouling-release properties when immobilized onto maleic anhydride copolymer films. Results confirmed the initial hypotheses related to the enzymatic degradation of the biological adhesives: the immobilized protease was effective at reducing the adhesion strength of *Ulva* spores and *Navicula* diatoms in a manner that correlated with the enzyme activity and surface concentration, and deterred settlement of *Balanus amphitrite* barnacle cyprids even at the lowest surface activity tested (Figure 5.2). The immobilized enzyme was more effective than an equivalent amount of enzyme in solution to promote the release of *Ulva* and *Navicula*, whereas both immobilized and soluble enzyme inhibited cyprid

settlement at equal extent. The relative efficacy of the immobilized *vs.* soluble enzyme was higher for *Ulva* than for *Navicula* in agreement with the relative fractions of protein *vs.* glycan of the adhesives secreted by both organisms (*Ulva*: predominantly protein with ~ 17 % *N*-linked glycan; *Navicula*: mostly polysaccharide with minor protein fractions) [7; 15].

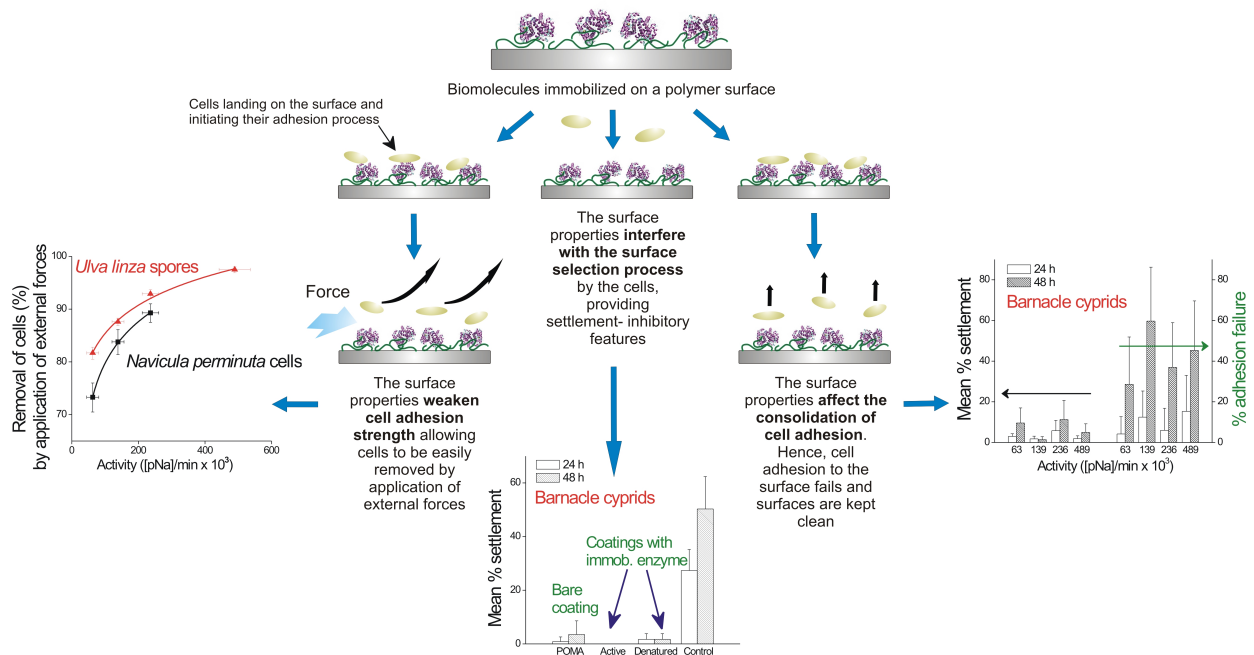


Fig. 5.2. Mechanisms of biofouling control with immobilized Subtilisin A.

The surface properties weaken cell adhesion strength: the adhesion strength of *Ulva* spores and *Navicula* diatoms to the enzyme-containing coatings decreased with increasing the activity of the surface-bound enzyme. At constant removal force, the decrease in adhesion strength with surface activity translated into a raise in the percentage removal. **The surface properties interfere with the surface selection process by the cells:** Subtilisin A immobilized onto POMA films displayed inhibitory features towards barnacle cyprids in either active or denatured form. The inhibitory character of these coatings is probably a consequence of the ‘determining’ effect exerted by the settlement-preventing POMA copolymer carrier. **The surface properties affect the consolidation of cell adhesion:** barnacle cyprids were found to settle in low numbers onto a series of bioactive coatings of increasing activity and were observed to fail in their adhesion attempts to the bioactive surfaces in much higher proportions than onto the control coatings. The encountered low settlement levels are therefore the result of a non-consolidated adhesion to the surface rather than a response to any surface inhibitory feature.

The localized action of the enzyme at the interface between surface and adhesive may account for the higher impact of the immobilized catalyst when compared to an equivalent amount of enzyme in solution: the immobilized enzyme destabilizes the direct bonding of the adhesive molecules to the surface, thus promoting an adhesive failure.

The comparison between coatings of similar activity but of different copolymer base coatings demonstrated that Subtilisin A immobilized onto PEMA layers had a greater potential to effect the consolidation of adhesion of *Ulva* and *Navicula*: consolidation of adhesion appears then to be co-determined by the physicochemical properties of the carrier used for immobilization.

Settlement of barnacle cyprids was kept at a minimum threshold *via* the degradation of the cyprid permanent cement, the evidence being the high number of larvae failing in their attempts to form a strong holdfast to the surface. The settlement and subsequent metamorphosis processes were not inhibited by the bioactive layers and proceeded as normal, but consolidation of adhesion failed. The cyprid temporary adhesive used during exploration is also likely to have been degraded by the immobilized enzyme [24], therefore reducing the cues for the settlement of conspecifics. Furthermore, the settlement-inhibitory character observed for POMA1 may reflect the ‘determining’ effect of the POMA copolymer carrier onto the final biological response as POMA itself discouraged settlement of barnacle cyprids almost completely.

By facilitating the removal of biofilm-forming diatoms and of spores of the troublesome alga *Ulva linza*, as well as by interfering with the consolidation of adhesion of the calcareous *Balanus amphitrite* macrofouler, the enzyme-containing coatings here disclosed are considered to constitute an appealing and promising alternative to control marine biofouling without jeopardizing marine life.

Chapter 6

Summary

The here presented strategy for the random covalent immobilization of the enzyme Subtilisin A to maleic anhydride copolymer thin films allowed to generate bioactive surfaces with tunable properties obtained by appropriate selection of the immobilization platform and of the enzyme concentration used for immobilization. Extensive characterization of the immobilized enzyme layer revealed the existence of distinctive enzyme molecular arrangements onto the two copolymer films employed, highlighting the role of the base immobilization carrier as modulator of the resulting properties of the immobilized catalyst. The bioactive layers obtained onto either copolymer film were shown to be essentially nanorough and hydrophilic and demonstrated susceptibility to incubation in aqueous media, although no differences in residual activity and protein amount could be pointed out when solutions of different ionic strength were considered. Enzyme layers of higher surface concentration and activity were obtained onto the hydrophilic, 3D-like PEMA copolymer films in opposition to the lower surface concentrations and activities attained onto the more hydrophobic and 2D-like POMA surfaces. The bioactive surfaces could successfully be employed to prove the concept that subtilisins are effective, promising agents to influence settlement and adhesion processes of distinct marine organisms. The surface-tethered enzyme reduced the adhesion strength of spores of the alga *Ulva linza* and cells of the diatom *Navicula perminuta* in a manner that correlates with the enzyme surface concentration and activity and deterred settlement of larvae of the barnacle *Balanus amphitrite* at very low surface concentrations. This work is

therefore considered to be of interest to those involved in antifouling and fouling release applications as well as to those interested in evaluating surface-related mechanisms with bioactive layers of graded activity (*e.g.* adhesion of bacterial or animal cells, exploratory behavior of more surface-selective foulers, or anti-adhesive character towards other proteins, like serum proteins).

Chapter 7

Materials and Methods

The experimental assays described in this chapter were performed at three different locations:

- the Max Bergmann Center of Biomaterials Dresden (director Prof. Carsten Werner) within the Leibniz Institute of Polymer Research Dresden (Dresden, Germany) for the preparation and characterization of the enzyme-containing MA copolymer thin coatings,
- the laboratory of Prof. James A. Callow at the School of Biosciences, University of Birmingham (Birmingham, UK) for the assays with zoospores of the green alga *Ulva linza* and cells of the brown diatom *Navicula perminuta*, and
- the laboratory of Prof. Anthony S. Clare at the School of Marine Sciences and Technology, University of Newcastle-upon-Tyne (Newcastle-upon-Tyne, UK) for the assays with cyprids of the barnacle *Balanus amphitrite*.

7.1 Materials

Glass coverslips (hydrolytic class 1 glass, 24 x 24 mm², thickness: 0.13 – 0.16 mm) were obtained from Menzel-Gläser (Braunschweig, Germany). Silicon wafers (native oxide, 22 x 22 mm², thickness: 525 µm) were purchased from Si-Mat (Landsberg am Lech, Germany). Ultrasonically cleaned microscope

Nexterion® Glass B slides (25 x 75.6 mm², thickness: 1.0 mm ± 0.05 mm) were obtained from SCHOTT (Jena, Germany). The acid-washed glass slides employed as internal lab controls in the experiment with marine organisms were from Fisher Scientific (Leicestershire, UK). The acid-wash treatment involved 2 h in 50% methanol: 50% hydrochloric acid followed by 2 h in 100% hydrochloric acid. 24-well plates were from IWAKI and bought from Scientific Laboratory Supplies Ltd. (Yorkshire, UK). 96-well plates (Rotilabo, F-profile) were obtained from Carl Roth GmbH (Karlsruhe, Germany). Quadriperm dishes were from Greiner Bio-One Ltd. (Stonehouse, UK). PD-10 desalting columns packed with Sephadex™ G-25 medium were obtained from GE Healthcare (Buckinghamshire, UK). De-ionized double distilled water was obtained from the Milli-Q water purification system (Milli-Q Gradient A10, Millipore, Molsheim, France).

Chemicals and solvents

Unless otherwise stated, all chemicals used were of the highest available grades.

<i>Product</i>	<i>Producer</i>
Acetone	Acros Organics (Geel, Belgium)
Amino acid standard solution	Sigma-Aldrich (Steinheim, Germany)
3-aminopropyldimethylethoxysilane (97 vol.%)	ABCR GmbH (Karlsruhe, Germany)
Ammonium hydroxide solution (28 – 30 wt.%)	Acros Organics (Geel, Belgium)
Boric acid	Sigma-Aldrich (St. Louis, US)
Calcium chloride	Merck (Darmstadt, Germany)
5-(and-6)-carboxytetramethylrhodamine, succinimidyl ester (TAMRA)	Invitrogen (Eugene, Oregon, US)
Citric acid	Sigma-Aldrich (St. Louis, US)
Dimethylsulfoxide (DMSO)	Fluka (Steinheim, Germany)

Ethanol	VWR International (Fontenay sous Bois, France)
Glutaraldehyde (25 vol.%)	Sigma-Aldrich (UK)
Hydrochloric acid solution	Fluka (Buchs, Switzerland)
Hydrogen peroxide solution (35 vol.%, not stabilized)	Merck (Darmstadt, Germany)
Immersion oil for microscopy	Zeiss (Oberkochen, Germany)
Magnesium chloride hexahydrate	Merck (Darmstadt, Germany)
2-mercaptoethanol (for molecular biology)	Sigma-Aldrich (Steinheim, Germany)
Methanol for HPLC	Acros Organics (Geel, Belgium)
Mowiol ® mounting agent	Calbiochem (La Jolla, US)
<i>N</i> -succinyl-Ala-Ala-Pro-Phe-pNA (<i>N</i> -Suc-AAPF-pNA)	Sigma-Aldrich (St. Louis, US)
<i>o</i> -phthalaldehyde (OPA)	Sigma-Aldrich (Steinheim, Germany)
Paraformaldehyde	Fluka (Buchs, Switzerland)
Phenol for GC	Fluka (Buchs, Switzerland)
Phosphate buffered saline tablets (PBS)	Sigma-Aldrich (St. Louis, US)
Poly(ethylene- <i>alt</i> -maleic anhydride) (PEMA)	Aldrich (Munich, Germany)
Poly(octadecene- <i>alt</i> -maleic anhydride) (POMA)	Polysciences Inc. (Warrington, US)
Potassium chloride	Riedel-de Haen (Seelze, Germany)
Propyl gallate	Fluka (Buchs, Switzerland)
Sodium acetate anhydrous	Fluka (Buchs, Switzerland)
Sodium bicarbonate	Sigma-Aldrich (St. Louis, US)
Sodium chloride	Riedel-de Haen (Seelze, Germany)

5 M sodium hydroxide solution (for molecular biology)	Sigma-Aldrich (St. Louis, US)
Sodium sulphate	Fluka (Steinheim, Germany)
Subtilisin A	Sigma-Aldrich (St. Louis, US)
Tetrahydrofuran (THF)	Fluka (Steinheim, Germany)
Tetrahydrofuran (THF) for HPLC	Carl Roth GmbH (Karlsruhe, Germany)
Toluene	Acros Organics (Geel, Belgium)
'Tropic Marin' artificial seawater (ASW)	Aquarientechnik GmbH (Wartenberg, Germany)

7.2 Experimental marine organisms

Zoospores of *Ulva linza*

Biological assays with zoospores of *Ulva* and cells of *Navicula perminuta* were conducted using 'Tropic Marin' commercial artificial seawater (ASW). Assays were based on those described fully in Callow *et al.* 1997 [57] and Pettitt *et al.* 2004 [23]. Briefly, fertile plants of *Ulva linza* were collected from Llanwit Major beach, Glamorgan, UK (52° 23' N; 3° 30' W), squeezed to remove excess water, wrapped in absorbent paper, transported to the lab in a cool box, and stored in a freezer.

The day of the assay, the tips of the plants were cut and transferred into glass vials to which ASW (0.2 µm-filtered) was added to start the release of spores. The volume of ASW added depended upon the concentration of spores required for the assay. The spore suspension was stored in ice and allowed to warm up to room temperature (RT) shortly before the assays. The concentration of spores in the suspension was determined through absorbance spectroscopy at 660 nm, based on the use of a calibration curve [57].

Cells of *Navicula perminuta*

Cultures of the diatom *Navicula perminuta* were isolated by Prof. Rick Wetherbee (University of Melbourne, Australia) and maintained at the lab in static culture using Guillard's F/2 medium [217] made up in natural seawater at 18 °C with a 16h:8h light:dark cycle. For the assays, cultures were allowed to warm up to RT, and thereafter cells were re-suspended in ASW to a final concentration of 0.1 µg.ml⁻¹ of extracted chlorophyll A. Absorbance spectroscopy of chlorophyll extracts in DMSO at two wavelengths was used to determine the concentration of cells in ASW [23].

Barnacle cyprids of *Balanus amphitrite*

Adult barnacles were provided by Prof. Daniel Rittschof from the Duke University Marine Lab and kept in tanks filled with strongly aerated natural seawater (salinity of 31 ppt, filtered through a 1 µm mesh size filter, and UV-sterilized) at 20 – 25 °C and with 16:8 h light:dark cycles. Barnacles were fed everyday with freshly hatched *Artemia* sp. (ca. 50 cells.ml⁻¹; Artemia International LLC, Texas, US) for 2 – 3 h and were additionally fed once or twice a week with algae^(*) (*Skeletonema costatum* or *Tetraselmis suecica*) overnight. Once a week, barnacles were scrubbed using a small brush under fresh seawater to remove adhered organisms or debris.

The release of nauplii by the adults proceeded in a tank placed in a dark area with a single-point cold light source at one end of the tank. Released nauplii moved towards the light source, where they were gently pipetted out of the tank and into a beaker containing a small amount of natural seawater and *Skeletonema costatum*. Nauplii were grown into cyprids inside a bucket containing 0.5 µm-filtered natural seawater at 28 °C, with aeration and under a 12:12 h light:dark cycle. Nauplii were added at a rate of one nauplii per ml seawater. *Skeletonema costatum* was added at 100 ml per liter seawater when at a strength of around 20 x 10⁶ cells.ml⁻¹. At the start of the culture, antibiotics^{(*)(*)} were added. When cyprids were present (usually after 4 – 5 days counting from

the day of nauplii's release), the content of the bucket was passed through three sequential filters (300 μm , 250 μm , and 160 μm mesh size filters) for the separation of cyprids to take place. All filters were washed off using cold (6 °C), 0.2 μm -filtered natural seawater into acid-rinsed glass evaporation dishes, where algae, nauplii, and moults were removed from the cyprids. Prior to use, cyprids were stored in a fridge at 6 ± 1 °C. For the settlement inhibition assays, cyprids are aged for four days in the fridge (and are defined as three-days-old cyprids because the filtering day is taken as day zero).

(*) Algal culture: *Skeletonema costatum* is cultured in standard F/2 media [217] at 19 °C in aerated natural seawater. Either a 24 h light or 12:12 h light:dark cycle is employed for fast or slow growth of *Skeletonema costatum*, respectively. Cultures proceed on a standard batch culture system.

(*)(*) Antibiotic solution: the antibiotic solution contains 36.5 $\text{mg}\cdot\text{ml}^{-1}$ Streptomycin and 21.9 $\text{mg}\cdot\text{ml}^{-1}$ Penicillin G (sodium salt), both antibiotics obtained from Sigma-Aldrich (UK). The solution is added at a rate of 1 ml per liter of natural seawater in the bucket. The solution is frozen in aliquots until needed.

7.3 Experimental techniques

7.3.1 Ellipsometry

The thickness of the immobilized Subtilisin A layer was determined by single-wavelength ellipsometry using a PCSA arrangement (EL X-02C, Dr. Riss Ellipsometerbau GmbH, Ratzeburg, Germany, angle of incidence: 70°, HeNe laser = 632.8 nm). Samples were prepared onto Si wafers and evaluated immediately after enzyme immobilization to avoid dehydration. The thickness of the immobilized enzyme layer was estimated by a five-layer (silicon/silicon dioxide/MA bound to aminosilane/enzyme layer/air) model approximation [168]

using the measured Δ and $\tan(\psi)$ values, assuming the model layers to be homogeneous, parallel and distinct. The parameters required by the model are listed in Table 7.1 (see Osaki and Werner 2003 [31] and Werner *et al.* 1999 [218] for more details). The refractive index of the enzyme layer was not determined; a comparative value of 1.375 was used instead [218]. The silicon dioxide and MA bound to aminosilane layer thicknesses were measured in advance onto additional samples to provide the required constants for the five-layer model. The enzyme layer thickness was measured in dependence of the enzyme concentration used for immobilization on both maleic anhydride copolymer films. Six independent samples were analyzed for each condition (three measurements on each sample).

Table 7.1. Parameters used for the analysis of ellipsometry data

<i>Layer</i>	<i>Refractive Index</i> $n + ji$	<i>Thickness</i> d (nm)
air	$1.0 + j 0$	
enzyme layer	$1.375 - j 0.0177$ ^{a)}	determined by the model
maleic anhydride + aminosilane	$1.5037 + j 0.0000$ ^{b)}	*
silicon dioxide	$1.4571 + j 0.0000$ ^{c)}	*
silicon	$3.8705 - j 0.0168$ ^{c)}	

*: measured in advance to provide the required constants to the five-layer model.

^{a)}: as described in Werner *et al.* 1999 [218].

^{b)}: as described in Pompe *et al.* 2003 [32] and Freudenberg *et al.* 2005 [157].

^{c)}: values taken from [219].

7.3.2 High performance liquid chromatography

The amount of immobilized Subtilisin A was determined by Amino Acid Analysis (AAA) based on High Performance Liquid Chromatography (HPLC). Chromatographic separation and analysis of the obtained amino acids were

performed with the Agilent 1100 capillary LC system (Agilent Technologies Deutschland, Böblingen, Germany) equipped with a vacuum degasser, a quaternary pump, an autosampler, a column compartment, and a fluorescent detector. The ZORBAX SB-C₁₈ column (internal diameter = 4.6 mm, length = 150 mm, particle size = 3.5 µm; Agilent Technologies GmbH, Waldbronn, Germany) was employed.

The quantification of protein amount via AAA/HPLC relied on the acidic hydrolysis of the immobilized enzyme followed by chromatographic analysis of the obtained amino acids. Extensive description of the procedure can be found elsewhere [160]. Briefly, the immobilized enzyme layer was exposed to 4 ml of 6 M hydrochloric acid (containing 1% phenol w/v) during 24 h at 110 °C in vacuum conditions. Afterwards, samples were neutralized, dried again under vacuum, and stored at -18 °C until further chromatographic analysis. Hydrolyzates were removed from the MA-coated glass slide by repetitive rinsing with 50 mM sodium acetate buffer (pH = 6.8) and thereafter derivatized with the *o*-phthalaldehyde (OPA) reagent. For that, 10 µl of the hydrolyzates sample were mixed with 30 µl of OPA reagent (25.2 mg OPA dissolved in 500 ml methanol, 20 µl 2-mercaptoethanol, 4.5 ml 0.2 M borate buffer made from boric acid, pH = 10.2 adjusted with potassium hydroxide) in the autosampler. 5 µl of the derivatized sample were injected into the system for binary gradient separation. Eluent A was 50 mM sodium acetate (pH = 6.8):methanol:tetrahydrofuran (THF) (volume ratio 80:19:1) and eluent B was methanol:50 mM sodium acetate (volume ratio 80:20). Within 30 min, a linear gradient was established from 0 % to 100 % eluent B, followed by 3 min of constant 100 % eluent B, and finally switched to 100 % eluent A. Fluorescent detection of the separated amino acids occurred at 455 nm using 355 nm as excitation wavelength.

Amino acid standards (166, 83, 42, 21 pmol) were included together with the samples. The analysis of the chromatograms was carried out with the Chemstation software Rev. 08.01 (Agilent Technologies Deutschland, Böblingen, Germany). Due to the hydrolysis and derivatization conditions, only 15 amino acids are available for the quantification of the immobilized protein amount. The

measured amino acid amounts are utilized to calculate the immobilized protein content through a MATLAB-based (v. 6, MathWorks, Natick, MA, US) algorithm. The linear equation system $AX = B$ requires the expected amino acid fractions of the protein under scrutiny (as vector A) and the measured amino acid fractions (as vector B) to determine the best fitting X matrix in the least-square sense. The final amount of protein is then provided on the basis of the best fitting calculation for the 15 amino acids included. To account for possible errors in the measured values, up to three amino acids can be excluded from the calculation when their measured fractions differ in more than 50% from the expected ones. The reported immobilized protein amounts are averages of 6 measurements per condition.

7.3.3 Absorbance spectroscopy

The activity of the immobilized enzyme was determined by following the conversion of the substrate *N*-Succinyl-Ala-Ala-Pro-Phe-pNA (*N*-Suc-AAPF-pNA) into peptides and phenylnitroaniline (pNa) through absorbance spectroscopy (TECAN Magellan GENios, Tecan, Austria) at 405 nm. *N*-Suc-AAPF-pNA was selected due to the preference of the subtilisin family of proteins for amino acid residues with aromatic or long aliphatic side-chains when ester substrates are hydrolyzed [113]. In a typical setup, enzyme-containing coatings were exposed to 1 ml of the substrate solution inside the immobilization chambers at RT for variable time periods depending on the kinetic of the reaction. Samples were analyzed immediately after the last washing step at the end of the immobilization process, or at the end of the incubation time for the aging experiments. The substrate solution was experimentally determined through the screening of different buffers, pHs, and substrate concentrations. A 0.2 mM substrate solution in PBS (pH = 7.4) obtained by dilution of a 2 mM substrate stock solution in DMSO was selected as it provided high initial conversion rates in solution as well as improved substrate stability during the assay. Periodic

extraction of aliquots of the supernatant (95 μl at each time point) allowed following the conversion of the substrate by the determination of the aliquots' optical densities (OD) at 405 nm. Aliquots were poured into the cavities of a 96-well plate already containing 5 μl of 0.1 M citric acid solution. Citric acid was added to avoid a further conversion of the substrate inside the well, either due to any possibly desorbed enzyme molecule or to the innate substrate hydrolysis.

The resulting set of OD values for each enzyme-containing coating was thereafter converted into phenylnitroaniline concentration ([pNa]) by means of a calibration curve ($[pNa] = (OD - 0.0462) / 2.7664$). The shape of the [pNa] vs. time conversion curve was fitted by an exponential function ($y = y_0 + A_1 \exp(-t/t_1)$) using the Origin software (v. 8, OriginLab Corporation, Northampton, MA, US). The initial activity was obtained as the first derivative of the fitted conversion curve at $t = 0$. Reported initial activity values are averages of 6 measurements each condition.

7.3.4 Confocal laser scanning microscopy

Confocal laser scanning microscopy (cLSM) was utilized to quantify the total immobilized protein amount in two cases: the low range of surface concentrations of the immobilized enzyme onto PEMA films, and the retained amount of immobilized enzyme after incubation in aqueous media. The quantification of protein amount was based in a combination of cLSM and AAA/HPLC: reliable surface concentrations obtained by AAA/HPLC were used to convert qualitative fluorescence data into amount of immobilized protein on the surface.

Mean fluorescence intensity values of TAMRA-labeled Subtilisin A immobilized onto MA copolymer films were assessed by cLSM (TCS SP, Leica, Bensheim, Germany) using a HeNe laser (543 nm incident light), a 40x/1.25 (numerical aperture) oil immersion objective (Immersion® oil), laser intensity below 70%, and pinhole aperture of 101.75 μm . For details about the fluorescent-labeling of Subtilisin A, see section 7.6. Fluorescent detection occurred at 590 nm.

Images (512 x 512 pixels) were processed with the Leica confocal software (Leica Microsystems Heidelberg GmbH, Mannheim, Germany) and analyzed for mean intensities with the ImageJ 1.38x software (intensity distribution determination; Wayne Rasband, National Institutes of Health, US) and the Origin v. 8 software (Gaussian-fitting of the intensity distribution function; OriginLab Corporation, Northampton, MA, US). Areas of comparable size at different spots in the specimen were analyzed. The microscope setting parameters were kept constant along measurements to allow for comparison. Prior to imaging, samples were fixed with 4 vol.% paraformaldehyde in PBS for 10 min, washed five times in PBS, and mounted in a microscope slide. A glycerol-based mounting media (Mowiol®, prepared as indicated by the producer, and modified by the addition of propyl gallate) was used to prevent photo-bleaching of the sample due to prolonged laser exposure. The mounted sample was subsequently sealed along the edges with a line of colorless nail polish. Special care was taken to avoid the formation of bubbles in the mounting media, which may blur the image.

cLSM for the low surface concentration range of the immobilized enzyme onto PEMA films

Samples consisting of TAMRA-labeled Subtilisin A immobilized onto PEMA films at various surface concentrations were analyzed via cLSM. The labeled enzyme was immobilized onto PEMA copolymer films as for the non-labeled enzyme (see section 7.5). Samples consisted of a reference sample, PEMA3 (which surface concentration was accurately determined by AAA/HPLC, Table 4.2) and several other samples of lower surface concentration than PEMA3 obtained from enzyme concentrations in solution ($[Es] = 0.5 - 10 \text{ mg.ml}^{-1}$). With equal microscope settings as those detailed above, all samples were sequentially (*i.e.* from the lowest to the highest intensity sample) imaged to assess the fluorescence emission intensity of the labeled-enzyme layer. For comparison purposes, a common laser intensity had to be determined beforehand, which could provide good imaging of all surfaces (*i.e.* enough brightness onto the low surface

concentration samples, and no photobleaching on the high surface concentration samples). Moreover, to minimize the effects of laser fluctuations with time, samples were scanned over a time frame of 1 h. Average mean intensities were determined for each condition, as explained above ($N = 3$; 3 images per sample). The ratio of the average intensities to the average intensity of PEMA3 (reference sample) was calculated and used to obtain the surface concentration of all samples assuming the image intensity has a linear dependence with the total immobilized amount. The reported surface concentrations resulted from the product between the corresponding ratio and the surface concentration of PEMA3 ($2.2 \pm 0.2 \mu\text{g}\cdot\text{cm}^{-2}$). Values are expressed as mean \pm propagated error.

cLSM for the quantification of the retained surface concentration after aging in aqueous media

Samples POMA1, PEMA1, PEMA2, PEMA3, and PEMA4 (see Table 7.3 for details) were incubated in aqueous media and analyzed for the quantification of the retained protein amount on the surface after treatment. Aged and non-aged samples of each condition (*e.g.* PEMA1 samples with and without aging) were imaged together, at equivalent microscope settings to those described above, and during a maximum time period of 45 min to reduce the impact of laser intensity variations with time. Mean intensities and intensity ratios of aged and non-aged samples of a given set were obtained as previously explained, taking the non-aged sample as a reference ($N = 4$; 5 images per sample). The surface concentrations after aging were calculated as a product between the intensity ratios and the AAA/HPLC-determined surface concentration of the reference sample. AAA/HPLC-derived values were utilized due to the high correspondence found between the surface concentrations without aging determined by cLSM and AAA/HPLC (see results in section 4.1.2). Results are reported as mean \pm propagated error.

7.3.5 Atomic force microscopy

The surface topography of the bioactive coatings was investigated using the BioScope AFM (Digital Instruments, Darmstadt, Germany). An area of $20 \times 20 \mu\text{m}^2$ was scanned in tapping mode at a speed of 0.4 lines.s^{-1} . A Si-SPM-cantilever (Tap300, Budget Sensors, Bulgaria) of spring constant of 40 N.m^{-1} and resonance frequency of *ca.* 300 kHz was used. The curvature radius of the tip was lower than 10 nm. The surface root mean square (RMS) roughness was calculated by using the WSxM 4.0 Develop software [220]. Reported RMS values are averages of 4 images per condition ($N = 2$). To avoid dehydration, surfaces were analyzed right after enzyme immobilization (active samples) or overnight exposure to the enzyme buffer (conditioned samples). Denatured samples were scanned immediately after thermal treatment. See Table 7.3 for details about active, conditioned, and denatured samples.

7.3.6 Surface wettability

Static water contact angles of samples in dry state were measured in the optical goniometer OCA30 (DataPhysics Instruments GmbH, Filderstadt, Germany) using sessile drops. $3 \mu\text{l}$ droplets of degassed Milli-Q water were deposited on the surface at a speed of $0.5 \mu\text{l.s}^{-1}$. An elliptical drop-shape fitting algorithm was used for the identification of contact angles above five degrees. A total of 6 measurements per condition was considered ($N = 2$). Samples were analyzed short after the end of the enzyme immobilization (active coatings), exposure to the enzyme buffer (conditioned coatings), or heat denaturing treatment (denatured coatings) steps. Active, conditioned, and denatured coatings are described in Table 7.3.

7.3.7 Cell density

Zoospores of *Ulva linza* and cells of *Navicula perminuta*

Zoospores and diatom cells were visualized by virtue of autofluorescence of chlorophyll using a Zeiss Axioplan epifluorescence microscope (Carl Zeiss AG, Germany) coupled to a short-arc mercury vapor lamp, as described in Callow *et al.* 2002 [221]. The excitation and emission wavelengths were set at 546 and 590 nm, respectively. Semi-automated cell counts were made using Zeiss Kontron 3000 image analysis software (Carl Zeiss AG, Germany) with 30 random fields of view being quantified for each replicate (N = 3). The fields of view were taken in the central area of the sample, along its long axis. Results are reported as mean ± 2 x standard error for each condition.

Barnacle cyprids of *Balanus amphitrite*

Settled and unsettled (divided into dead, floating, and swimming) cyprids were quantified by means of traditional optical microscopy. Samples were thoroughly inspected to determine the total number of settled cyprids and their location in the area covered by the enzyme (*i.e.* central or close-to-the-borders area). Settled cyprids were differentiated into permanently-settled and newly-metamorphosed cyprids. The identification of fallen-off cyprids, and their posterior quantification, was performed with particular care by an experienced microscopist (Ms. Sheelagh Conlan). Larvae that did not settle after the 48 h experimental period were observed for signs of abnormal behavior or compromise in their normal physiological functions. All referred observations were reported as part of the results. Twelve (active coatings) or six (denatured and conditioned base coatings) replicates each condition were considered (see Table 7.3 for details about these coatings). Results are reported as mean $\pm 95\%$ confidence limit.

7.3.8 Cell adhesion strength

The strength of adhesion of the evaluated marine organisms was assessed by using a water jet apparatus [214] (*Ulva* zoospores) or a flow channel device [215] (diatom cells).

Water jet apparatus

The automated water jet device utilized in the assays with zoospores of *Ulva* comprised a sample holder with computer-controlled planar movements, a nozzle (1.6 mm internal exit diameter) mounted 25 mm from the surface of the sample, and a water tank pressurized by means of a compressed air supplier SCUBA tank. In operation, the sample holder was horizontally moved at a speed of 10 mm.s⁻¹ and, at the end of the horizontal traverse, displaced 2 mm down for another line to be jetted. A total of 10 sweeps resulted in an exposed area of around 500 mm² in the mid-region of each sample. The pressure on the surface was determined from a calibration curve built-up by using a force transducer and by observing the area impinged by the water jet at each setting of the compressed air regulator [216].

Flow channel device

The turbulent flow channel device employed to evaluate the adhesion strength of the microfouler *Navicula perminuta* was equipped as generally described in 3.7. The settling chamber was composed of a series of perforated or porous honeycomb-like parallel plates, which reduced the flow turbulence levels. A nozzle placed at the end of the settling chamber accelerated the flow before entering the test zone. The sample holder accommodated six microscope slides with their long axis parallel to the flow. Slides were held in place by the application of vacuum from their reverse sides [215]. A calibration curve relating the flow rate to the wall shear stress was determined for this device over a range of velocities, according to Schultz *et al.* 2000 [215].

7.4 Polymer film preparation

Substrate cleaning

Silicon wafers and glass coverslips were cleaned by sonication in Milli-Q water and thereafter in ethanol p.a. for 30 min to remove adhered particles and organic residues, respectively. Oxidation of the samples' surface was performed by immersing the samples into a water:hydrogen peroxide:ammonia (volume ratio 5:1:1) solution at 70 °C during 10 min. Special quartz containers were employed for this aim. Upon completion of the oxidizing treatment, samples were rinsed three times with Milli-Q water, dried with a N₂-gas stream, and heat-treated at 120 °C for 1 h.

Aminosilanization

Immediately after the heat-treatment, samples were placed inside a Petri dish containing 100 µl of 3-aminopropyldimethylethoxysilane. The dish was sealed with Parafilm and kept at room temperature overnight to complete the evaporation of the dispensed aminosilane. Aminosilane molecules not bound to the glass or silicon surfaces were removed by thorough rinsing in toluene (5 x immersions) followed by drying under N₂-gas stream. Aminosilane-modified slides were treated at 120 °C for 1 h, after what the spin-coating of the maleic anhydride (MA) copolymer solutions was carried out.

Maleic anhydride copolymer

Maleic anhydride copolymer films were prepared as described previously [32]. Briefly, copolymer solutions of poly(ethylene-*alt*-maleic anhydride) (PEMA) and poly(octadecene-*alt*-maleic anhydride) (POMA) were prepared at concentrations of 0.15 and 0.08 wt.%, respectively. The copolymer solutions were made one day prior to use by dissolving PEMA in a mixture of THF:acetone (2:1 weight ratio) and POMA in THF, then stored overnight in the dark to complete the dissolution

of the copolymer powder, and finally filtered through a 0.2 μm polytetrafluoroethylene syringe filter before spin-coating. The prepared copolymer solutions were stored in the dark at RT. Aminosilane-modified silicon or glass surfaces were spin-coated (RC5, Suess Microtec, Garching, Germany) at 4000 rpm and $1500 \text{ rpm}\cdot\text{s}^{-1}$ during 30 s using freshly prepared (or not older than seven days) PEMA and POMA copolymer solutions. Stable covalent binding of the deposited maleic anhydride films was achieved by annealing at $120 \text{ }^\circ\text{C}$ during 2 h to generate imide bonds with the aminosilane-modified silica surface.

7.5 Covalent immobilization of Subtilisin A

Reactive immobilization of Subtilisin A onto PEMA and POMA copolymer films was achieved by exposing the copolymer layers to enzyme solutions of variable concentration. Prior to enzyme immobilization, the anhydride moieties of the copolymers were hydrolyzed into the diacid form by autoclaving ($120 \text{ }^\circ\text{C}$, 20 min and saturated water vapor for PEMA or 15 min and unsaturated water vapor for POMA) and subsequently regenerated upon annealing at $120 \text{ }^\circ\text{C}$ for 2 h. Enzyme immobilization was performed immediately after annealing of the copolymer surfaces to avoid the slow conversion of the reactive anhydride groups upon exposure to ambient humidity.

The enzyme solution (Es) was freshly prepared short before enzyme immobilization by dissolving lyophilized Subtilisin A in PBS modified by the addition of calcium chloride and sodium chloride at concentrations of 2 mM and 0.1 M, respectively [222]. The addition of Ca^{2+} ions to the enzyme solution has its roots on the calcium dependent behavior of the subtilisin-like family of proteases: bound calcium ions play a key role in protecting subtilisin-like proteases against autolysis and thermal denaturation [100; 115]. The pH of the enzyme solution was set to 8.6 (adjusted with 1 M and 5 M sodium hydroxide solutions), in agreement with the reported optimum pH range for this enzyme

[114; product datasheet]. The enzyme solution concentration ($[Es]$) was varied between 0.5 and 30 $\text{mg}\cdot\text{ml}^{-1}$.

Enzyme immobilization was performed using in-house constructed immobilization chambers, essentially a device allowing samples to be placed at the bottom of a cavity onto which the enzyme solution is poured. Two types of immobilization chambers were employed: one for the glass coverslips and silicon wafers, and another one for the microscope slides used in the biological assays (Figure 7.1). The volume of Es employed was of 500 μl for the glass and silicon surfaces, and of 1.875 μl for the microscope slides, so the height of the liquid Es column was the same irrespective of the different immobilization area (*i.e.* 2 cm^2 for the glass/silicon surfaces or 7.5 cm^2 for the microscope slides).

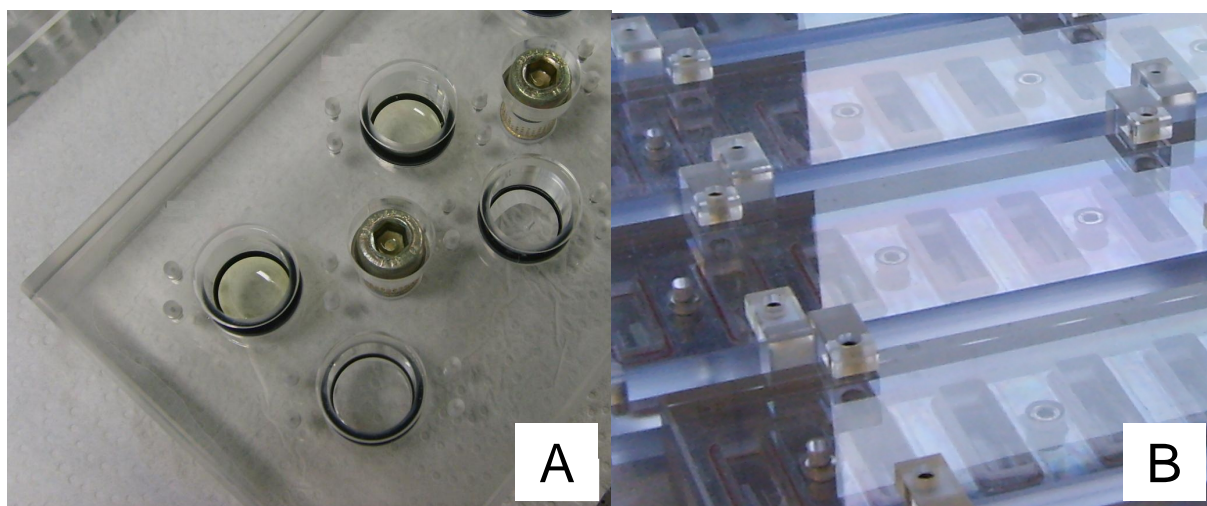


Fig. 7.1. Immobilization chambers employed for the obtainment of an immobilized enzyme layer. Immobilization chambers used with (A) glass coverslips and silicon wafers, (B) microscope slides.

Enzyme immobilization proceeded overnight at RT and in steady conditions (*i.e.* without shaking or oscillation of the immobilization chambers). After overnight exposure to Es, samples were gently rinsed 10 times with Milli-Q water to remove any unbound protein prior to the enzyme layer characterization steps (described below).

7.6 Enzyme layer characterization

Enzyme layer thickness

The thickness of the immobilized Subtilisin A layer was determined by single-wavelength ellipsometry onto freshly prepared samples as described in section 7.3.1.

Immobilized protein amount

The amount of protein immobilized onto MA copolymer films was determined by amino acid analysis (AAA) based on High Performance Liquid Chromatography (HPLC) and by confocal Laser Scanning Microscopy (cLSM) using fluorescently-labeled Subtilisin A. AAA via HPLC was performed for the whole range of enzyme concentrations in solution and for both copolymer types employed in this work, following the protocol described in section 7.3.2. For the low range of enzyme surface concentrations obtained by HPLC (corresponding to protein amounts close to the detection limit of HPLC and usually associated with several amino acids excluded from the calculation), the use of cLSM of immobilized TAMRA-labeled Subtilisin A was proposed. The methodology details associated to the fluorescence microscopy of TAMRA-labeled enzyme can be found in section 7.3.4.

TAMRA-labeled Subtilisin A was obtained by mixing 2 ml of 5 mg.ml⁻¹ enzyme in sodium bicarbonate buffer (100 mM, pH = 8.3) with 100 µl of 5 mg.ml⁻¹ TAMRA in DMSO and additional 400 µl of sodium bicarbonate buffer. The reaction was let to proceed for 90 min at RT in a horizontal shaker and in the dark. The conjugate was separated by using a SephadexTM G-25 desalting column and PBS as eluting buffer. The protein content was determined by absorbance spectroscopy at 280 nm (NanoDrop ND-1000 UV-Vis spectrophotometer, Wilmington, Delaware, US) and recalculated by means of a calibration curve (data not shown). The degree of labeling was determined as the ratio between the absorbance of the fluorophore solution in PBS at 555 nm and the molar extinction

coefficient of the dye at 555 nm ($65,000 \text{ cm}^{-1} \cdot \text{M}^{-1}$) multiplied by the protein concentration in molar units. Degrees of labeling from 0.2 to 0.6 mol of dye per mol of enzyme molecule were attainable.

Activity

The catalytic activity of the immobilized enzyme layer was determined by following the conversion of the chromogenic substrate N-Suc-AAPF-pNA into peptides and pNa through absorbance spectroscopy at 405 nm, as explained in section 7.3.3. The activity of the immobilized layer is reported as the initial (*i.e.* at $t = 0$) slope of the [pNa] vs. time reaction curve for all bioactive coatings.

Specific activity

The specific activity stands for the ratio between the activity provided by a bioactive layer and the amount of immobilized protein (per unit area) constituting that layer. The specific activity is then an indicator of the catalytic capability provided per immobilized enzyme molecule (active or not), and allows for a comparison between different immobilization platforms and/or surface concentrations. Due to the random immobilization strategy employed in this work, only a fraction of the immobilized enzyme molecules is active, hence resulting in lower specific activity values than those expected for bioactive layers of higher activity retention after immobilization (as with site-directed immobilization [154]). Taken together, the specific activity value can be exploited as a useful indicator of the “effectiveness” of a given polymeric platform in providing higher activity yields per immobilized molecule.

Surface morphology and wettability

The surface morphology and wettability of the bioactive, denatured and conditioned base coatings employed in the biological assays (see Table 7.3 for details about these coatings) were investigated as described in sections 7.3.5 and 7.3.6. AFM was employed to determine the RMS roughness of all coatings in dry

state. Static water contact angles of active and control coatings were measured in air and utilized as an indicator of the surface wettability.

7.7 Enzyme layer stability in aqueous media

The stability in aqueous media of the enzyme-containing coatings was evaluated by incubating selected samples in Milli-Q water and in a substitute of commercial artificial sea water (ASW*) for 6 and 24 h at RT. ASW* was employed instead of natural or commercial ASW to guarantee the reproducibility of the experimental aging solution and the absence of organic contaminants. The ASW* contained the five main salts present in seawater, according to the ASTM D1141-98 standard [223] (Table 7.2).

Table 7.2. Composition of the substitute of artificial seawater, ASW*

<i>Salt</i>	<i>Concentration</i> (<i>mM</i>)
sodium chloride	420
magnesium chloride hexahydrate	54.6
sodium sulphate	28.8
calcium chloride	10.45
potassium chloride	9.3

The evaluated bioactive coatings included two samples with similar initial activity immobilized onto polymer coatings of different physicochemical properties (PEMA1 and POMA1) and samples with increasing initial activities (PEMA1, PEMA2, PEMA3, and PEMA4). The selected group of samples coincides with that used for the biological assays, and it is described in Table 7.3.

After exposure to the aging solution for 6 or 24 h, the stability of the enzyme layer was assessed by evaluating both initial activity and enzyme surface

concentration. These two characteristic properties were monitored in an attempt to correlate depletion in activity after aging with possible decrease in immobilized protein amount. The catalytic activity of the enzyme layer after aging was determined following the reaction conversion of N-Suc-AAPF-pNA, as described in section 7.3.3. The initial activity was determined for 5 samples exposed to each condition. The surface concentration was evaluated by cLSM using immobilized TAMRA-labeled Subtilisin A (see sections 7.3.4 and 7.6 for details). Aging experiments were repeated twice.

Since the biological assays with barnacle cyprids implied the exposure of the enzyme-containing coating to ASW for a maximum length of 48 h, the activity of those coatings after 48 h incubation in ASW* was also investigated to determine the levels of activity retention after that time period. The activity assays after 48 h incubation in ASW* proceeded as described above for 6 or 24 h aging. Milli-Q water was not included as incubation media at 48 h due to the lack of substantial differences found between both incubation solutions at 6 and 24 h regarding their effect onto the residual activity (see results in section 4.2).

7.8 Biological assays with micro and macrofoulers

The biological assays described in this section were performed with cells of the diatom *Navicula perminuta* and zoospores of the alga *Ulva linza* (microfoulers), and with barnacle cyprids of *Balanus amphitrite* (macrofouler) (see section 3.1.1 for additional information about the marine organisms). Two main cases were considered during the biological assays: one in which the organisms were exposed to variable concentrations of the enzyme in solution using the MA copolymer films as substrates, and another one consisting in the exposure of the organisms to the enzyme bound to MA copolymer films at increasing concentration and activity on the surface. These two cases made it possible to compare soluble and tethered enzyme by correlating enzyme concentrations in solution with equivalent amounts of enzyme immobilized on the surface. Additionally, negative controls (obtained

by denaturing the immobilized enzyme layer) were included. The denatured coatings allowed to compare active and inactive enzyme layers at equal enzyme surface concentration and distribution. Table 7.3 below provides a list of the samples employed during the biological assays together with their mode of preparation. All samples were prepared *in-situ* to guaranty the properties of the coatings were as determined during the characterization steps.

Table 7.3. Samples utilized in the biological assays with micro and macrofoulers

<i>Coating type</i>	<i>Coating label</i>	<i>[Es]</i> <i>(mg.mL⁻¹)^b</i>	<i>Mode of preparation</i>
Active coatings ^{a)}	POMA1	7	Overnight enzyme immobilization from solutions of variable concentration. Removal of unbound enzyme and rinsing prior to assay (as detailed in 7.5) ^(*) .
	PEMA1	3	
	PEMA2	10	
	PEMA3	20	
	PEMA4	30	
Denatured coatings ^{a)}	POMA1 – D	7	Active coatings submitted to heat-denaturing treatment (45 min at 120 °C). Rinsing prior to assay.
	PEMA1 – D	3	
	PEMA2 – D	10	
	PEMA3 – D	20	
	PEMA4 – D	30	
Conditioned base coatings	POMA	0	Overnight exposure of the base MA copolymer films to the enzyme buffer ^(*) . Rinsing prior to assay.
	PEMA	0	

^{a)}: POMA and PEMA refer to the maleic anhydride copolymer film used as immobilization platform; ^{b)}: enzyme concentration in solution used during the immobilization process; ^(*): the enzyme buffer was different to that described in section 7.5; it consisted of PBS (without the addition of calcium chloride and sodium chloride), pH increased to 8.6 with sodium hydroxide solution.

The active coatings were prepared as outlined in section 7.5, but changing the enzyme buffer to PBS alone (*i.e.* without calcium chloride and sodium chloride), pH = 8.6 modified by addition of sodium hydroxide solution. The denatured coatings were obtained by heat-denaturing treatment (45 min at 120 °C) of the active coatings short after the end of the enzyme immobilization process. The conditioned base coatings consisted of MA copolymer films prepared as for enzyme immobilization but exposed overnight to the enzyme buffer alone (instead of exposed to the enzyme solution). For all coatings, a rinsing step was carried out at the end of the respective treatments, involving 10x immersion in a beaker containing distilled water. Samples with and without enzyme were rinsed separately, as well as samples of different enzyme surface concentration, to avoid cross-contamination.

Assays with zoospores of *Ulva linza*

Spores from a single release of plant tissue were used for all assays. Active, denatured, and conditioned base coatings were exposed to 10 ml of a suspension of 1.5×10^6 spores.ml⁻¹ in ASW for 45 min in the dark, as described in Callow *et al.* 1997 [57]. All slides were then rinsed gently in ASW to remove unsettled (motile) spores, leaving just those that had settled and adhered to each coating. Active and denatured coatings were incubated in 10 ml of ASW for 1.5 h, whilst conditioned base coatings were incubated with 10 ml of 0, 8, 25 or 50 µg.ml⁻¹ Subtilisin A in ASW for the same duration. Once the incubation period had elapsed, three replicate slides of each coating were fixed in 2.5 vol.% glutaraldehyde in ASW for 15 min and subsequently washed in ASW, 50 vol.% ASW, and distilled water before drying. These slides give the initial settlement density of spores on each coating. The remaining three replicate slides were exposed to an impact pressure of 34 kPa in the water-jet apparatus (see section 7.3.8), prior to fixation. The difference in spore numbers between unexposed slides and those subjected to impact pressure was used to calculate the

mean spore removal as a percentage of the initial settled population. Quantification of spores' number proceeded as explained in section 7.3.7.

Data were tested for normality using the Anderson-Darling test for conformity. Percentage removal data departed from a normal distribution, and were arcsine-transformed prior to applying parametric tests. Analysis of variance, either nested one-way or two-way in design, was used to determine the significance of the collective difference, with a post-hoc Tukey's HSD test to determine the significance of pair-wise comparisons within the analysis.

Assays with cells of *Navicula perminuta*

The assays with cells of the diatom *Navicula* followed the same general schema as that conducted with spores of *Ulva*, and is described fully in Pettitt *et al.* 2004 [23]. Diatom cells are not motile in the water column and in laboratory assays reach a surface as a result of gravity. Thus, at the end of the incubation period, there is the same number of cells present on every surface. Any differences in the number of cells attached after gentle washing is therefore a consequence of differences in the ability of cells to initially adhere to the substratum. A $0.1 \mu\text{gchla.ml}^{-1}$ suspension of cells was allowed to settle and adhere to active, denatured, and conditioned base coatings for 2 h. Slides were rinsed to remove non-attached cells as for the assay with *Ulva* and incubated for 3 h in 10 ml of ASW (active and denatured coatings) or 10 ml of 0, 8, 25 or $50 \mu\text{g.ml}^{-1}$ Subtilisin A in ASW (conditioned base coatings) prior to fixation or exposure to hydrodynamic shear. As diatom cells generally adhere less strongly than spores of *Ulva*, an alternative method for cell removal was employed, *viz.* application of 35 Pa wall shear stress in the flow-channel apparatus (see section 7.3.8). Cell fixation, visualization and quantification, as well as the statistical analysis of the data, were as described for *Ulva*.

*Assays with cyprids of *Balanus amphitrite**

Barnacle drop settlement assay was performed adapting a methodology described elsewhere [59]. Active and denatured samples were placed in quadriperm dishes and 1 ml of ASW (30 ppt) was deposited onto the surfaces. To that volume, additional 0.5 ml of ASW containing 40 (day 3 of age) cyprids were added. The conditioned base coatings were treated as the active and denatured ones, but using ASW modified by the addition of Subtilisin A at concentrations of 0, 0.5, 1, or 1.5 $\mu\text{g}\cdot\text{ml}^{-1}$. Dishes were thereafter placed in a dark incubator at 28 °C for 24 and 48 h prior to settlement and mortality enumeration. The quadriperm dishes were wrapped with damp paper towels to provide sufficient moisture as to prevent desiccation of the drop during incubation. After 24 and 48 h, slides were taken out the incubator for settlement quantification, which proceeded as described in 7.3.7. Twelve (active coatings) or six (denatured and conditioned base coatings) replicates each condition were considered.

Due to the high hydrophilicity of the bioactive MA copolymer coatings tested, the abovementioned methodology for the settlement assays with barnacle cyprids needed a modification to avoid the otherwise observed spreading of the dispensed drop onto the surfaces. For that, a thin layer of wax was deposited around the central area occupied by the enzyme on the microscope slides. Deposition was carried out by dip-coating the microscope slides alongside their four edges in a wax pool (paraffin, 60 °C) at the end of the immobilization process. This wax ‘fence’ helped confining cyprids to the area in which the enzyme was immobilized and prevented cyprids from settling in enzyme-free areas, like the grooves resulting from the use of O’rings as sealants in the immobilization chambers, or the regions non-exposed to the enzyme in solution.

Six acid-washed glass (AWG) slides and a 24-well polystyrene plate were run alongside each settlement assay. AWG slides were used as controls to ensure the health, viability, and settlement levels of cyprids were within an acceptable range and to account for any variation between batches. The 24-well plate was used as an internal laboratory standard. AWG slides were assayed as the coatings

under evaluation. For the 24-well plate, 2 ml of ASW were added to each well prior to the incorporation of ten cyprids (day 3 of age) in the absolute minimum of ASW. The 24-well plate was thereafter placed in the incubator and treated as the rest of the samples.

Settlement results are given as mean percentage settlement (*i.e.* mean of the number of settled cyprids expressed as a percentage of the total number of dispensed cyprids) with 95% confidence intervals. Settlement data were analyzed for statistical differences using the Kruskal-Wallis method.

Abbreviations

2D	Two dimensional
3D	Three dimensional
AAA	Amino acid analysis
AF	Antifouling
AFM	Atomic force microscopy
ASW	'Tropic Marin' artificial seawater
ASW*	Substitute of commercial artificial sea water
AWG	Acid-washed glass
cLSM	Confocal laser scanning microscopy
DMSO	Dimethylsulfoxide
EPS	Extracellular polymeric substances
Es	Enzyme solution
[Es]	Concentration of the enzyme solution
FC	Flow channel

FR	Fouling-release
HeNe	Helio-Neon
HPLC	High performance liquid chromatography
IR	Infrared
MA	Maleic anhydride
Milli-Q water	De-ionized double distilled water
N	Number of samples
NA	Numerical aperture
N-Suc-AAPF-pNA	<i>N</i> -succinyl-Ala-Ala-Pro-Phe-pNA
OD	Optical density
OPA	<i>o</i> -phthalaldehyde
PBS	Phosphate buffered saline
PCSA	Polarizer-compensator-sample-analyzer
PEMA	Poly(ethylene- <i>alt</i> -maleic anhydride)
pNa	Phenylnitroaniline
[pNa]	Concentration of phenylnitroaniline
pNA	Phenylnitroanilide
POMA	Poly(octadecene- <i>alt</i> -maleic anhydride)
RMS	Root mean square roughness
RPC	Reverse phase chromatography
RT	Room temperature
SEM	Scanning electron microscope

$t_{1/2}$	Time to consume half of the available substrate
TAMRA	5-(and-6)-carboxytetramethylrhodamine, succinimidyl ester
THF	Tetrahydrofuran
UV	Ultraviolet
WJ	Water jet

List of Figures

1.1	Use of proteolytic enzymes to prevent biofouling	3
2.1	Strategy towards the goal	6
3.1	Examples of biofouling	10
3.2	Temporal sequence of the biofouling process	11
3.3	Zoospore of <i>Ulva linza</i> and settlement process	14
3.4	Cell of <i>Navicula</i> sp. diatom	15
3.5	Cyprid of <i>Balanus amphitrite</i> and settlement process	16
3.6	Schematic depiction of the enzyme molecular structure	22
3.7	Crystal structure of HIV protease with its substrate	23
3.8	Hydrolysis of peptide bonds by subtilisins	25
3.9	Depiction of the molecular structure of Subtilisin A	27
3.10	Immobilization strategies	29
3.11	Schematic representation of random and site-directed enzyme immobilization	30

3.12 Schematic depiction of the preparation of maleic anhydride copolymer thin films	32
3.13 Covalent immobilization of biomolecules to maleic anhydride copolymer films by aminolysis	33
3.14 Basic PCSA ellipsometry setup	34
3.15 Schematic representation of an HPLC unit	37
3.16 Principle of absorbance spectroscopy	38
3.17 Principle of the confocal microscope	40
3.18 Tapping mode AFM setup	41
3.19 Contact angle formation on a solid surface	43
3.20 Schematic view of the water jet apparatus	44
3.21 Illustrative depiction of the turbulent flow channel device	45
4.1 Schematic depiction of maleic anhydride copolymer films	48
4.2 Thickness of the immobilized enzyme layer	49
4.3 Immobilized amount of protein	50
4.4 Correspondence between thickness and surface concentration	52
4.5 Schematic representation of the bioactive layers	52
4.6 Initial activity of the bioactive layers	53
4.7 $t_{1/2}$ (time to consume half of the substrate)	54
4.8 Specific activity of immobilized Subtilisin A	56
4.9 Initial activity, immobilized amount of enzyme, and specific activity after aging	60
4.10 Initial activity of the bioactive coatings after 48 h incubation in ASW*	61

4.11 Removal of spores of <i>Ulva</i> from conditioned MA films after incubation with Subtilisin A in solution	63
4.12 Removal of cells of <i>Navicula</i> from conditioned MA films after incubation with Subtilisin A in solution	65
4.13 Mean percentage settlement of <i>Balanus amphitrite</i> cyprids to conditioned MA films in the presence of Subtilisin A in solution	66
4.14 Adhesion strength of spores of <i>Ulva</i> to denatured and active coatings with increasing activity of Subtilisin A	69
4.15 Removal of spores of <i>Ulva</i> from active PEMA coatings of increasing activity	70
4.16 Epifluorescence microscopy images of settled <i>Ulva</i> spores onto PEMA3 and PEMA3 – D	71
4.17 Adhesion strength of spores of <i>Ulva</i> to coatings of similar activity but onto different copolymer platforms	72
4.18 Adhesion strength of spores to PEMA + 8 $\mu\text{g.ml}^{-1}$, PEMA3, and control coatings	74
4.19 Adhesion strength of cells of <i>Navicula</i> to denatured and active coatings with increasing activity of Subtilisin A	76
4.20 Removal of cells of <i>Navicula</i> from active PEMA coatings of increasing activity	77
4.21 Adhesion strength of cells of <i>Navicula</i> to coatings of similar activity but onto different copolymer platforms	78
4.22 Adhesion strength of diatom cells to PEMA + 8 $\mu\text{g.ml}^{-1}$, PEMA3, and control coatings	79
4.23 Mean percent settlement of barnacle cyprids onto PEMA active coatings of increasing activity	81
4.24 Settlement distribution of barnacle cyprids onto PEMA1 and PEMA1– D	82
4.25 Relative number of cyprids metamorphosed and fallen-off for PEMA active coatings of increasing activity	84

4.26	Mean percent settlement of barnacle cyprids onto PEMA + 1 $\mu\text{g}\cdot\text{ml}^{-1}$, PEMA1, and control coatings	85
5.1	Structure-property relationships for Subtilisin A immobilized onto PEMA and POMA films	89
5.2	Mechanisms of biofouling control with immobilized Subtilisin A	91
7.1	Immobilization chambers	112

List of Tables

3.1	Survey of properties of the MA copolymer films	31
4.1	Surface roughness and wettability of the surfaces tested in the biological assays	57
4.2	Initial activity and surface concentration of the active coatings used in the biological assays	68
7.1	Parameters used for the analysis of ellipsometry data	101
7.2	Composition of the substitute of artificial seawater, ASW*	115
7.3	Samples utilized in the biological assays	117

References

- [1] D. M. Yebra, *Prog. Org. Coat.* **2004**, *50*, 75.
- [2] J. B. Kristensen et al., *Biotech. Adv.* **2008**, *26*, 471.
- [3] P. Landini, G. Jubelin and C. Dorel-Flamant, “The Molecular Genetics of Bioadhesion and Biofilm Formation”, in: *Biological Adhesives*, A. M. Smith and J. A. Callow, Eds., Springer-Verlag, Heidelberg 2006.
- [4] M. E. Callow and J. A. Callow, *Biologist* **2002**, *49(1)*, 1.
- [5] I. W. Sutherland, *Microbiology* **2001**, *147*, 3.
- [6] K. Kamino, “Barnacle Underwater Attachment”, in: *Biological Adhesives*, A. M. Smith and J. A. Callow, Eds., Springer-Verlag, Heidelberg 2006.
- [7] A. Chiovitti, T. M. Dugdale and R. Wetherbee, “Diatom Adhesives: Molecular and Mechanical Properties”, in: *Biological Adhesives*, A. M. Smith and J. A. Callow, Eds., Springer-Verlag, Heidelberg 2006.
- [8] J. A. Callow and M. E. Callow, “The *Ulva* Spore Adhesive System”, in: *Biological Adhesives*, A. M. Smith and J. A. Callow, Eds., Springer-Verlag, Heidelberg 2006.
- [9] P. J. Molino and R. Wetherbee, *Biofouling* **2008**, *24(5)*, 365.

- [10] T. M. Dugdale et al., *Biophys. J.* **2006**, 90(8), L58.
- [11] T. M. Dugdale et al., *Biophys. J.* **2006**, 90(8), 2987.
- [12] T. M. Dugdale et al., *Biophys. J.* **2005**, 89(6), 4252.
- [13] A. Chiovitti et al., *Soft Matter* **2008**, 4, 811.
- [14] C. Leroy et al., *J. Appl. Microbiol.* **2008**, 105, 791.
- [15] M. S. Stanley et al., *Planta* **1999**, 210, 61.
- [16] A. S. Clare et al., *J. Mar. Biol. Assoc.* **1994**, 74, 243.
- [17] K. Matsumura et al., *Proc. R. Soc. London B* **1998**, 265, 1825.
- [18] A. S. Clare and K. Matsumura, *Biofouling* **2000**, 15(1–3), 57.
- [19] C. Dreanno et al., *Biol. Lett.* **2006**, 2, 423.
- [20] C. Dreanno et al., *Proc. Natl. Acad. Sci. U.S. A.* **2006**, 103(39), 14396.
- [21] B. P. Lee, J. L. Dalsin and P. M. Messersmith, “Biomimetic Adhesive Polymers Based on Mussel Adhesive Proteins”, in: *Biological Adhesives*, A. M. Smith and J. A. Callow, Eds., Springer-Verlag, Heidelberg 2006.
- [22] S. M. Olsen et al., *Biofouling* **2007**, 23(5), 369.
- [23] M. E. Pettitt et al., *Biofouling* **2004**, 20(6), 299.
- [24] N. Aldred et al., *Biofouling* **2008**, 24(2), 97.
- [25] C. Leroy et al., *Biofouling* **2008**, 24(1), 11.
- [26] J. H. Paul and W. H. Jeffrey, *Appl. Environ. Microbiol.* **1985**, 50(2), 431.
- [27] Y. D. Kim et al., *Biotechnol. Bioeng.* **2001**, 72(4), 475.
- [28] S. Dobretsov et al., *Mar. Biotechnol.* **2007**, 9(3), 388.
- [29] R. L. Townsin, *Biofouling* **2003**, 19(Suppl), 9.

- [30] P. S. Murthy, V. P. Venugopalan, K. V. K. Nair and T. Subramoniam, "Larval Settlement and Surfaces: Implications in Development of Antifouling Strategies", in: *Marine and Industrial Biofouling*, H.-C. Flemming, P. S. Murthy, R. Venkatesan and K. E. Cooksey, Eds., Springer-Verlag, Berlin 2009.
- [31] T. Osaki and C. Werner, *Langmuir* **2003**, *19*, 5787.
- [32] T. Pompe et al., *Biomacromolecules* **2003**, *4*, 1072.
- [33] T. Pompe et al., *Macromol. Biosci.* **2005**, *5*, 890.
- [34] P. Uhlmann et al., *Langmuir* **2005**, *21*, 6302.
- [35] C. Sperling et al., *Biomaterials* **2004**, *25*, 5101.
- [36] K. Alberti et al., *Nat. Methods* **2008**, *5*, 645.
- [37] M.-F. Gouzy et al., *Biomaterials* **2004**, *25*, 3493.
- [38] K. Salchert et al., *Acta Biomater.* **2005**, *1*, 441.
- [39] D. E. Wendt et al., *Biofouling* **2006**, *22(1)*, 1.
- [40] J. F. Schumacher et al., *Biofouling* **2007**, *23(1)*, 55.
- [41] M. P. Schultz, *Biofouling* **2007**, *23(5)*, 331.
- [42] A. Allion et al., *Biofouling* **2006**, *22(5)*, 269.
- [43] P. Majumdar et al., *Biofouling* **2008**, *24(3)*, 185.
- [44] T. Vladkova, "Surface Modification Approach to Control Biofouling", in: *Marine and Industrial Biofouling*, H.-C. Flemming, P. S. Murthy, R. Venkatesan and K. E. Cooksey, Eds., Springer-Verlag, Berlin 2009.
- [45] S. Dobretsov et al., *Biofouling* **2006**, *22(1/2)*, 43.
- [46] M. E. Callow, *Biodeterior. Abstr.* **1996**, *10*, 411.

- [47] A. P. Haag, “Mechanic Properties of Bacterial Exopolymeric Adhesives and Their Commercial Development”, in: *Biological Adhesives*, A. M. Smith and J. A. Callow, Eds., Springer-Verlag, Heidelberg 2006.
- [48] J. F. Schumacher et al., *Biofouling* **2007**, *23(5)*, 307.
- [49] A. J. Scardino et al., *Biofouling* **2008**, *24(1)*, 45.
- [50] S. Schilp et al., *Biointerphases* **2007**, *2*, 143.
- [51] L. K. Ista et al., *Appl. Environ. Microbiol.* **2004**, *70(7)*, 4151.
- [52] S. S. Branda et al., *Trends Microbiol.* **2005**, *13*, 20.
- [53] M. Otto, *Curr. Top. Microbiol. Immunol.* **2006**, *306*, 251.
- [54] A. I. Railkin, “*Marine Biofouling: Colonization Processes and Defences*”, CRC Press, US 2004, p. 1–8.
- [55] N. Aldred and A. S. Clare, *Biofouling* **2008**, *24(5)*, 351.
- [56] C. J. Kavanagh et al., *J. Adhes.* **2005**, *81*, 843.
- [57] M. E. Callow et al., *J. Phycol.* **1997**, *33*, 938.
- [58] J. A. Callow et al., *Planta* **2000**, *211*, 641.
- [59] Y. Tang et al., *Biofouling* **2005**, *21(1)*, 59.
- [60] J. A. Finlay et al., *Integr. Comp. Biol.* **2002**, *42*, 1116.
- [61] M. L. Carman et al., *Biofouling* **2006**, *22(1)*, 11.
- [62] J. A. Callow et al., *J. R. Soc. Interface* **2005**, *2*, 319.
- [63] A. Statz et al., *Biofouling* **2006**, *22(6)*, 391.
- [64] D. M. McMaster et al., *Biofouling* **2009**, *25(1)*, 21.
- [65] M. K. Chaudhury et al., *Biofouling* **2005**, *21(1)*, 41.
- [66] J. Bowen et al., *J. R. Soc. Interface* **2007**, *4(14)*, 473.
- [67] J. Kim et al., *Biofouling* **2008**, *24(4)*, 313.

- [68] R. E. Pérez-Roa et al., *Biofouling* **2008**, 24(3), 177.
- [69] L. Gipperth, *J. Environm. Management* **2009**, 90, S86.
- [70] R. F. Brady and I. L. Singer, *Biofouling* **2000**, 15(1–3), 73.
- [71] J. Kim et al., *Biofouling* **2007**, 23(2), 113.
- [72] N. Fusetani and A. S. Clare (Eds.), “*Antifouling Compounds*”, series Progress in Molecular and Subcellular Biology, vol. 42, Springer-Verlag, Berlin 2006.
- [73] T. Ekblad et al., *Biomacromolecules* **2008**, 9(10), 2775.
- [74] C. Baum et al., *Comp. Biochem. Physiol., Part A* **2001**, 130, 835.
- [75] J. G. Burgess et al., *Biofouling* **2003**, 19(Suppl.), 197.
- [76] C. Holmstrom et al., *FEMS Microbiol. Ecol.* **2002**, 41(1), 47.
- [77] R. de Nys and P. D. Steinberg, *Curr. Opin. Biotechnol.* **2002**, 13(3), 244.
- [78] M. Loisel and K. W. Anderson, *Biofouling* **2003**, 19(2), 77.
- [79] M. Marotta et al., *Proc. Biochem.* **2002**, 38(1), 101.
- [80] B. Orgaz et al., *Enzyme Microb. Technol.* **2006**, 40(1), 51.
- [81] N. Oulahal et al., *Innov. Food Sci. Emerg. Technol.* **2007**, 8(2), 192.
- [82] P. Asuri et al., *Small* **2007**, 3(1), 50.
- [83] N. C. Price and L. Stevens, “*Fundamentals of Enzymology: the Cell and Molecular Biology of Catalytic Proteins*”, 3rd edition, Oxford University Press, New York 1999, p. 1–2.
- [84] P. Carter and J. A. Wells, *Nature* **1988**, 332, 564.
- [85] R. A. Copeland, “*Enzymes: A Practical Introduction to Structure, Mechanism, and Data Analysis*”, 2nd edition, Wiley-VCH Inc., New York 2000, p. 151–154.

- [86] K. F. Tipton, "Principles of Enzyme Assay and Kinetic Studies", in: *Enzyme Assays*, 2nd edition, R. Eisenthal and M. J. Danson, Eds., Oxford University Press, New York 2002.
- [87] E. Fisher, *Chem. Ber.* **1894**, 27, 2985.
- [88] R. A. Copeland, "*Enzymes: A Practical Introduction to Structure, Mechanism, and Data Analysis*", 2nd edition, Wiley-VCH Inc., New York 2000, p. 146–150.
- [89] E. Smyth, "The Trouble with Inhibitors", in: *Background, Horizon Symposia 2003*, Nature Publishing Group 2003.
<http://www.nature.com/horizon/teases/index.html>
- [90] D. R. Davies et al., *J. Biol. Chem.* **1988**, 263(22), 10541.
- [91] T. J. Tsomides and H. N. Eisen, *J. Biol. Chem.* **1991**, 266(6), 3357.
- [92] U. M. Hegazy, *J. Biol. Chem.* **2004**, 279(10), 9586.
- [93] B. Kiely and A. Martonosi, *J. Biol. Chem.* **1968**, 243(9), 2273.
- [94] E. Heyde and S. Ainsworth, *J. Biol. Chem.* **1968**, 243(9), 2413.
- [95] N. D. Rawlings and A. J. Barrett, "Introduction: Serine Peptidases and Their Clans", in: *Handbook of Proteolytic Enzymes*, 2nd edition, vol. 2, A. J. Barrett, N. D. Rawlings and J. F. Woessner, Eds., Academic Press, London 2004, p. 1425.
- [96] A. Chatterjee and R. V. Hosur, *Biophys. Chem.* **2006**, 123(1), 1.
- [97] J. H. Hehemann et al., *Biochem. Biophys. Res. Comm.* **2008**, 370(4), 566.
- [98] J. Pietzsch, "Signaling Scissors: New Perspectives on Proteases", in: *Background, Horizon Symposia 2003*, Nature Publishing Group 2003.
<http://www.nature.com/horizon/teases/index.html>
- [99] F. S. Markland and E. L. Smith, "Subtilisins: Primary Structure, Chemical and Physical Properties", in: *The Enzymes*, vol. 3, P. D. Boyer, Ed., Academic Press, New York and London 1971, p. 561–608.

- [100] A. V. Bacheva et al., *Biochemistry (Moscow)* **2003**, 68(11), 1261.
- [101] A. Stavrakoudis et al., *Lett. Pept. Sci.* **1997**, 4, 481.
- [102] K. E. S. Dean et al., *Bioorg. Med. Chem. Lett.* **2003**, 13, 1653.
- [103] D. Gabel, *FEBS Lett.* **1974**, 49(2), 280.
- [104] S. S. Twining, *Anal. Biochem.* **1984**, 143, 30.
- [105] L. X. Tang et al., *Anal. Lett.* **1996**, 29(12), 2085.
- [106] C. Y. Hsia et al., *Anal. Biochem.* **1996**, 242, 221.
- [107] J. Varani et al., *Anal. Biochem.* **1980**, 107, 377.
- [108] M. T. Gisslow et al., *Anal. Biochem.* **1975**, 68, 70.
- [109] O. H. Kwon et al., *Biotechnol. Bioeng.* **1999**, 66(4), 265.
- [110] R. Bovara et al., *Biotechnol. Bioeng.* **1997**, 54(1), 50.
- [111] K. Linderstrom-Lang and M. Ottesen, *Nature* **1947**, 159, 807.
- [112] A. V. Güntelberg and M. Ottesen, *Compt. Rend. Trav. Lab. Carlsberg, Ser. Chim.* **1954**, 29(4), 36.
- [113] M. Ottesen and I. Svendsen, "The Subtilisins", in: *Methods in Enzymology*, vol. 19, G. E. Perlmann and L. Lorand, Eds., Academic Press, London 1970, p. 199–215.
- [114] T. P. Graycar, M. D. Ballinger and J. A. Wells, "Subtilisins", in: *Handbook of Proteolytic Enzymes*, 2nd edition, vol. 2, A. J. Barrett, N. D. Rawlings and J. F. Woessner, Eds., Academic Press, London 2004, p. 1786–1792.
- [115] M. W. Pantoliano et al., *Biochemistry* **1988**, 27, 8311.
- [116] D. W. Heinz et al., *J. Mol. Biol.* **1991**, 217, 353.
- [117] F. A. A. Mulder et al., *J. Mol. Biol.* **1999**, 292, 111.
- [118] P. N. Bryan, *Biochim. Biophys. Acta* **2000**, 1543, 203.

- [119] N. D. Rawlings and A. J. Barrett, *Methods Enzymol.* **1994**, *244*, 19.
- [120] E. L. Smith et al., *J. Biol. Chem.* **1966**, *241(24)*, 5974.
- [121] L. Polgár, *Cell. Mol. Life Sci.* **2005**, *62*, 2161.
- [122] J. Kraut, “Subtilisin: X-Ray Structure”, in: *The Enzymes*, vol. 3, P. D. Boyer, Ed., Academic Press, New York and London 1971, p. 552.
- [123] D. J. Neidhart and G. A. Petsko, *Protein Eng.* **1988**, *2(4)*, 271.
- [124] R. J. DeLange and E. L. Smith, *J. Biol. Chem.* **1968**, *243(9)*, 2134.
- [125] F. Rusmini et al., *Biomacromolecules* **2007**, *8*, 1775.
- [126] R. L. Hill, *Adv. Protein Chem.* **1965**, *20(37)*, 89.
- [127] D. G. Smyth, “Use of Papain, Pepsin, and Subtilisin in Sequence Determination”, in: *Methods in Enzymology*, vol. 11, C. H. W. Hirs, Ed., Academic Press, London 1967, p. 421.
- [128] S. F. D’Souza, *Curr. Sci. India* **1999**, *77(1)*, 69.
- [129] A. Schmid et al., *Nature* **2001**, *409*, 258.
- [130] C. Walsh, *Nature* **2001**, *409*, 226.
- [131] L. Cao, “*Carrier-Bound Immobilized Enzymes: Principles, Application and Design*”, Wiley-VCH Verlag GmbH, Weinheim 2005, p. 7–9.
- [132] J. M. Goddard and J. H. Hotchkiss, *Prog. Polym. Sci.* **2007**, *32*, 698.
- [133] J. F. Liang et al., *J. Pharma. Sci.* **2000**, *89(8)*, 979.
- [134] D. Shan et al., *Biosens. Bioelectron.* **2007**, *22*, 1612.
- [135] J. Kim et al., *Chem. Eng. Sci.* **2006**, *61*, 1017.
- [136] D.-J. van Unen et al., *Biotechnol. Bioeng.* **2001**, *75(2)*, 154.
- [137] P. Wang et al., *Biotechnol. Bioeng.* **2001**, *74(3)*, 249.
- [138] P. Asuri et al., *Langmuir* **2007**, *23*, 12318.

- [139] M. E. Marín-Zamora et al., *J. Biotechnol.* **2006**, *126*, 295.
- [140] C. Mateo et al., *Enzyme Microb. Technol.* **2007**, *40*, 1451.
- [141] C. S. McDaniel et al., *Prog. Org. Coat.* **2006**, *55*, 182.
- [142] S. P. Bizily et al., *Proc. Natl. Acad. Sci. USA* **1999**, *96*, 6808.
- [143] K. E. LeJeune et al., *Nature* **1998**, *395*, 27.
- [144] R. McDaniel et al., *Nature* **1995**, *375*, 549.
- [145] L. P. Wackett et al., *Am. Soc. Microbiol. News* **1999**, *65(2)*, 87.
- [146] M. Trevan, “*Immobilized Enzymes*”, Wiley-VCH Inc., London 1980, p. 3.
- [147] J. Kim et al., *Enzyme Microb. Technol.* **2006**, *29*, 474.
- [148] F. Peissker and L. Fischer, *Bioorg. Med. Chem.* **1999**, *7*, 2231.
- [149] X. Tong, *Biotechnol. Prog.* **2008**, *24*, 714.
- [150] S. A. Barker et al., *Carbohydr. Res.* **1969**, *9(3)*, 257.
- [151] L. Cao, *Curr. Opin. Chem. Biol.* **2005**, *9*, 217.
- [152] L. Ferreira et al., *J. Mol. Catal. B: Enzym.* **2003**, *21*, 189.
- [153] L. Goldstein et al., *Biochemistry* **1964**, *3(12)*, 1913.
- [154] S. Viswanath et al., *Biotechnol. Bioeng.* **1998**, *60(5)*, 608.
- [155] J. Wang et al., *Fresenius J. Anal. Chem.* **2001**, *369*, 280.
- [156] U. Schmidt et al., *J. Appl. Polym. Sci.* **2003**, *87(8)*, 1255.
- [157] U. Freudenberg et al., *Biomacromolecules* **2005**, *6*, 1628.
- [158] T. Pompe et al., *J. Biomed. Mater. Res. A* **2003**, *67A*, 647.
- [159] K. Salchert et al., *J. Mater. Sci. Mater. Med.* **2005**, *16*, 581.
- [160] K. Salchert et al., *J. Chromatogr. A* **2003**, *1005*, 113.

- [161] L. Renner et al., *J. Mater. Sci. Mater. Med.* **2004**, *15*, 385.
- [162] L. Renner et al., *Langmuir* **2004**, *20*, 2928.
- [163] L. Renner et al., *Langmuir* **2005**, *21*, 4571.
- [164] T. Klose et al., *Colloids Surf., B* **2006**, *51*, 1.
- [165] T. Pompe et al., *Tissue Eng.* **2004**, *10(5)*, 841.
- [166] Tasso et al., *Macromol. Biosci.* **2009**, *9(9)*, 922.
- [167] Tasso et al., *Biofouling* **2009**, *25(6)*, 505.
- [168] R. Azzam and N. Bashara, “*Ellipsometry and Polarized Light*”, Elsevier, Amsterdam 1987.
- [169] R. A. Synowicki et al., *AIP Conf. Proc.* **2005**, 788, 324.
- [170] H. Arwin, *Sens. Actuators, A* **2001**, *92*, 43.
- [171] A. Laskarakis and S. Logothetidis, *Appl. Surf. Sci.* **2006**, *253(1)*, 52.
- [172] J. Wang et al., *Appl. Opt.* **2007**, *46(16)*, 3221.
- [173] H. Arwin et al., *Appl. Opt.* **2004**, *43(15)*, 3028.
- [174] S. Lousinian and S. Logothetidis, *Thin Solid Films* **2008**, *516(22)*, 8002.
- [175] H. Arwin, *Thin Solid Films* **2000**, *377*, 48.
- [176] Y. M. Bae et al., *Biosens. Bioelectron.* **2004**, *20(4)*, 895.
- [177] H. Elwing, *Biomaterials* **1998**, *19*, 397.
- [178] H. Fujiwara, “*Spectroscopic Ellipsometry: Principles and Applications*”, John Wiley and Sons Inc., West Sussex 2007, p. 147–204.
- [179] R. Cunico, K. Gooding and T. Wehr, “*Basic HPLC and CE of Biomolecules*”, Bay Bioanalytical Laboratory Inc., Richmond (CA) 1998.

- [180] S. P. Elliott and K. A. Hale, *J. Anal. Toxicol.* **1998**, 22(4), 279.
- [181] S. X. Peng, *Biomed. Chromatogr.* **2000**, 14(6), 430.
- [182] M. Sandvoss et al., *Magn. Reson. Chem.* **2005**, 43(9), 762.
- [183] X. Xu et al., *J. Forensic Sci.* **2004**, 49(6), 1171.
- [184] D. Dias and S. Urban, *Phytochem. Anal.* **2008**, 19(5), 453.
- [185] J.-A. Raust et al., *J. Chromatog. A* **2008**, 1203(2), 207.
- [186] I. D. Wilson, *J. Chromatog. A* **2000**, 892(1–2), 315.
- [187] E. Gelpí, *J. Chromatog. A* **1995**, 703(1–2), 59.
- [188] E. Gelpí, *J. Chromatog. A* **2003**, 1000(1–2), 567.
- [189] B. A. Buchholz et al., *Nucl. Instrum. Methods Phys. Res., Sect. B* **2000**, 172(1–4), 910.
- [190] Y. Yang et al., *J. Biotechnol.* **2000**, 81, 113.
- [191] K. Krane, “*Modern Physics*”, 2nd edition, J. Wiley and Sons Inc., New York 1996, p. 235–263.
- [192] R. K. Poole and U. Kalnenieks, “Introduction to Light Absorption: Visible and Ultraviolet Spectra”, in: *Spectrophotometry and Spectrofluorimetry: A practical Approach*, 2nd edition, M. G. Gore, Ed., Oxford University Press Inc., New York 2000, p. 1–31.
- [193] W. Song et al., *Methods* **2008**, 46(4), 295.
- [194] H. Ishiguro and T. Horimizu, *Int. J. Heat Mass Transfer* **2008**, 51, 5642.
- [195] M. Wagner et al., *Water Res.* **2009**, 43(1), 63.
- [196] V. Vukojevic et al., *Proc. Natl. Acad. Sci. USA* **2008**, 105(47), 18176.
- [197] K. Yang et al., *Chem. Eng. Sci.* **2008**, 63(16), 4045.

- [198] S. E. C. Dale and P. R. Unwin, *Electrochem. Commun.* **2008**, *10*(5), 723.
- [199] J. B. Pawley (Ed.), “*Handbook of Biological Confocal Microscopy*”, 3rd edition, Springer-Verlag, New York 2006, p. 1–58.
- [200] S. Minko and Y. Roiter, *Curr. Opin. Colloid. Interface. Sci.* **2005**, *10*, 9.
- [201] V. Karagkiozaki et al., *Mater. Sci. Eng., B* **2008**, *152*, 16.
- [202] D. J. Muller, *Biochemistry* **2008**, *47*(31), 7986.
- [203] Y. F. Dufrene, *Analyst* **2008**, *133*(3), 297.
- [204] B. Garipcan et al., *Langmuir* **2008**, *24*(16), 8944.
- [205] V. J. Morris, A. P. Gunning and A. R. Kirby, “*Atomic Force Microscopy for Biologist*”, Imperial College Press, London 1999, p. 5–74.
- [206] A. Bouafsoun et al., *Mater. Sci. Eng., C* **2007**, *27*(4), 709.
- [207] O. I. Wilner et al., *Chem. Eur. J.* **2008**, *14*(26), 7774.
- [208] M. Gindl et al., *Colloids Surf., A* **2001**, *181*, 279.
- [209] E. Chibowski and R. Perea-Carpio, *Adv. Colloid. Interface Sci.* **2002**, *98*, 245.
- [210] M. Zenkiewicz, *Polym. Test.* **2007**, *26*, 14.
- [211] E. Chibowski and R. Perea-Carpio, *Adv. Colloid. Interface Sci.* **2002**, *98*(2), 245.
- [212] M. Zenkiewicz, *Polym. Test.* **2007**, *26*(1), 14.
- [213] D. Y. Kwok and A. W. Neumann, *Adv. Colloid. Interface Sci.* **1999**, *81*(3), 167.
- [214] J. A. Finlay et al., *Biofouling* **2002**, *18*(4), 251.
- [215] M. P. Schultz et al., *Biofouling* **2000**, *15*(4), 243.
- [216] G. W. Swain and M. P. Schultz, *Biofouling* **1996**, *10*(1–3), 187.

-
- [217] R. R. L. Guillard and J. H. Ryther, *Can. J. Microbiol.* **1962**, 8, 229.
- [218] C. Werner et al., *Colloids Surf., A* **1999**, 156, 3.
- [219] J. A. Woollam, “*User Manual VASE and M-44 Ellipsometers WVASE 32TM*”, J. A. Woollam Co. Inc., Lincoln (NE).
- [220] I. Horcas et al., *Rev. Sci. Instrum.* **2007**, 78(1), 013705.
- [221] M. E. Callow et al., *Biofouling* **2002**, 18(3), 237.
- [222] M. Philipp and M. L. Bender, *Mol. Cell. Biochem.* **1983**, 51, 5.
- [223] ASTM D1141-98(2003), Standard practice for the preparation of substitute ocean water.

Acknowledgements

My acknowledgements go to:

Prof. Carsten Werner for the opportunity of joining his group,

Dr Ana Cordeiro for general supervision and useful corrections to my work,

Christine Arnhold, Tina Lenk, Milauscha Grimmer, Juliane Drichel, Grith Eberth, Nelly Rein, Martin Espig, Claudia Sperling, Manfred Maitz, Marion Fischer, Ralf Zimmermann, Ralf Helbig, Martin Kaufmann, Petra Welzel, Dimitar Stamov, and Andreas Janke, all from the MBC, for lab support, advice with several techniques, and (in some cases) huge help during the execution of my work,

Dr Michala Pettitt and Ms. Sheelagh Conlan for the tremendous efforts dedicated to carry out together with me the biological assays, and mostly for friendliness and kindness at any time,

Prof. James Callow, Dr Maureen Callow, Prof. Anthony Clare, and Dr Nicholas Aldred for detailed insights into the biofouling phenomena, instructive discussions and encouragement,

Prof. Katrin Salchert for guidance (especially at the very beginning), suggestions, and openness for challenging and productive discussions,

Theresia Klose, Petra Welzel, Tilo Pompe, and Lars Renner for fruitful conversations,

Dimitar Stamov, Kristin Alberti, Yvonne Müller, Lidia Sobkow, Agnieszka Kuriata, Eli Elias, Ringo Grombe, Claudia Hinüber, Zeynep Özyürek, Woranan Panyanuwat, Mikhail Tsurkan, Manfred Maitz, Salim Ok, Michael Lang and Rebecca Schober for friendship and valuable support in difficult moments, Theresia Klose and her family, my several flatmates, partners of volleyball, swimming, dancing and German courses, as well as the PhDs of the MBC&IPF for the many enjoyable moments together, The teams at the universities of Birmingham and Newcastle-upon-Tyne for the warm welcome and help, and the AMBIO partners for supportive words and nice discussions,

and, with all my heart, my thanks go to my family, to Benjamin Kürten and his family, and to my closest friends.

This work was supported by the AMBIO project (NMP4-CT-2005-011827) funded by the 6th framework program of research and technological development of the European community. The work herein presented was carried out at the Max Bergmann Center of Biomaterials Dresden within the Leibniz Institute of Polymer Research Dresden, Germany (Prof. Carsten Werner) as well as in the facilities of the Universities of Birmingham (Prof. James Callow) and Newcastle-upon-Tyne (Prof. Anthony Clare), both in UK.

Erklärung

Hiermit versichere ich, dass ich die vorliegende Arbeit ohne unzulässige Hilfe Dritter und ohne Benutzung anderer als der angegebenen Hilfsmittel angefertigt habe. Die aus fremden Quellen direkt oder indirekt übernommenen Gedanken sind als solche kenntlich gemacht. Die Arbeit wurde bisher weder im Inland noch im Ausland in gleicher oder ähnlicher Form einer anderen Prüfungsbehörde vorgelegt.

Die vorliegende Arbeit mit dem Titel „Bioactive coatings to control marine biofouling“ wurde in der Zeit von Februar 2006 bis Juni 2009 am Max Bergmann Zentrum für Biomaterialien des Leibniz-Instituts für Polymerforschung Dresden e. V. unter der Leitung von Herrn Prof. Dr. rer. nat. Carsten Werner durchgeführt.

Dresden, 10.07.2009

Mariana Tasso